

University of Nebraska - Lincoln

DigitalCommons@University of Nebraska - Lincoln

Theses, Dissertations, and Student Research
from Electrical & Computer Engineering

Electrical & Computer Engineering, Department
of

8-2014

EXPECTED COST PENALTY DUE TO DEVIATION FROM SECURITY- CONSTRAINED DISPATCH

Veravut Dherapasart

University of Nebraska-Lincoln, vdherapasart2@unl.edu

Follow this and additional works at: <https://digitalcommons.unl.edu/elecengtheses>



Part of the [Computer Engineering Commons](#), and the [Other Electrical and Computer Engineering Commons](#)

Dherapasart, Veravut, "EXPECTED COST PENALTY DUE TO DEVIATION FROM SECURITY-CONSTRAINED DISPATCH" (2014). *Theses, Dissertations, and Student Research from Electrical & Computer Engineering*. 121.

<https://digitalcommons.unl.edu/elecengtheses/121>

This Article is brought to you for free and open access by the Electrical & Computer Engineering, Department of at DigitalCommons@University of Nebraska - Lincoln. It has been accepted for inclusion in Theses, Dissertations, and Student Research from Electrical & Computer Engineering by an authorized administrator of DigitalCommons@University of Nebraska - Lincoln.

University of Nebraska - Lincoln

DigitalCommons@University of Nebraska - Lincoln

Digital Commons / Institutional Repository
Information

Digital Commons - Information and Tools

2014

EXPECTED COST PENALTY DUE TO DEVIATION FROM SECURITY- CONSTRAINED DISPATCH

Veravut Dherapasart

Follow this and additional works at: http://digitalcommons.unl.edu/ir_information

 Part of the [Power and Energy Commons](#)

This Article is brought to you for free and open access by the Digital Commons - Information and Tools at DigitalCommons@University of Nebraska - Lincoln. It has been accepted for inclusion in Digital Commons / Institutional Repository Information by an authorized administrator of DigitalCommons@University of Nebraska - Lincoln.

EXPECTED COST PENALTY DUE TO DEVIATION
FROM SECURITY-CONSTRAINED DISPATCH

by

Veravut Dherapasart

A THESIS

Presented to the Faculty of
The Graduate College at the University of Nebraska
In Partial Fulfillment of Requirements
For the Degree of Master of Science

Major: Electrical Engineering

Under the Supervision of Professor Sohrab Asgarpoor

Lincoln, Nebraska

August 2014

EXPECTED COST PENALTY DUE TO DEVIATION
FROM SECURITY-CONSTRAINED DISPATCH

Veravut Dherapasart, M.S.

University of Nebraska, 2014

Adviser: Sohrab Asgarpoor

This thesis introduces and evaluates a new index called "Expected Cost Penalty Due to Deviation From Security Constrained Dispatch" (ECP_SCD) for interconnected power systems planning. This index represents the optimal operating cost of the system taking into account the uncertainties such as random failure of generating units, transformer, and transmission lines in interconnected power systems. The significance of this index is that it represents the minimum operating cost for a contingency event and can be used for contingency screening (ranking). This index also indicates the impact of equipment reliability on the average cost penalty of all contingency events. Moreover, this index unit is in dollars per hour which makes it easier to understand for the power system operator. Monte-Carlo simulation and a normal Statistics Numerical Algorithms are used to evaluate this index. System studies are performed to determine the variation of expected cost penalty with respect to changes in load values, probability outage of components, and transmission line loading limit.

Acknowledgement

First of all, I would like to thank my advisor, Dr. Sohrab Asgarpoor, for his assistance and support in the process of my thesis. Being his research assistance gave me an opportunity to gain a lot of valuable experiences and broaden my horizons. In addition, his great efforts in revising my thesis are truly appreciated. Also, I would like to thank Dr. Jerry Hudgins and Dr. Steven Cohn for serving as committee members. Lastly, I owe a debt of gratitude to my dear family and friends for their encouragement, love, and support during the past two years while I was working on this thesis. Thank you ☺

Contents

Acknowledgments	iii
Contents	iv
List of Figures	vi
List of Tables	vii
Chapter 1: Introduction	1
1.1 Motivation of Work	1
1.2 Literature Review	4
1.3 Thesis Organization	21
Chapter 2: Background, Models and Tools	23
2.1 Power Flow Analysis	23
2.1.1 Bus Classifications	24
2.1.2 Bus admittance matrix	25
2.1.3 Power balance equations	26
2.1.4 Jacobian matrix	28
2.1.5 Power flow by Newton-Raphson method	30
2.2 Optimal Power Flow Analysis	32
2.2.1 Objective function	33
2.2.2 Constraints	36
2.2.3 Interior-point algorithm	37

2.3 Contingency Analysis	40
2.3.1 Contingency Screening	40
2.3.2 Contingency Screening	43
2.4 Security Constraint Optimal Power Flow	45
2.5 Security Constraint Dispatch	49
2.6 Expected Cost Penalty	52
2.6.1 Expected Value	52
2.6.2 Variance and Standard Deviation	54
2.6.3 Coefficient of Variation	55
2.7 Monte Carlo Simulation	57
Chapter 3: Case Study	61
3.1 IEEE 30 Bus Test Case	61
3.2 ECP_SCD of The Test System	62
3.2.1 Procedure and results of ECP_SCD calculation	62
3.2.2 ECP_SCD by Monte Carlo Simulation	72
3.2.3 ECP_SCD with decreasing the probability outage rate	75
3.2.4 ECP_SCD when increasing the line limit	77
3.3 Contingency Screening by SCD	80
Chapter 4: Conclusion	87
References	89
Appendix	96
A1 Example of Power Flow Analysis on 3 Bus System	96

A2 IEEE 30 Bus Test System Data

102

A3 DPL Code

110

List of Figure

Figure 1: Results of 3-bus system power flow analysis on Matpower	31
Figure 2: Results of 3-bus system power flow analysis on PowerWorld	32
Figure 3: Fuel cost curve example	34
Figure 4: Fuel cost curve approximated using piece-wise smooth	35
Figure 5: The OPF based on interior-point method flow chart	39
Figure 6: The contingency analysis method flow chart	42
Figure 7: Optimal dispatch state	47
Figure 8: Post contingency State	47
Figure 9: Secure dispatch state	48
Figure 10: Secure Post Contingency State	48
Figure 11: Security Constrained Dispatch analysis flow chart	51
Figure 12: Overview of the Monte Carlo Simulation module for ECP_SCD	60
Figure 13: One-line diagram of the IEEE-30 bus system in DIgSILENT-PowerFactory	63
Figure 14: The ECP_SCD result with the same load shedding cost penalty for all the load points	65
Figure 15: Daily load curve of IEEE 30 bus test system	67
Figure 16: ECP_SCD result with the daily load curve	67
Figure 17: Result of ECP_SCD	69
Figure 18: Variance of CP_SCD	69

Figure 19: Standard deviation of CP_SCD	70
Figure 20: C.V. of CP_SCP	70
Figure 21: ECP_SCD by Monte Carlo Simulation	74
Figure 22: Frequency of ECP_SCD by Monte Carlo Simulation	74
Figure 23: Result of ECP_SCD when decreasing the probability outage rate	76
Figure 24: Variance of ECP_SCD when decreasing the probability outage rate	76
Figure 25: SD of ECP_SCD when decreasing the probability outage rate	77
Figure 26: Result of OPF simulation	78
Figure 27: ECP_SCD when increasing the line-loading limit	80
Figure 28: Load flow analysis when transmission line 06-08 out of service	82

List of Tables

Table 1: Potential cost savings of increased efficiency of dispatch	2
Table 2: The advantages of AI OPF Method	5
Table 3: Cost penalty of load shedding for each load point.	66
Table 4: Result of ECP_SCD	68
Table 5: Probability outage data	75
Table 6: Line loading result	79
Table 7: Contingency Screening by Performance Index	83
Table 8: Contingency Screening by SCD	85
Table 9: Comparison results of Contingency Screening by PI vs. SCD	85
Table 10: Contingency screening by SCD with different load scaling factor	86
Table A1: Buses classify result	91
Table A2: Bus Data Format	102
Table A3: Generator Data Format	104
Table A4: Transmission Line Data Format	105
Table A5: Transformer Data Format	107
Table A6: Generator Cost Data in Piecewise Linear Format	108

Chapter 1

Introduction

1.1 Motivation of Work

Nowadays, the power system networking is getting more complex and stressed due to global warming phenomenon, increasing population size and rapid infrastructure development which contribute to continuous changes in supply and demand patterns, increased interconnection and stringent environmental constraints. These activities can lead to the system contingencies or in the worst case is the blackout. To deal with the complex power system, a serious attention and studies have been focused on appropriate planning and control action to avoid and/or minimize its occurrences. One of the main studies in power system planning is the Optimal Power Flow Analysis (OPF), which is the study of a power flow in the system plus optimizing the objective function (cost, loss, etc.). Unfortunately, even 50 years after the Optimal Power Flow (OPF) problem was first formulated, OPF still lack a fast and robust solution technique for the full solution. Therefore, the Independent System Operator (ISO) in power market planning still uses approximations, decompositions and engineering judgment to obtain reasonably acceptable solutions to OPF problem [1].

In power system planning, if the operator can increase the efficiency of the power system just by a small amount, the total production cost of system operating will be saved a lot in billion dollars per year. The easiest way to do this is by improving the potential of operating software. In example, using EIA data on wholesale electricity prices of U.S. and World Energy production [1], Table 1 gives a range of potential cost savings from a 5% increase in market efficiency due to improvements to the OPF simulation software. Small increases in efficiency of dispatch are measured in billions of dollars per year. Since the usual cost of purchasing and installing new software for an existing ISO market is less than \$10 million dollars, the potential benefit/cost ratios of better software are in the range of 10 to 1000.

Table 1: Potential cost savings of increased efficiency of dispatch

	2009 gross electricity production (MWh)	Production cost (\$billion/year) assuming \$30/MW energy price	Savings (\$billion/year) assuming 5% increase in efficiency	Production cost (\$billion/year) assuming \$100/MWh energy price	Savings (\$billion/year) assuming 5% Increase in efficiency
U.S.	3,724,000	112	6	372	19
World	17,314,000	519	26	1731	87

Beside the optimal power flow simulation, contingency analysis tools are also widely used in power system planning. Contingency analysis in power system is a study of unpredictable conditions, outage of elements such as transmission lines,

transformers and generators, and investigation of the resulting effects on line power flows and bus voltages of the remaining system [2]. When contingency event occur, the cost of operation can increase more than 10 times of the operating cost in normal situation. Also, the operator usually studies the contingency events in advance to see how each contingency can be fixed. Therefore, when contingency occur, the operator can take an action fast enough to keep the remaining system operate in steady state.

As discussion above, improving OPF and contingency analysis tool can save a lot of money for both operator and demand side. Therefore, this thesis introduces an index called Expected Cost Penalty due to Deviation from Security Constrained Dispatch (ECP_SCD), which is an optimal operating cost of the system following contingency and security corrections event. Additional, the SCD analysis is a self-healing (corrective switching) AC optimal power flow with unit commitment over the optimal network. Also, this analysis tool will analyze all contingency events that can occur in the power system and determine the minimum cost for each contingency event.

The power system operator can use this index to represent the cost penalties associated with daily events by averaging the cost penalties of all contingency events. Also, this index can be used for contingency screening analysis that easier to understand for the power system operators since its unit is in dollars per hour.

1.2 Literature Review

This section contains a brief review of literature helpful for understanding the material presented in this thesis. The references in this section are relevant to the Security Constrained Dispatch as a whole and to the material presented in Chapter 2 and 3 in particular. This literature summarizes and concludes selected related works from the past to present, and divides in five topics. The five topics are: Optimal Power Flow (OPF), Contingency Analysis, Security Constrained Optimal Power Flow (SCOPF), Load Shedding, and Statistics Numerical Value.

Optimal Power Flow

The first optimal power flow equation was formulated in 1962 by J. Carpentier [3]. Over fifty years of study, many different OPF formulations have been developed to address specific instances of the problem, using varying assumptions and selecting different objective functions, controls, and system constraints. Optimization problems can be formulated and described differently depending on the objective function, control variables, the constraints under consideration, and the method of calculation.

In 1999, J. A. Momoh et al. [4] did a literature survey, which reviewed some of selected optimal power flows research up to 1993. In their review, the techniques to solve OPF problem can be classified into 6 categories as: Nonlinear programming (NLP), Quadratic programming (QP), Newton-based solution (NR), Linear programming (LP), Mixed integer programming (MIP), and Interior point methods

(IP). These six categories are known as classical OPF methods. He also concluded that linear programming is accurate and very fast, suitable for large systems.

Interior point method features good starting point and fast convergence.

Almost ten years later, 2008, K. S. Pandya and S. K. Joshi [5] did a literature survey of optimal power methods. Their survey includes classical method from the past and adds the modern techniques called Artificial Intelligence (AI). Since OPF has become more complex in recent year, AI methods have been emerged which can solve highly complex OPF problems. In their survey, AI methods are divided into the following categories: Artificial neural networks (ANN), Fuzzy logic methods (FL), Genetic algorithm methods (GA), Miscellaneous AI methods, Evolutionary programming (EP), Ant colony optimization (ACO), and Particle Swarm Optimization (PSO). In their conclusion, they summarized and made a table that shows the suitable methods for solving the various optimization problems. Also, they point out all the AI methods advantages.

Table 2: The advantages of AI OPF Method

Method	Advantages
Artificial neural networks (ANN)	Possesses learning ability, fast, appropriate for non-linear modeling, etc.
Fuzzy logic methods (FL)	Accurately represents the operational constraints and FL' constraints are softer than traditional constraints.
Genetic algorithm methods (GA)	GA only uses the values of the objective function and less likely to get trapped at a local optimum.

Method	Advantages
Evolutionary programming (EP)	Adaptability to change, ability to generate good enough solutions and rapid convergence.
Ant colony optimization (ACO)	Positive feedback for recovery of good solutions, distributed computation, which avoids premature convergence.
Particle Swarm Optimization (PSO)	PSO can be used to solve complex optimization problems, which are non-linear, non-differentiable and multi-model. The main merits of PSO are its fast convergence speed and it can be realized simply for less parameters need adjusting.

In 2012, S. Frank et al. [6-7] did a bibliographic survey about OPF. Their survey divides into two parts. The first part provides an introduction and deterministic methods that have been applied to OPF, and the second part examines non-deterministic and hybrid methods for OPF. They also claimed that his survey is the most comprehensive review of OPF algorithms for electric power systems available to date, both in the number of referenced articles as well as in the number of methods surveyed. In his survey, the total 18 methods are divided into 3 categories as follows:

Deterministic optimization methods

- Gradient Methods
- Newton's Method
- Simplex Method

- Sequential Linear Programming
- Sequential Quadratic Programming
- Interior Point Methods

Non-deterministic optimization methods

- Ant Colony Optimization
- Artificial Neural Network
- Bacterial Foraging Algorithm
- Chaos Optimization Algorithm
- Evolutionary Algorithms
- Particle Swarm Optimization
- Simulated Annealing
- Tabu Search

Hybrid methods

- Deterministic Methods Combined
- Deterministic and Non-deterministic Methods Combined
- Non-deterministic Methods Combined
- Fuzzy Logic Combined with OPF

The objective functions of OPF problem can be varied. The most common OPF objective function is minimization of total system operating cost. Besides that, the more common objectives include minimization of system losses, voltage deviation, voltage stability and load shedding schedule under emergency conditions. Furthermore, there are more than one set of solutions that can be solve in OPF

problem called multi-objective function. Some OPF problems solved in past 10 years, which have a multi-objective function, are as follows:

In 2003, D. B. Das and C. Patvardhan [8] presented a multi-objective hybrid evolutionary strategy, which combined Genetic Algorithms and Simulated Annealing techniques to solve OPF problem. Four objective functions are considered in their research: minimization of generation cost, transmission losses, emissions, and maximization of a security index. Two year later, 2005, J. G. Vlachogiannis and K.Y. Lee [9] successfully implemented parallel vector evaluated Particle Swarm Optimization, minimizing both the real power losses in the transmission lines and the voltage magnitudes at the load busses.

In 2007, M. Tripathy and S. Mishra [10] applied a new Evolutionary Algorithm know as Bacterial Foraging Algorithm for solving the multi-objective multivariable OPF problem. The objectives functions are optimizing the real power losses and voltage stability limits of a mesh power network. Later in the same year, Z. L.Gaing and X. H. Liu [11] used a Particle Swarm Optimization for solving an OPF problem. The four objective functions are minimization of total generation cost, enhancement transmission security, reduce transmission loss, and improvement of the bus voltage profile under pre- and post-contingency states. In addition, Aminudin et al. [12] applied Evolutionary Algorithm Programming to improve the load margin of a power system, considering operational cost and loss reductions.

Abido [13] applied Particle Swarm Optimization technique to multi-objective OPF problem in 2008. The OPF problem has been formulated with competing fuel

cost and voltage stability enhancement objectives. Later, M. Varadarajan and K. S. Swarup [14] presented a Differential Evolutionary Algorithm approach to solve an OPF problem with multiple objectives. For the active power dispatch problem, total emissions and generation costs were considered, while power losses and voltage deviation were the objective functions considered for the reactive power dispatch problem. K. Zehar and S. Sayah [15] also minimized same objective functions, the fuel generation costs and pollutants emissions, but used a successive linear programming technique.

In 2009, B. Gasbaoui and B. Allaoua [16] used Ant Colony Optimization technique to solve an OPF problem with multiple objective functions. The research tested on the standard IEEE 57-bus test system with different objectives that reflect fuel cost minimization, voltage profile improvement, and voltage stability enhancement. A year later, M. S. Kumari and K. Maheswarapu [17] solved a multi-objective OPF by an Enhanced Genetic Algorithm based computation technique. The combinations of generation costs, system transmission losses, and a system voltage stability index are considered as a multi-objective function. Later in 2012, J. Aghaei et al. [18] used Fuzzy Optimization method to solve an OPF problem. The simulation on the IEEE 30-bus test system shows the performance, which minimizes the total generation fuel cost and active power losses.

From the contents of these reviews, the OPF analysis took a very long time to become a successful algorithm that could be applied in everyday use. The most common of the objective function is minimizing the total operation cost. When the

problem becomes more complex or considering multi-objective functions, the Artificial Intelligence techniques, such as Particle Swarm Optimization and Evolutionary Algorithm, will be used.

Contingencies Analysis

A contingency in a power system can be described by the loss of a major piece of equipment, such as a power transmission line, transformer, and generator [2]. Many problems, which occur in the power system, can have serious consequences within a short time that the operator could not take appropriate actions fast enough. Also the operator usually needs to know if the present operation of the system is secure and what will happen if a particular outage occurs.

Because of this aspect of system operation, modern power system operation software, such as PowerWorld or DigSilent-Power Factory, are equipped with a contingency analysis tool. This tool used to study outage events and alarm the operators to any potential overloads or out of limit voltages before they arise. Therefore, contingency analysis is the study of the outage of elements that uses a computer simulation to evaluate the effects of removing individual elements from a power system and investigation of the resulting effects on line power flows and bus voltages of the remaining system [2].

The main objective of contingency analysis is to determine the level of protection and rank all the components in the system by priority. In general, contingency events are ranked by comparing the power flow violation of the system,

system using severity indices called Performance Index (PI). There are two types of performance indices; the first one called Active Power Performance Index (PIP), which reflects the violation of line active power flow. Another one called Reactive Power Performance Index (PIV), which reflects the violation of bus over voltage [2]. In 2001, J. A. Momoh et al. [19] used PI of line over loads to find the worst contingency case in order to determine the priority of phase shifters location to solve the OPF with phase shifter problem. IEEE 30-bus system is used to test the proposed scheme, and simulation results show that the proposed integrated OPF with phase shifter scheme is effective. Also, S. Gope and T. Malakar [20] used PI to determine the most severe contingency scenarios of IEEE 30 bus test system with wind farm in 2011. This study shows that the average PI value is less with the presence of wind farm than when it is not present even though the top five severe contingencies are totally different. Therefore, using wind farm makes the security of power system improves significantly under the single line contingency condition.

Many similar ranking indices, for contingency analysis, were proposed and used. R. N. Banu and D. Devaraj [21] ranked the line outage contingency events using proposed approach called Single Contingency Sensitivity (SCS) index. In their project, SCS is used to define the best branch location for installing the Flexible AC transmission system (FACTS) devices to eliminate line over loads in the system. The SCS for each branch is defined as the sum of the sensitivity of considered branch to all considered contingencies. In general, the larger SCS value a branch has, the more sensitive it will be. Also, C. Nnonyelu and T.C. Madueme [22] determined the

security level of the Nigeria power system by ranking contingency events using calculation of System Line Overload Index (SLOI). SLOI index calculates contingencies based on the line loadability, which is defined as transmission line voltages decrease (when heavily loaded) and increase (when lightly loaded). Also, this ranking result were used for suggestion on the level of protection to be applied on the Nigeria power system's transmission line with aim of improving system security.

In 2011, Z. Hussain et al. [23] proposed two techniques of accurate and precise contingency ranking for modern complex power system. One is Exact Ranking Index (E_{RI}), which aims at finding the exact number of possible violations following a contingency. Another one is Precise Ranking Index (P_{RI}), which concern to identify the ranking result in same number of violations and takes into account in case there is any line or bus reaching near to its limit following a particular contingency. They also compared these two techniques with other three: Loss Based ranking, PI Based ranking and Actual Number of Violation Based ranking. The result shows that the proposed ranking technique, which considers apparent power instead of real power, is more realistic approach.

Security Constrained Optimal Power Flow

The contingency analysis can be applied into various power system problems, such as economic dispatch, unit commitment, and optimal power flow. It has been recognized that with the basic OPF formulation it may not be possible to

keep the system in a normal state after a contingency occurs, or even when it is possible, the cost of such a solution may be very high. Security Constrained OPF (SCOPF), also called Contingency Constrained OPF (CCOPF) dispatch, guarantees that the system will operate successfully and optimally under the base case and the contingency case [24]. Basically, the SCOPF is a combination of contingency analysis with an optimal power flow.

Following the definitions in [25], the pre-contingencies or base case (N-0) refers to “the power system in its normal steady-state operation, with all elements in service that are expected to be in service”. The first loss of a bus or a line is referred to as the Primary Contingency (N-1), while the second loss is referred to as the Secondary Contingency (N-1-1). The post-contingencies refer to the system that already incorporates remedial actions after contingency events occur. System remedial actions may include the open or close of a transmission line, re-dispatch of a generator, change of transformer tap, change of the switched shunt set point, and the curtailment of load or load shedding.

F. Milano et al. [26], P. E. O. Yumbla et al. [27], Z. L. Gaing and C. H. Lin [28] solved a SCOPF problem with N-1 contingency criterion. F. Milano et al. used Interior Point method demonstrated two cases studies, 6 and 24 buses, to solve the SCOPF problem that include voltage stability limits in the operation of competitive electricity markets. Their objective function considered both proper market conditions and security margins. P. E. Onate Yumbla et al. used PSO with reconstruction operators, where the major aim is to minimize the total operating

cost. Their proposed methodology has been applied to two power systems. The first one is a 39 buses system, and the second system has 26 buses. Also, Z. L. Gaing and C. H. Lin used Simplex-Based Chaotic Particle Swarm Optimization (SCPSO) on 26 and IEEE 57 bus system. The associated objective is to minimize the total generation cost, reduce transmission loss, and improve the bus-voltage profile under pre- or post-contingent states as well as enhancing the security of the system even if the system suffers transmission line outages.

V. C. Ramesh and X. Li [29], and N. Fan et al. [30] solved a SCOPF problem with N-1-1 contingency criterion. V. C. Ramesh and X. Li used a Fuzzy Logic technique on IEEE 14 bus test system. Three objective functions were the minimization of operating cost, and minimization of both pre- and post- contingency correction times. Unfortunately, the results were unclear and had some issues remain open. One is the choice of a suitable metric for measuring correction time. Another is the selection of an appropriate mechanism for assigning weights to different contingencies. N. Fan et al. used a DC Mixed-Integer Optimization method on IEEE 30-Bus and RTS-96 test systems. Their model requires full compliance in the primary contingency, but allows for line overloads and load shedding during the secondary contingency.

F. Zaoui and S. Fliscounakis [31] considered both N-1 and N-1-1 contingency criterion for the SCOPF problem, using Interior Point method. Three different sizes of test cases were presented, small (3 buses), medium (95 buses), and large (1207 buses). Minimization of total operating cost was solving for both in the base case

and contingency cases. In addition, in case of a priority infeasibility of the contingency problem, load-shedding and investment variables are added to help to obtain a solution.

Load Shedding

Load shedding during contingency conditions is one of the most important issues in planning, security, and operation of power systems. Increasing demands in power systems at present may cause overloading and might lead to severe blackout unless proper load shedding is performed in time. Load shedding scheme must be effective and optimal in order to protect the power system instability.

Since traditional load management systems require that load shedding have to be done manually, in 1985, L. A. Finley et al. [32] demonstrated a method of software called Load Management Control System (LMCS) which computes optimum load shed for a requested load shed amount. This software was developed for Houston Lighting & Power Company (HL&P), and it was decided that the optimum load shed schedule should maximize customer acceptance, require minimum dispatcher intervention, and provide flexibility for future development. Therefore, this load management software designs from basic load shed toward an integrated energy control operation.

In 2005, G. B. Shrestha and K. C. Lee [33] proposed the concept of an overall load shedding scheme considering the probabilistic outages of a number of most significant contingencies. In the study case with small system, the load shedding

schemes for two different contingencies were combined to obtain the overall shedding scheme, which can be expected to perform well under both contingencies in practice. Unfortunately, this proposed method needs refinement and has not produced optimal results; they have provided quite reasonable results that provide insight into the system performance under load shedding.

In 2008, B. F. Rad and M. Abedi [34] presented an optimal load shedding approach solved by Genetic and Particle Swarm Optimization Algorithms, in which weighting factors are determined using Analytical Hierarchy Process (AHP) method. The AHP is the method to compare two items based on questions asked from experts. In this case, the questions can be simply classified as: How is the importance of i^{th} bus respect to j^{th} bus? Or how is the importance of i^{th} line respect to j^{th} line? The proposed method was tested on the IEEE 30 bus system, and the results were comparison of load shedding from each bus with GA and PSO method. In conclusion, the authors confirmed that in terms of time consumed to run the program, PSO is faster than GA but, for the problems in which variables are not continuous, GA has been better than PSO.

In 2010, M.T. Hagh and S. Galvani [35], and B. Charoenphan and K. Audomvongseree [36] solved the minimum weighted load shedding problem during contingency conditions. M.T. Hagh and S. Galvani used a modified version of Non-Dominated Sorting Genetic Algorithm (NSGA-II) as an optimization tools to determine the location and amount of load shedding as well as generator rescheduling in post contingency conditions. Also simultaneous minimizing of total

load shedding with respect to loads importance, transmission lines overloading and voltage violations are taken into consideration. Single and double contingency of IEEE 14 bus test system were used as a case study. Later in the same year, B. Charoenphan and K. Audomvongseree used the linearized optimization method to test with EGAT Thailand system in peak load situation with single line contingency. With this proposed method, the load shedding solution can be obtained faster than the conventional nonlinear optimization method by comparing computation time.

Load shedding not only used to prevent the system instability, S. Su and K. Tanaka [37] used an estimated necessary load shedding amount for ranking contingency events. Two model systems were used in this research. The 6-bus system was used mainly for verifying the accuracy of the concept, and the modified IEEE 30 bus system used for the accuracy of the proposed ranking method. From the results, it can be clarified that the proposed ranking method obtains enough accuracy of the necessary amount of load shedding for arranging contingency case including unstable load buses in descending order.

Statistic Numerical Value

Expected value and variance are the most important descriptive measure in statistics and probability. Expected value is calculated by multiplying each of the possible outcomes with the probability that each outcome will occur, and summing all of those values [38].

In power system, expected value can be used in several ways. For example, some researchers used expected value to determine the system operating cost, system losses, and fault resistance in power systems. The following papers are the example of research that use expected value to find the expected cost of SCOPF:

J. Condren et al. [39-40] published two papers in 2006. The first one discusses the expected-security-cost optimal power flow (ESCOPF). In this paper, the ESCOPF has been applied to linearized DC IEEE 14-bus and IEEE 30-bus test system and to the full AC IEEE 14-bus test system. Also, a five-bus system was presented as a simple example, and the results of the OPF and ESCOPF were compared. Since the contingency event may cause the system to become unstable, transient and small signal stability analysis should be included as the constraints. Therefore, in second paper, they did improve the ESCOPF with small-signal stability constraints. In this paper, the small-signal stability ESCOPF problem was solved for a nine-bus test case. As expected, the optimal value of the objective function, which is the expected value of social welfare, decreases as the stability margin is increased.

L. Yang et al. [41] presented the formulation, which improved and corrected for ESCOPF using a novel parallel Interior-point algorithm based on multiple centrality-weighted correctors as a method in 2009. Unfortunately, no case study was presented in this paper. A year later, 2010, R. S. Wibowo et al. [42] proposed an approach to optimally allocate flexible ac transmission systems (FACTS) devices based on ESCOPF. Two optimization problems are considered in this paper. The main optimization problem was intended to find optimal location and size of

Thyristor-Controlled Series Capacitors (TCSC), which is used for eliminating overload under single contingency. The other one is aimed to minimize operating cost while keeping voltage and line flow within limit. Hybrid PSO method is used in this research. The results show that adding TCSCs is able to considerably reduce operating cost only when contingencies occur in some lines, but not for all lines. Fortunately, expected cost can be reduced and investment cost TCSC can be covered by obtained benefit. Moreover, H. J. Cheng et al. [43] also proposes a technique for optimizing the balance between probabilistic measures of economy and security in the operation of a power system called an optimal probabilistic security (OPS) method. The objective of the OPS is to minimize the expected social cost, which is the sum of the expected operating cost and the expected interruption cost. An improved PSO technique is used to solve this problem. Also, comparison between OPS, OPF and SCOPF was shown as the results, and prove that the OPS achieve a smaller overall social cost than the other two methods.

The variance (σ^2) is a measure of how far each value in the data set from the mean (or expected value) [38]. A small variance indicates that the data tend to be very close to the mean. On the other hand, a high variance indicates that the data are very spread out from the mean. Same as expected value, variance has been used in power system area with related to the optimal power flow analysis in many ways. Some examples of variance with OPF problem, which published as a paper, are showing below:

M. E. El-Hawary and G. A. N. Mbamalu [44] presented a method that reformulates the OPF problem including power demand uncertainty. In this paper, they used variances, of the active power loss and the active power generation, to predict the degree of uncertainty associated with their optimal values and thus compare with the spinning reserve that is available for that interval. In their conclusion, their reformulated model appears to have more realistic results when compared on the basis of system fuel cost, and system losses.

A. Schellenberg et al. [45] used a variance minimization of the active power generation at the slack bus as an objective function of a Cumulant Method based solution for Stochastic Optimal Power Flow (S-OPF). M. Dadkhah and B. Venkatesh [46] also used mean and variance to check the efficiency and accuracy of the Cumulant Method, which use for solving the Probabilistic Optimal Power Flow (P-OPF). In these two researches, the Cumulant Method was compared against the Monte Carlo simulation. The results show that the Cumulant Method possesses high degree of accuracy, significantly faster and more practical than a Monte Carlo Simulation. In generally, Cumulant Method is one of the data analysis methods, and much more detailed information is available in [47].

M. Davari et al. [48] calculated the mean and variance of the Locational Marginal Pricing (LMP) based on deterministic load flow and Optimal Power Flow (OPF) using Two Point Estimate Method (T-PEM). The proposed LMP mean and variance calculation methods are applied to the PJM 5-bus system and the results have been compared with the deterministic calculations results. Furthermore, the

LMP mean and variance calculation can be used for price forecasting and system planning.

In 2010, I. Erlich et al. [49] proposed a new optimization algorithm called the Mean-Variance Optimization (MVO). The MVO algorithm borrows ideas of selection, mutation and crossover from evolutionary computation algorithms. However, the main distinct features of the MVO algorithm is based on the strategic transformation of mutated genes of the offspring based on the mean-variance of the n-best population. The performance of MVO algorithm has been compared with the PSO and demonstrated on standard benchmark optimization functions. The results show that an MVO algorithm finds the near optimal solution and is simple to implement. A year later, in 2011, Erlich et al. [50] successfully applied MVO to solve the optimal reactive power dispatch (ORPD) of wind farms. Later on, W. Nakawiro et al. [51] used MVO method to solve the ORPD problem on the IEEE 57- and 118- bus standard test systems.

1.3. Organization of Thesis

The rest of the chapters in this thesis are organized as follows:

Chapter 2: Describes on the methodology and development process of the thesis. The overview of the power flow analysis, Optimal Power Flow Analysis, Contingency Analysis, Security Constrained Optimal Power Flow, Security

Constrained Dispatch, Monte Carlo Simulation as well as the explanations on the Statistic Numerical Algorithms are discussed.

Chapter 3: Presents the results achieved throughout the case study. Besides, the comparison studies between Monte Carlo Simulation and Statistic Numerical results, also, the comparison results between Contingency Screening by Security Constrained Dispatch and Performance Index are also carried out in this chapter.

Chapter 4: Summarizes the overall research. Recommendation on future research work is also discussed.

Chapter 2

Background, Models and Tools

2.1 Power Flow Analysis

A power flow study, also known as load-flow study, is a steady-state analysis, whose target is to determine the voltages, currents, real and reactive power flows in a system under given loading conditions. A power-flow study usually uses simplified notation such as one-line diagrams and per-unit systems. The purpose of power flow studies is to plan ahead and account for various situations [52-54]. For example, if a transmission line is taken off for maintenance, it is desired to determine if the remaining lines in the system can handle the required loads without exceeding their rated values. Furthermore, a power flow study is fundamental to the study of power systems, and is often used to be the starting point for many other types of power system analysis, such as optimal power flow analysis, contingency analysis, stability studies, and the implementation of real-time monitoring systems. The topics related to power flow analysis, are described in this section as follows: Bus classifications, Bus admittance matrix, Power balance equations, Jacobian matrix, Power flow by Newton Raphson method, and Example of power flow analysis problem.

2.1.1 Bus Classifications

In load flow study, there are four quantities of interest associated with each bus: real power (P), reactive power (Q), voltage magnitude ($|V|$), and voltage angle (δ). At every bus of the system, two out of four quantities will be specified and remaining two are required to be obtained through the solution of the analysis [52-54]. Therefore, each system bus is classified according to the two quantities specified at the bus. The buses are classified as described in the following three categories:

1. Load bus (PQ bus); a bus at which the real and reactive power quantities are specified. Real and reactive powers supplied to a power system are defined to be positive, while the powers consumed from the system are defined to be negative. All busses having no generators are load busses. It is desired to find out the voltage magnitude and phase angle of the load bus through the load flow solution.

2. Generator bus (PV bus); a bus where only generator is connected. At this bus, the injected active power input and magnitude of the bus voltage are kept constant. It is required to find out the reactive power generation and the phase angle of the bus voltage.

3. Slack bus; is also known as swing bus or reference bus. In general, only one bus is taken as a slack bus for the entire system. All of the values computed in the power flow analysis are with respect or relative with the slack bus. Its voltage assumes to be fixed in both magnitude and phase angle, and can be set to any

arbitrary value, usually at 1.0 per unit value of voltage and at an angle of 0 degree.

Generally, slack bus is chosen so that it has the largest generator connected to it.

2.1.2 Bus admittance matrix

The first step in solving the power flow analysis is to create the bus admittance matrix, also known as Y_{bus} matrix. This matrix represents the nodal admittance of the buses in power system. The equations used to construct the Y_{bus} matrix come from the application of Kirchhoff's current law, in which the sum of currents entering a node is zero. These principles are applied to all the nodes in the system and thereby determine the elements of the admittance matrix [52-54]. The example of formulating Y_{bus} matrix of 3-bus system shows below:

From the Ohm's law:

$$I = Z^{-1}V$$

$$I = YV$$

This relation can be written in terms of the bus voltages V_1 to V_3 and injected currents I_1 to I_3 as follows

$$\begin{bmatrix} I_1 \\ I_2 \\ I_3 \end{bmatrix} = Y_{bus} \begin{bmatrix} V_1 \\ V_2 \\ V_3 \end{bmatrix}$$

Consider buses 1, 2, and 3 are all connected to each other. Then applying KCL at this node

$$\begin{aligned} I_1 &= Y_{11}V_1 + Y_{12}(V_1 - V_2) + Y_{13}(V_1 - V_3) \\ &= (Y_{11} + Y_{12} + Y_{13})V_1 - Y_{12}V_2 - Y_{13}V_3 \end{aligned}$$

Similar for bus 2 and 3

$$\begin{aligned}
I_2 &= Y_{22}V_2 + Y_{12}(V_2 - V_1) + Y_{23}(V_2 - V_3) \\
&= -Y_{12}V_1 + (Y_{22} + Y_{12} + Y_{23})V_2 - Y_{23}V_3 \\
I_3 &= Y_{33}V_3 + Y_{13}(V_3 - V_1) + Y_{23}(V_3 - V_2) \\
&= -Y_{13}V_1 - Y_{23}V_2 + (Y_{33} + Y_{13} + Y_{23})V_3
\end{aligned}$$

Combining KCL equation of bus 1 to 3

$$\begin{bmatrix} I_1 \\ I_2 \\ I_3 \end{bmatrix} = \begin{bmatrix} Y_{11} + Y_{12} + Y_{13} & -Y_{12} & -Y_{13} \\ -Y_{12} & Y_{22} + Y_{12} + Y_{23} & -Y_{23} \\ -Y_{13} & -Y_{23} & Y_{33} + Y_{13} + Y_{23} \end{bmatrix} \begin{bmatrix} V_1 \\ V_2 \\ V_3 \end{bmatrix}$$

From the example, bus admittance matrix formulation can form as below:

$$\therefore Y_{bus} = \begin{bmatrix} Y_{11} & Y_{12} & \dots & Y_{1n} \\ Y_{21} & Y_{22} & \dots & Y_{2n} \\ \vdots & \vdots & \ddots & \vdots \\ Y_{n1} & Y_{n2} & \dots & Y_{nn} \end{bmatrix}$$

Therefore, the bus admittance matrix can be constructed from the line and transformer input data. The diagonal terms, Y_{kk} , are the self-admittance terms, equal to the sum of the admittances of all devices connect to bus k. The off-diagonal terms, Y_{kn} , are equal to the negative of the sum of the admittances connected between buses k and n.

2.1.3 Power balance equations

When analyzing a power system, neither the complex bus voltages nor the complex current injections are known. Therefore, the Y_{bus} equations cannot use directly to solve the solution of power flow analysis. Additionally, the power flow analysis of the power system consists of nonlinear equations. The possible

equations to use are power balance equations, which can be written for real and reactive power for each bus [52-54].

Let the voltage at the i^{th} bus be denoted by

$$V_i = |V_i| \angle \delta_i = |V_i| (\cos \delta_i + j \sin \delta_i)$$

Also let us define the self admittance at bus i as

$$Y_{ii} = |Y_{ii}| \angle \theta_{ii} = |Y_{ii}| (\cos \theta_{ii} + j \sin \theta_{ii}) = G_{ii} + jB_{ii}$$

Similarly the mutual admittance between the buses i and j can be written as

$$Y_{ij} = |Y_{ij}| \angle \theta_{ij} = |Y_{ij}| (\cos \theta_{ij} + j \sin \theta_{ij}) = G_{ij} + jB_{ij}$$

Let the power system contains a total number of n buses. The current injected at bus i is given as

$$\begin{aligned} I_i &= Y_{i1}V_1 + Y_{i2}V_2 + \dots + Y_{ik}V_k \\ &= \sum_{k=1}^n Y_{ik}V_k \end{aligned}$$

It is to be noted that we shall assume the current entering a bus to be positive and that leaving the bus to be negative. As a consequence the power and reactive power entering a bus will also be assumed to be positive. The complex power at bus i is then given by

$$\begin{aligned} P_i - jQ_i &= V_i^* I_i = V_i^* \sum_{k=1}^n Y_{ik}V_k \\ &= |V_i| (\cos \delta_i - j \sin \delta_i) \sum_{k=1}^n |Y_{ik}V_k| (\cos \theta_{ik} + j \sin \theta_{ik}) (\cos \delta_k + j \sin \delta_k) \end{aligned}$$

$$= \sum_{k=1}^n |Y_{ik} V_i V_k| (\cos\delta_i - j\sin\delta_i)(\cos\theta_{ik} + j\sin\theta_{ik})(\cos\delta_k + j\sin\delta_k)$$

Note that

$$\begin{aligned} & (\cos\delta_i - j\sin\delta_i)(\cos\theta_{ik} + j\sin\theta_{ik})(\cos\delta_k + j\sin\delta_k) \\ &= (\cos\delta_i - j\sin\delta_i)[\cos(\theta_{ik} + \delta_k) + j\sin(\theta_{ik} + \delta_k)] \\ &= \cos(\theta_{ik} + \delta_k - \delta_i) + j\sin(\theta_{ik} + \delta_k - \delta_i) \end{aligned}$$

Therefore the real and reactive power equation can obtain by substituting all the equations above:

$$\begin{aligned} P_i &= \sum_{k=1}^n |Y_{ik} V_i V_k| \cos(\theta_{ik} + \delta_k - \delta_i) \\ Q_i &= - \sum_{k=1}^n |Y_{ik} V_i V_k| \sin(\theta_{ik} + \delta_k - \delta_i) \end{aligned}$$

2.1.4 Jacobian matrix

Since the Power-flow solutions by Newton-Raphson are based on the nonlinear equations, Jacobian matrix is used [52-54]. From calculating the real and reactive power mismatch by using Y_{bus} and power balance equations, the result of voltage magnitude ($|V|$) and voltage angle (δ) mismatch can be expressed as:

$$\begin{bmatrix} \Delta P_2 \\ \vdots \\ \Delta P_N \\ \Delta Q_2 \\ \vdots \\ \Delta Q_N \end{bmatrix} = J \begin{bmatrix} \Delta\delta_2 \\ \vdots \\ \Delta\delta_N \\ \Delta|V_2| \\ \vdots \\ \Delta|V_N| \end{bmatrix}$$

Note that the swing bus variables δ_1 and V_1 are omitted since they are already known.

The Jacobian matrix (J) in power flow analysis can be partitioned into four blocks, and the size of this matrix depend on the size of the power system:

$$J = \begin{array}{c} \begin{array}{cc} J1 & J2 \end{array} \\ \left[\begin{array}{cc|cc} \frac{\partial P_2}{\partial \delta_2} & \dots & \frac{\partial P_2}{\partial \delta_N} & \frac{\partial P_2}{\partial V_2} & \dots & \frac{\partial P_2}{\partial V_N} \\ \vdots & \ddots & \vdots & \vdots & \ddots & \vdots \\ \frac{\partial P_N}{\partial \delta_2} & \dots & \frac{\partial P_N}{\partial \delta_N} & \frac{\partial P_N}{\partial V_2} & \dots & \frac{\partial P_N}{\partial V_N} \\ \hline \frac{\partial Q_2}{\partial \delta_2} & \dots & \frac{\partial Q_2}{\partial \delta_N} & \frac{\partial Q_2}{\partial V_2} & \dots & \frac{\partial Q_2}{\partial V_N} \\ \vdots & \ddots & \vdots & \vdots & \ddots & \vdots \\ \frac{\partial Q_N}{\partial \delta_2} & \dots & \frac{\partial Q_N}{\partial \delta_N} & \frac{\partial Q_N}{\partial V_2} & \dots & \frac{\partial Q_N}{\partial V_N} \\ \hline & & J3 & & & J2 \end{array} \right] \end{array}$$

Elements of the Jacobian matrix are shown below:

For $n \neq k$

$$J1_{kn} = \frac{\partial P_k}{\partial \delta_n} = V_k Y_{kn} V_n \sin (\delta_k - \delta_n - \theta_{kn})$$

$$J2_{kn} = \frac{\partial P_k}{\partial V_n} = V_k Y_{kn} \cos (\delta_k - \delta_n - \theta_{kn})$$

$$J3_{kn} = \frac{\partial Q_k}{\partial \delta_n} = -V_k Y_{kn} V_n \cos (\delta_k - \delta_n - \theta_{kn})$$

$$J4_{kn} = \frac{\partial Q_k}{\partial V_n} = V_k Y_{kn} \sin (\delta_k - \delta_n - \theta_{kn})$$

For $n = k$

$$J1_{kk} = \frac{\partial P_k}{\partial \delta_k} = -V_k \sum_{\substack{n=1 \\ n \neq k}}^N Y_{kn} V_n \sin (\delta_k - \delta_n - \theta_{kn})$$

$$J2_{kk} = \frac{\partial P_k}{\partial V_k} = V_k Y_{kk} \cos \theta_{kk} + \sum_{n=1}^N Y_{kn} V_n \cos (\delta_k - \delta_n - \theta_{kn})$$

$$J3_{kk} = \frac{\partial Q_k}{\partial \delta_k} = V_k \sum_{\substack{n=1 \\ n \neq k}}^N Y_{kn} V_n \cos (\delta_k - \delta_n - \theta_{kn})$$

$$J4_{kk} = \frac{\partial Q_k}{\partial V_k} = -V_k Y_{kk} \sin \theta_{kk} + \sum_{n=1}^N Y_{kn} V_n \sin (\delta_k - \delta_n - \theta_{kn})$$

2.1.5 Power flow by Newton-Raphson method

For power systems with a large number of buses, the load flow problem becomes computationally intensive. Therefore, for large power systems, the load flow is solved using specific software based on iterative techniques, such as the Newton-Raphson method. In this thesis, Matpower, PowerWorld and Digsilent-PowerFactory software are used to solve the power flow analysis problem [54-55]. An example of power flow analysis with step-by-step process on a 3-bus system using Newton-Raphson method and the result are given in Appendix A1.

The results in Appendix A1 are compared with the results from Matpower and PowerWorld simulation software. Results from three different calculations are reasonably close to each other, with only second decimal place difference, which

possibly results from the rounding errors. The results of 3-bus power flow analysis calculation run on Matpower and PowerWorld software show below:

```

Newton's method power flow converged in 3 iterations.

Converged in 0.01 seconds
=====
|   System Summary   |
=====
How many?           How much?           P (MW)           Q (MVar)
-----
Buses               3   Total Gen Capacity  718.0           -200.0 to 200.0
Generators          2   On-line Capacity   718.0           -200.0 to 200.0
Committed Gens     2   Generation (actual) 418.4           287.0
Loads              1   Load              400.0           250.0
  Fixed            1   Fixed              400.0           250.0
  Dispatchable    0   Dispatchable       -0.0 of -0.0    -0.0
Shunts             0   Shunt (inj)        -0.0            0.0
Branches           3   Losses (I^2 * Z)   18.42           37.03
Transformers       0   Branch Charging (inj) -              0.0
Inter-ties         0   Total Inter-tie Flow 0.0            0.0
Areas              1

                        Minimum                Maximum
-----
Voltage Magnitude    0.972 p.u. @ bus 2          1.050 p.u. @ bus 1
Voltage Angle        -2.70 deg @ bus 2          0.00 deg @ bus 1
P Losses (I^2*R)     -                          9.85 MW @ line 2-3
Q Losses (I^2*X)     -                          19.69 MVar @ line 2-3
=====
|   Bus Data         |
=====
Bus #   Voltage           Generation           Load
      Mag(pu) Ang(deg)   P (MW)  Q (MVar)  P (MW)  Q (MVar)
-----
1   1.050   0.000*  218.42  140.85   -       -
2   0.972  -2.696   -       -       400.00  250.00
3   1.040  -0.499  200.00  146.18   -       -
      Total:  418.42  287.03  400.00  250.00
=====
|   Branch Data      |
=====
Brnch #  From Bus  To Bus  From Bus Injection  To Bus Injection  Loss (I^2 * Z)
      P (MW)  Q (MVar)  P (MW)  Q (MVar)  P (MW)  Q (MVar)
-----
1   1   2   179.36  118.73  -170.97  -101.95  8.393  16.79
2   1   3   39.06   22.12   -38.88   -21.57   0.183  0.55
3   2   3  -229.03 -148.05  238.88   167.75   9.847  19.69
      Total:  18.423  37.03

```

Figure 1: Results of 3-bus system power flow analysis on MatPower

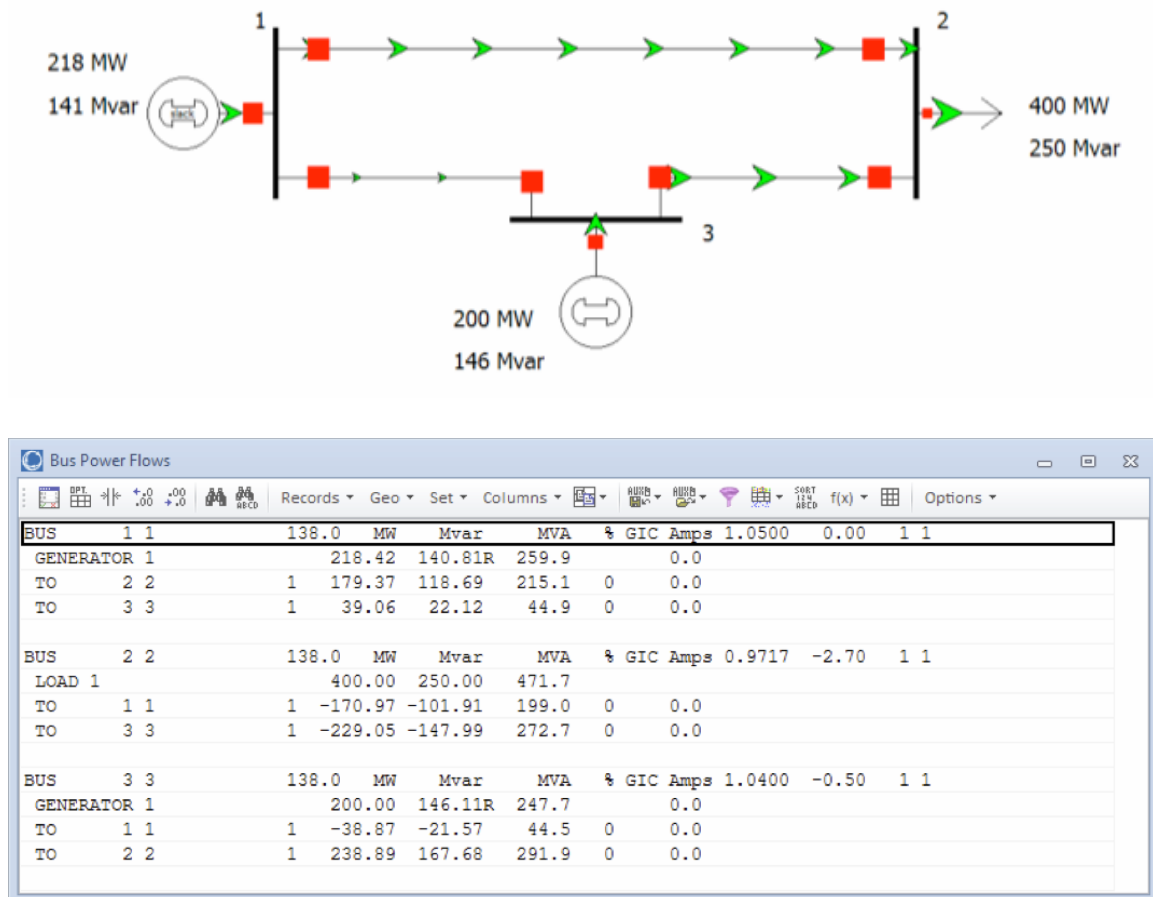


Figure 2: Results of 3-bus system power flow analysis on PowerWorld

2.2 Optimal Power Flow Analysis

Optimal power flow (OPF) is an optimization tool for power system operation analysis, scheduling and energy management. Essentially, OPF attempts to allocate available generation to meet the current load while keeping all components within their limits to satisfy the equality constraints (the load flow equations), inequality constraints (i.e. generator reactive power limits), and

objective function [1-7, 54]. In this section, the topics described are as follows: objective functions of OPF, OPF constraints, and Interior-point algorithm (the technique for solving OPF that is used in this thesis).

2.2.1 Objective function

The objective functions of OPF problem can be varied. The most common OPF objective function is minimization of total system operating cost (fuel costs). Besides that, the more common objectives include minimization of system losses, voltage deviation, voltage stability and load shedding schedule under emergency conditions. In this thesis, the objective functions of OPF analysis are minimization of fuel cost and minimization of load shedding [1-7, 54].

Minimization of fuel cost

The goal of OPF under this objective function is to supply the system under optimal operating costs. More specifically, the aim is to minimize the total operating cost of power dispatch based on non-linear operating cost functions for each generator [8, 11-18].

The most significant elements that are used to define the cost of electrical energy generation is the operating costs which dominated mostly by the fuel costs compared with the maintenance costs, emission costs, facility construction, ownership cost, etc. The fuel costs may be obtained from design calculations or from heat rate tests. The generator operating costs are typically represented by cost

curve, which can be in the form of third-order polynomial functions, quadratic functions and piecewise linear functions [54]. Thermal power plants usually use a quadratic fuel cost function described in equation below:

$$C_i(P_{Gi}) = a + bP_{Gi} + cP_{Gi}^2$$

Where:

i : Generator i

C_i : Operating cost of unit in \$/h

P_{Gi} : Electrical power output of generator i

a, b and c : Fuel cost coefficients of generator i

An example of fuel cost function plotted as a cost curve is shown in Figure 3. Normally, y-axis represents a cost in \$/h unit, and x-axis is the generator output power [2]. Generator cost curves is usually not smooth, however the curves can be adequately approximated using piece-wise smooth, functions as shown in Figure 4 (Blue line).

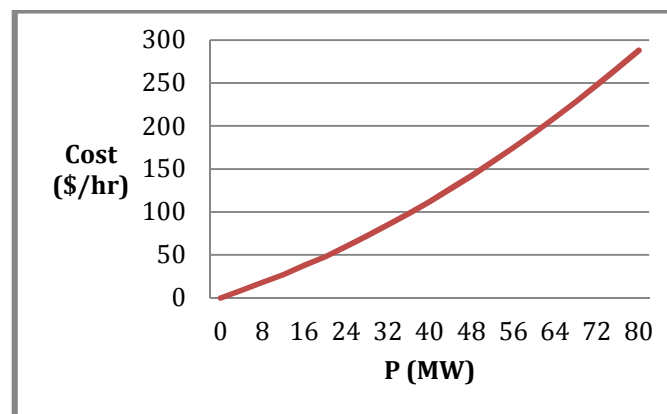


Figure 3: Fuel cost curve example

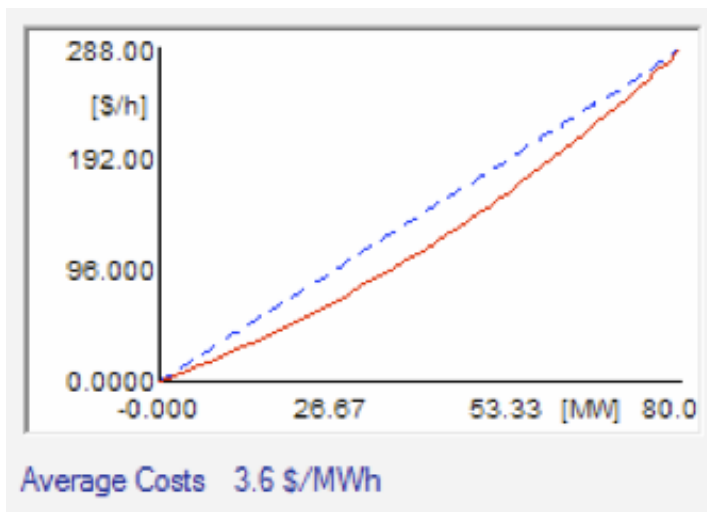


Figure 4: Fuel cost curve approximated using piece-wise smooth (blue line)

Minimization of load shedding

The goal of OPF under this objective function is to minimize the overall cost of load shedding, such that all constraints can be satisfied [32-37]. A typical application for this objective function is a case in which there are no feasible solutions. This is evidenced by a lack of converge of the optimization. In such cases, it is highly likely that not all loads can be supplied due to constraint restrictions. Hence it is recommended in these situations to firstly perform a Minimization of Load Shedding.

The cost of load shedding, also called interruption cost, is usually estimated from the impacts of interruptions in service to electric utility customers by conducting customer surveys [54, 56-57]. Such surveys are normally undertaken for each user group, e.g., commercial, industrial, and residential. The results of these surveys are used to calculate one of the load point reliability indices called the

Interrupted Energy Assessment Rate (IEAR). IEAR at a load point shows how vulnerable the load point is in terms of cost, which is expressed in dollars per kW/h of unserved energy. The higher the IEAR the higher priority this load point may have because a load curtailment at that load point will contribute to higher economic cost. Also, a priority order based on the IEAR was used for load curtailment ranking [57].

2.2.2 Constraints

In this thesis, four constraints of Optimal Power Flow Analysis are used as follows [54]:

1. Active Power Limits of Generators

$$P_{Gi}^{\min} \leq P_{Gi} \leq P_{Gi}^{\max}$$

2. Reactive Power Limits of Generators

$$Q_{Gi}^{\min} \leq Q_{Gi} \leq Q_{Gi}^{\max}$$

3. Branch Flow Limits (max. loading): the maximum current magnitude values for transmission lines and transformers are given due to limitation of the current carrying capability of conductors. As current increase, lines sag and equipment may be damaged by overheating.

$$S_i^{\min} \leq S_i \leq S_i^{\max}$$

$$(I_i^{real})^2 + (I_i^{img})^2 \leq (I_i^{max})^2$$

4. Voltage Limits of Busbars/Terminals: Too high or too low voltages could cause problems with respect to end-user power apparatus damage or instability in the power system. This could lead to unwanted and economically expensive partial unavailability of power for end-users.

$$V_i^{\min} \leq V_i \leq V_i^{\max}$$

2.2.3 Interior-point algorithm

In this thesis, the OPF performs a non-linear optimization based on an iterative interior-point algorithm, which is the AC optimization function in DigSilent-Powerfactory software [54]. The goal of the optimization is to minimize an objective function $f(\vec{x})$ subject to the equality and inequality constraints, which are imposed by the load flow equations and various power system elements respectively. This is summarized mathematically as follows:

$$\min f(\vec{x})$$

Subject to:

$$g(\vec{x}) = 0$$

$$h(\vec{x}) \leq 0$$

Where $g(\vec{x})$ represents the load flow equations and $h(\vec{x})$ is the set of inequality constraints. Introducing a slack variable for each inequality constraint, this can be reformulated as:

$$g(\vec{x}) = 0$$

$$h(\vec{x}) + \vec{s} = 0$$

$$\vec{s} \geq 0$$

Then incorporate logarithmic penalties and minimize the function:

$$\min \left[f(\vec{x}) - \mu \cdot \sum_i \log(s_i) \right]$$

Where μ is the penalty-weighting factor. In order to change the contribution of the penalty function:

$$f_{pen} = \sum_i \log(s_i)$$

To the overall minimization, the penalty weighting factor μ will be decreased from a user-defined initial value (μ_{max}) to a user-defined target value (μ_{min}). The smaller the minimum penalty-weighting factor, the lower the applied penalty will be for a solution, which is close to the constraint limits. This may result in a solution that is close to the limiting constraint [2, 54]. The Outlined to solve the OPF based on an interior-point method step as follow:

Step 1: Initialize primal and dual variables of the problem, paying attention as the non-negativity conditions, have to be satisfied. Choose the value of safety, centering and barrier parameters.

Step 2: Compute Newton direction by solving the system of equations.

Step 3: Determine the step size length and update the variables.

Step 4: Compute the barrier parameter.

Step 5: If convergence criteria are met, then optimal solution is found; otherwise go back to Step 2

The flow chart of OPF based on interior-point method show in Figure 5. Also, more details for each steps is in F. Capitanescu et al. “An interior-point method based optimal power flow” [67]

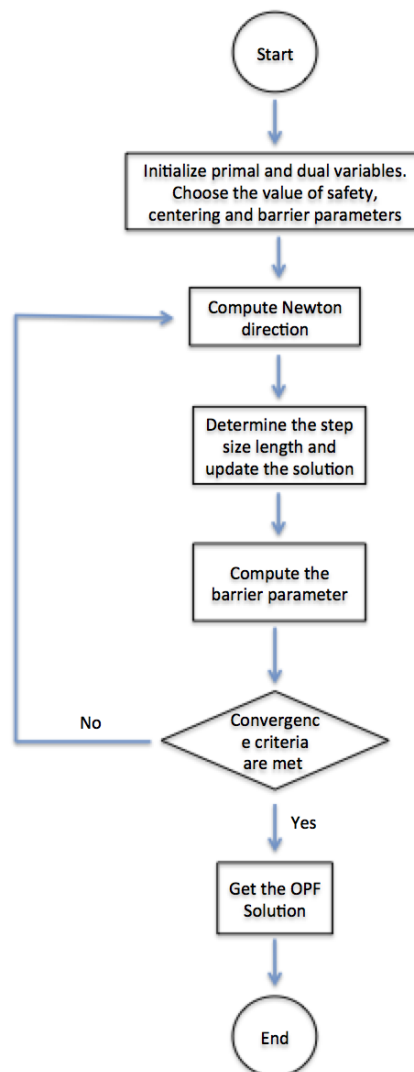


Figure 5: the OPF based on interior-point method flow chart

2.3 Contingency analysis

Contingency analysis in power system means a study of unpredictable conditions, outage of elements such as transmission lines, transformers and generators, and investigation of the resulting effects on line power flows and bus voltages of the remaining system [2]. Many problems, which occur in the power system, can have serious consequences within a short time that the operator could not take appropriate actions fast enough. Also the operator usually needs to know if the present operation of the system is secure and what will happen if a particular outage occurs. Both Contingency analysis method and contingency screening are described in this section.

2.3.1 Contingency Analysis Method

An overview of suggested analysis method is shown in Figure 5. This process can be used for studying both single and multiple contingency events. The step-by-step algorithm for contingency analysis are given as follows:

Step 1: Start with the base case of the system. The base case is the system operating in its normal steady state with all elements in service.

Step 2: Simulate the first contingency event by taking out one component from the system; the component can be transmission line, transformer or generator. Perform the power flow analysis to check the system violations.

Step 3: Alarm the operators to any potential overloads or out-of-limit voltages for all the components in the system.

Step 4: Change the component outage and do step 3 again until considering all the components in the system.

For double contingencies (n-2), the analysis process is the same except choosing two components each time. Similarly, the secondary contingency (n-1-1) is one component outage occur after another one. Therefore, the flow chart will have additional steps after performing the analysis of first contingency (primary contingency).

From the flow chart, in order to study outage events, the operator has to perform the contingency analysis with the AC power flow to determine the overloads and voltage limits violations. This process becomes very bored and time consuming when the power system network is large. In order to resolve this issue, the contingency screening is used.

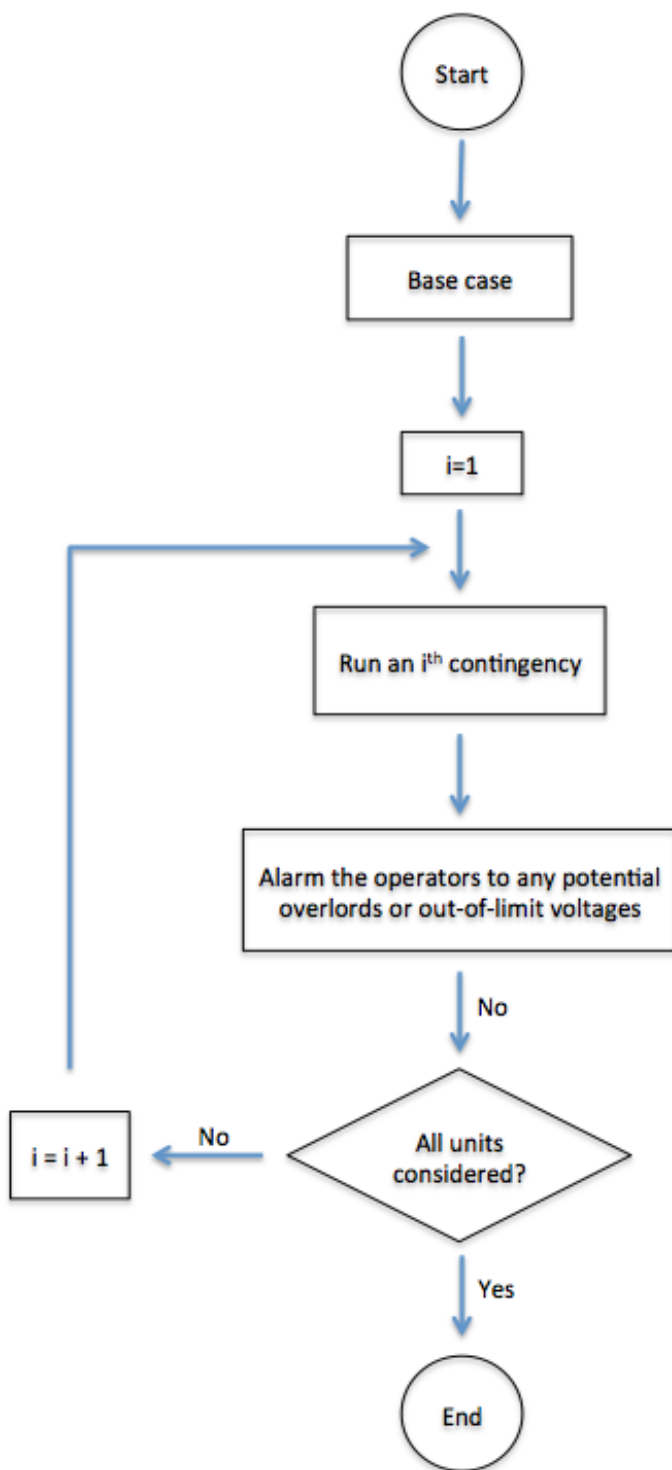


Figure 6: The contingency analysis method flow chart

2.3.2 Contingency Screening

Contingency screening, also called contingency selection, is used to identify the contingency that actually leads to the violation of the operational limits and rank all the components in the system by a priority order. In general, contingency events are ranked by comparing the power flow violation of the system after load flow analysis using severity indices known as Performance Index (PI) [2, 19-23].

There are two types of performance indices; the first one called Active Power Performance Index (PIP), which reflects the violation of line active power flow. Another one called Reactive Power Performance Index (PIV), which reflects the violation of bus over voltage [2]. These two indexes also can be combined into one equation for better performance as shows below:

$$PIP = \sum_{i=1}^N \left(\frac{P_i}{P_{imax}} \right)^{2n}$$

$$PIV = \sum_{j=1}^M \left(\frac{\Delta|E_j|}{\Delta|E_{max}|} \right)^{2m}$$

Then

$$PI = PIP + PIV$$

$$\therefore PI_k = \sum_{i=1}^N \left(\frac{P_i}{P_{imax}} \right)^n + \sum_{j=1}^M \left(\frac{\Delta|E_j|}{\Delta|E_{max}|} \right)^m$$

Where:

PI_k : performance index of contingency k

P_i : the active power flow in line i

P_{imax} : the maximum active power can flow in line i

N : the total number of transmission lines that overlimit in the system

$\Delta|E_j|$: the voltage magnitude difference between before and after contingency at bus j

$\Delta|E_{max}|$: the difference between maximum and minimum voltage limit at bus j

M : the total number of busbars that overlimit in the system

n, m : the specified exponent

Basically n and m are the weighting factor for designing which index has more significant in the system between the line power flow and violation of bus voltage. If n and m are large number, the PI will be a small number if both indexes are within limit, and it will be large if one or more lines and buses are overloaded.

From the above equation, the contingencies are ranked in a manner where the PI list is sorted so that the largest PI, most severe, appears at the top of the list and the non-severe contingencies at the bottom. Then, the contingency analysis can start by executing full power flows with the case that is at the top of the list, and then the second case, and so on down the list. This continues until either a fixed number of cases are solved (due to computation time), or until a predetermined number of cases are solved which do not have any violations.

2.4 Security Constraint Optimal Power Flow

Contingencies, in power system terminology, are unpredictable disturbances to the transmission or generation facilities. It has been recognized that with the

solution of basic OPF formulation, it may not be possible to keep the system in a normal state after a contingency occurs, or even when it is possible, the cost of such a solution may be very high. Programs, which can make control adjustments to the base or pre-contingency operation to prevent violations in the post-contingency conditions, are called “security-constrained optimal power flows” or SCOPF [2, 24-31]. The mathematical formulation of the general SCOPF is as follows:

$$\min f(x, u)$$

Subject to:

$$g(x, u) = 0$$

$$h(x, u) \leq 0$$

$$g_w(x_w, u_w) = 0 \quad w = 1, \dots, K$$

$$h_w(x_w, u_w) \leq 0 \quad w = 1, \dots, K$$

Where:

x, u : Pre – contingency state and controls

x_w, u_w : Post – contingency state and controls

$g(x, u)$: Power balance equations for base case

$h(x, u)$: Set of inequality constraints for base case

$g_w(x_w, u_w)$: Power balance equations for each contingency case

$h_w(x_w, u_w)$: Set of inequality constraints for each contingency case

ω : The set of possible contingencies

In general, $h_w(x_w, u_w)$ are contingency limits or security constraints that impose post-disturbance limits and may be substantially different from the base case limits. The computational times for security constrained OPF are considerably longer than for the base case OPF.

In SCOPF, a contingency analysis is integrated with an optimal power flow to make necessary changes to the optimal dispatch of generation, as well as other adjustments, so that following a security analysis, no contingencies result in violations. A.J. Wood and B. F. WollenBerg [2] show how SCOPF can be performed by dividing the power system into four operating states.

1. Optimal dispatch: the state that the power system is in prior to any contingency. It is optimal with respect to economic operation, but it may not be secure.

2. Post contingency: the state of the power system after a contingency has occurred, assuming that this condition has a security violation (line or transformer beyond its flow limit, or a bus voltage outside the limit).

3. Secure dispatch: the state of the system with no contingency outages, but with corrections to the operating parameters to account for security violations.

4. Secure post-contingency: the state of the system when the contingency is applied to the base-operating condition with corrections.

The above four states are illustrated in a power system consisting of two generators, one load, and two transmission lines. This power system assumed to be operating with both generators supplying the load as shown below:

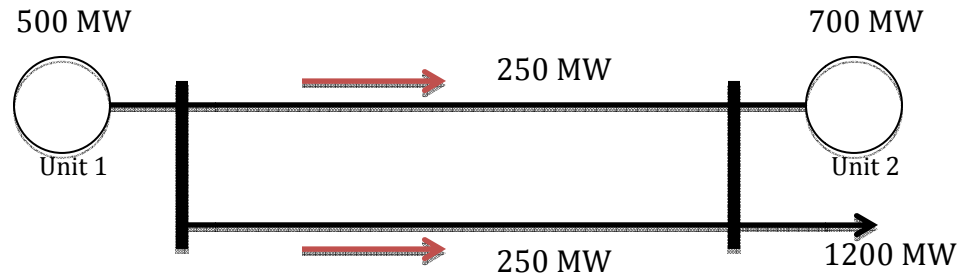


Figure 7: Optimal dispatch state

Assuming that the system as shown in Figure 6 is in economic dispatch, that is the 500 MW from unit 1 and the 700 MW from unit 2 is the optimum dispatch. Further, each transmission lines can carry a maximum of 400 MW, so that there is no loading problem in the base-operating condition.

Next, we shall postulate that one of the transmission line has been opened because of a failure. This results in Figure 7.

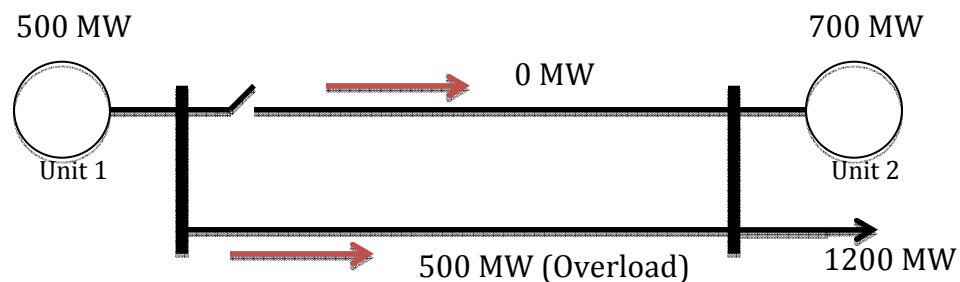


Figure 8: Post contingency State

As a result, there is an overload on the remaining circuit. Since the operators do not want this condition to arise, they will correct this situation by lowering the generation on unit 1 to 400 MW. Therefore, the secure dispatch state is

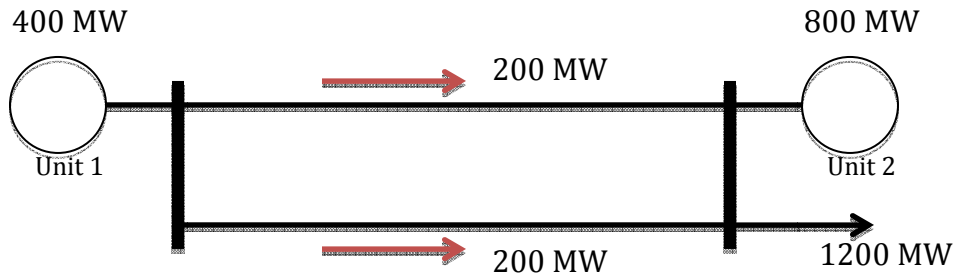


Figure 9: Secure dispatch state

Given that the same contingency analysis is performed, the post-contingency condition is

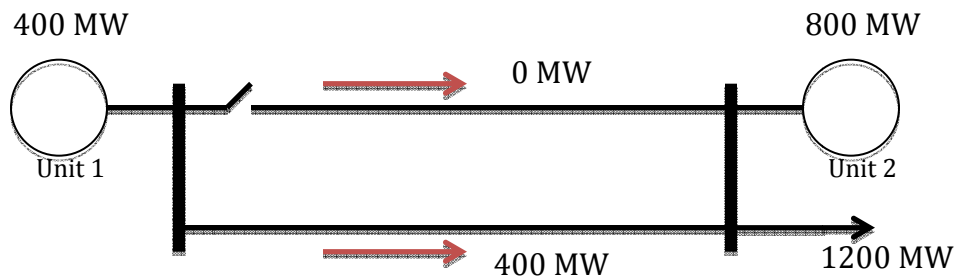


Figure 10: Secure Post Contingency State

By adjusting the generation on unit 1 and unit 2, the system prevents the post-contingency operating state from having an overloaded transmission line. This is the essence of the so called “security corrections.”

2.5 Security Constrained Dispatch

Concepts from the previous sections are extended for the formation of a new tool called Security Constraint Dispatch (SCD). SCD is an integration of contingency analysis, OPF, and SCOPF. This tool considers only three states of the power system that are optimal dispatch state, post contingency state, and secure post contingency state. Optimal dispatch is the state that the power system is operating with optimal cost prior to any contingency. Post contingency state corresponds to the state in which power system has one or more contingency event. Secure post contingency state is the state following a contingency with no violations through security corrections. The objective function of SCD is as same as OPF, which is a minimization of total operating cost in dollar per hour. In addition, instead of one solution such as SCOPF, SCD will analyze all contingency events that can occur in the power system and determine the minimum cost for each contingency event.

The result of SCD is the optimal operating cost of the system following contingency event and security corrections event. SCD solution will always have a cost greater or equal to the OPF solution of the base case due to the security corrections' cost. In particular, the cost for security correction by load shedding will be the most expensive because of the reliability cost assessment. This cost can go higher to more than 10 times the normal operating cost. In this case, if SCD has a high value, it means that the system has a poor reliability due to the high cost difference from the normal operating state cost. On the other hand, if SCD has a low value, close to the operating cost of the base case, means the system has a high

reliability because even when the contingency occur, the system still can operate within their limits.

An overview of suggested analysis method of SCD is shown in Figure 10. This flow chart is similar to the contingency analysis flow chart, but includes additional state of security corrections. The step-by-step algorithm for SCD is given as follows:

Step 1: Start with the base case of the system. The base case is the system operating in its normal steady state with all elements in service.

Step 2: Simulate the first contingency event by taking out one component from the system; the component can be transmission line, transformer or generator.

Step 3: Perform the SCD analysis that includes security corrections function. In this state, the security corrections can be the opening, closing, or re-dispatching of a generator; the changing of a phase shifting transformer angle; changing of a switched shunt set point. The SCD result will be the total operating costs of the system with that contingency event.

Step 4: If SCD cannot converge (infeasible), perform the security corrections called load shedding (load curtailment). This result will be the total operating costs of the system with that contingency event plus the penalty costs for load shedding.

Step 5: Continue with the next component outage and perform step 3 and 4 again until considering all the components in the system.

After finish the simulation, we will get the total operating costs for each contingency events. All of each result in SCD analysis will use for calculates the

expected cost penalty of security constraint dispatch (ECP_SCD), which described in next section.

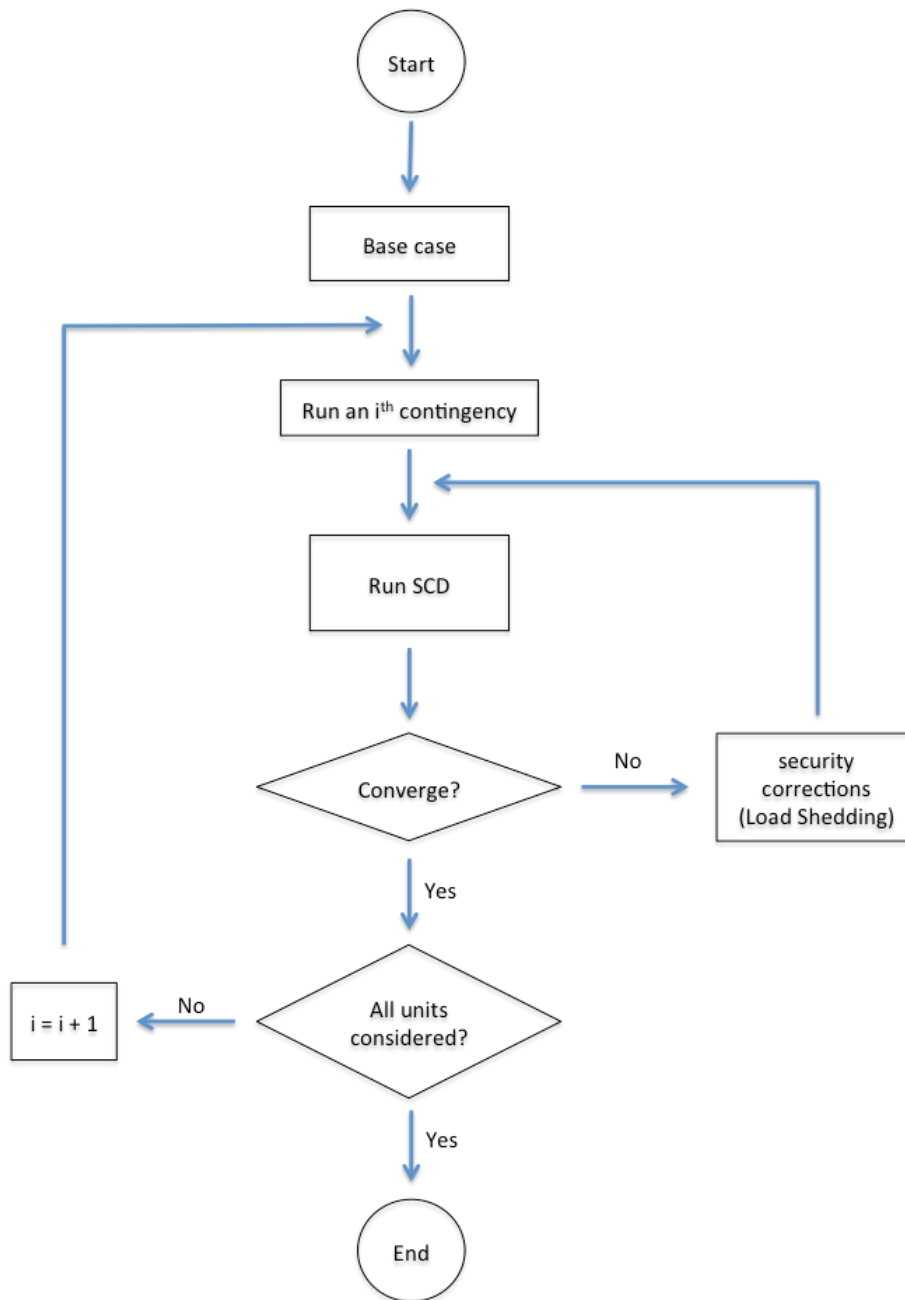


Figure 11: Security Constrained Dispatch analysis flow chart

2.6 Expected Cost Penalty

The expected cost penalty of security constraint dispatch (ECP_SCD) is a new index introduced in this thesis. This penalty is in dollar per hour, which shows the average cost that the utility has to pay extra when the contingency events occur in the system. Typically when the mean is calculated it is important to know the variance and standard deviation about that mean. In this thesis, three statistic numerical values are considered:

2.6.1 Expected Value

In mathematics, the expected value can be calculated by multiplying each of the possible outcomes with the probability that each outcome will occur, and summing all of those values [38]. Therefore, the expected value is a weighted average of all possible value. The expected value of random variable X defines as below:

$$E(X) = x_1p_1 + x_2p_2 + x_3p_3 + \dots + x_kp_k$$

Since all probabilities p_i add up to one ($p_1 + p_2 + \dots + p_k = 1$), the expected value can be viewed as the weighted average. The average value of a particular set of numbers with different levels of relevance:

$$E(X) = \frac{x_1p_1 + x_2p_2 + x_3p_3 + \dots + x_kp_k}{p_1 + p_2 + p_3 + \dots + p_k}$$

The concept of the expected value is used to calculate the ECP_SCD in this thesis. The p_i in the equation is the probability of the contingency event occurrences,

which is the same as the probability of the component failure in that event. The x_i is the cost penalty, which is the difference between the system operating cost in contingency and normal situations. For very complex power system, not all the contingency events can consider because it will become very time-consuming. Therefore, the ECP_SCD's equation with the weighted average can be expressed as follows:

$$ECP_SCD = \frac{(f_1 - f_0)p_1 + (f_2 - f_0)p_2 + \dots + (f_k - f_0)p_k}{p_0 + p_1 + p_2 + p_3 + \dots + p_k}$$

When:

$$CP_i = f_i - f_0$$

$$\therefore ECP_SCD = \frac{(CP_1)p_1 + (CP_2)p_2 + \dots + (CP_k)p_k}{p_0 + p_1 + p_2 + p_3 + \dots + p_k}$$

Where:

ECP_SCD: Expected cost penalty of the security constraint dispatch

CP_i: Cost penalty when contingency i occurred

f_i: The total operation cost when coningency i ocurred

f₀: The total operation cost in normal situation

p_i: Probability of coningency event i

p₀: Probability of the system normal situation

k: The total number of considered contingency events

2.6.2 Variance and Standard Deviation

The variance (σ^2) is a measure of how far each value in the data set is from the mean (or expected value) [38]. A small variance indicates that the data tend to be very close to the mean. On the other hand, a high variance indicates that the data are very spread out from the mean. The equation to define the variance is:

$$Var(X) = \frac{\sum_{i=1}^N (x_i - \mu)^2}{N}$$

When a weighted mean is used, the variance of the weighted sample is different from the variance of the unweighted sample. The weighted sample variance is defined similarly to the normal sample variance:

$$Var(X)_{weighted} = \frac{\sum_{i=1}^N p_i (x_i - \mu)^2}{\sum_{i=1}^N p_i}$$

Similarly to the expected cost penalty, the concept of the weighted variance is applied to find the variance of cost penalty of the system. The equation shows as below:

$$Var_{CP_SCD} = \frac{\sum_{i=1}^N p_i (CP_i - (ECP_SCD))^2}{\sum_{i=1}^N p_i}$$

Where:

Var_{CP_SCD} : Variance of of the cost penalty of the security constraint dispatch

ECP_SCD : Expected cost penalty of the security constraint dispatch

CP_i : Cost penalty when coningency i occur

p_i : Probability of coningency event i

N = the set of possible contingencies

The standard deviation of a random variable, statistical population, data set, or probability distribution is the square root of its variance which shows as equation below:

$$SD(X) = \sqrt{Var(X)} = \sqrt{\frac{\sum_{i=1}^N (x_i - \mu)^2}{N}}$$

Furthermore, the standard deviation of the weighted mean equation are used in this thesis to find a standard deviation of cost penalty is shows below:

$$SD_{CP_SCD} = \sqrt{\frac{\sum_{i=1}^N p_i (CP_i - (ECP_SCD))^2}{\sum_{i=1}^N p_i}}$$

Where

SD_{CP_SCD}: Standard deviation of the cost penalty of the security constraint dispatch

ECP_SCD: Expected cost penalty of the security constraint dispatch

CP_i: Cost penalty when coningency *i* occurs

p_i: Probability of coningency event *i*

N = the set of possible contingencies

2.6.3 Coefficient of Variation

The Standard deviation is an absolute measure of dispersion. It is expressed in terms of units in which the original figures are collected and stated.

Unfortunately, the SD of one unit cannot be compared with another SD with difference unit. For example, the SD of heights in inches of students cannot be

compared with the SD of weights of students, in pounds as both are expressed in different units. Therefore the SD must be converted into a relative measure of dispersion for the purpose of comparison. The relative measure is known as the coefficient of variation (C.V.) [38]. The coefficient of variation is defined as the ratio of the standard deviation to the mean and expressed in percentage. In this thesis, the C.V. of cost penalty of SCD express as:

$$C.V._{CP_SCD} = \frac{SD_{CP_SCD}}{ECP_SCD} \times 100$$

Where

$C.V._{CP_SCD}$: Coefficient of variation of *the cost penalty of the SCD*

SD_{CP_SCD} : *Standard deviation of the cost penalty of the SCD*

ECP_SCD : *Expected cost penalty of the SCD*

If we want to compare the variability of two or more data set with difference units, we can use C.V. The series or groups of data for which the C.V. is greater indicate that the group is more variable, less stable, less uniform and less consistent. On the other hand, if the C.V. is less, it indicates that the group is less variable or more stable, more uniform and more consistent. The big disadvantages of the C.V. happened when the mean value is close to zero; the coefficient of variation will approach infinity and is therefore sensitive to small changes in the mean. This is often the case if the values do not originate from a ratio scale.

2.7 Monte Carlo Simulation

Monte Carlo Simulation (MCS) is referred to as the stochastic simulation method, which is the fundamental of computer simulation, and usually used to simulate the reliability and probability of failure in the power system [58]. MCS can easily deal with the uncertainties. Since MCS' computation time nearly does not increase with power systems' scale and complexity, MCS is very suitable for sampling for the system with a large scale [59].

The basic idea of MCS is applying multiple random numbers complying with some probability distribution to mathematical model as the parameters and then the probability distribution of the focused variables can be obtained. Many paper have developed different kinds of Monte Carlo techniques to estimate the power system reliability [60-62]. Although, the main disadvantage of MCS is that it requires more time and larger computational effort to implement for the accurate result, it is very versatile to model random behavior of components. It may be the easiest way to evaluate adequately the impact of higher order contingencies in system reliability [63].

The MCS utilized in this thesis is applied to determine if and what component will fail for a given condition. In this case, a two-state model was used in this simulation, namely, the normal state and the contingency state. In normal state, all the system components are functional; on the other hand, the contingency state happens when one or more components are out of service [64]. The availability of each component in a single state is found by generating a random number in the

range of zero to one. If the random number is greater than the probability of failure, the component is considered operational and available. Otherwise the component is considered failed. Additionally, the probability of outage is given by the component forced outage rate (FOR). It is also assumed that component outages are independent events [65]. The equations of the system's components state can be expressed as:

$$s_i = \begin{cases} 0 \text{ (normal state)} & \text{if } x \geq FOR_i \\ 1 \text{ (contingency state)} & \text{if } 0 \leq x < FOR_i \end{cases} \quad (1)$$

Let s_i denote the state of the i^{th} component and FOR_i be its forced outage rate. Where x is the random number in the range of zero to one. The state of the system containing n components is expressed by the vector S :

$$S = (s_1, s_2, s_3, \dots, s_n)$$

When $S = 0$, the system is in the normal state. When $S \neq 0$, the system is in a contingency state due to component outage.

While Contingency Enumeration tests every state, Monte Carlo Simulation tests those states that are most probable. Each iteration (sampled time) of the simulation shows the result of one set of random events (one system state). With many sampled times, the average solution will give the most probable answer, the predicted ECP_SCD [66].

Figure 11 provides an overview of the MCS module in this thesis. Also, the ECP_SCD computation processes based on MCS is listed as follows:

Step 1: The first step is to initialize data of the study case. Then, select the master seed for the random number generator, which is used to determine a random number seed for each component on the system.

Step 2: The MCS randomly generate a possible outcome for each system' components to construct a series of system states by equation (1) and (2).

Step 3: After a system state is obtained, if $S = 0$ then it means the system is in the normal state; the cost penalty of SCD for this state is equal to zero.

Step 4: If $S \neq 0$, cost penalty of the SCD is calculated from the difference between the cost of operating in the normal state (where all system components are functional) and the cost of operating in this contingency state (The process to get the SCD is in the previous chapter).

Step 5: Repeat step 2-4 until number of iterations (N) reached.

Step 6: Then, the ECP_SCD is calculated by means of the cost penalty for all the iteration from Monte Carlo Simulation.

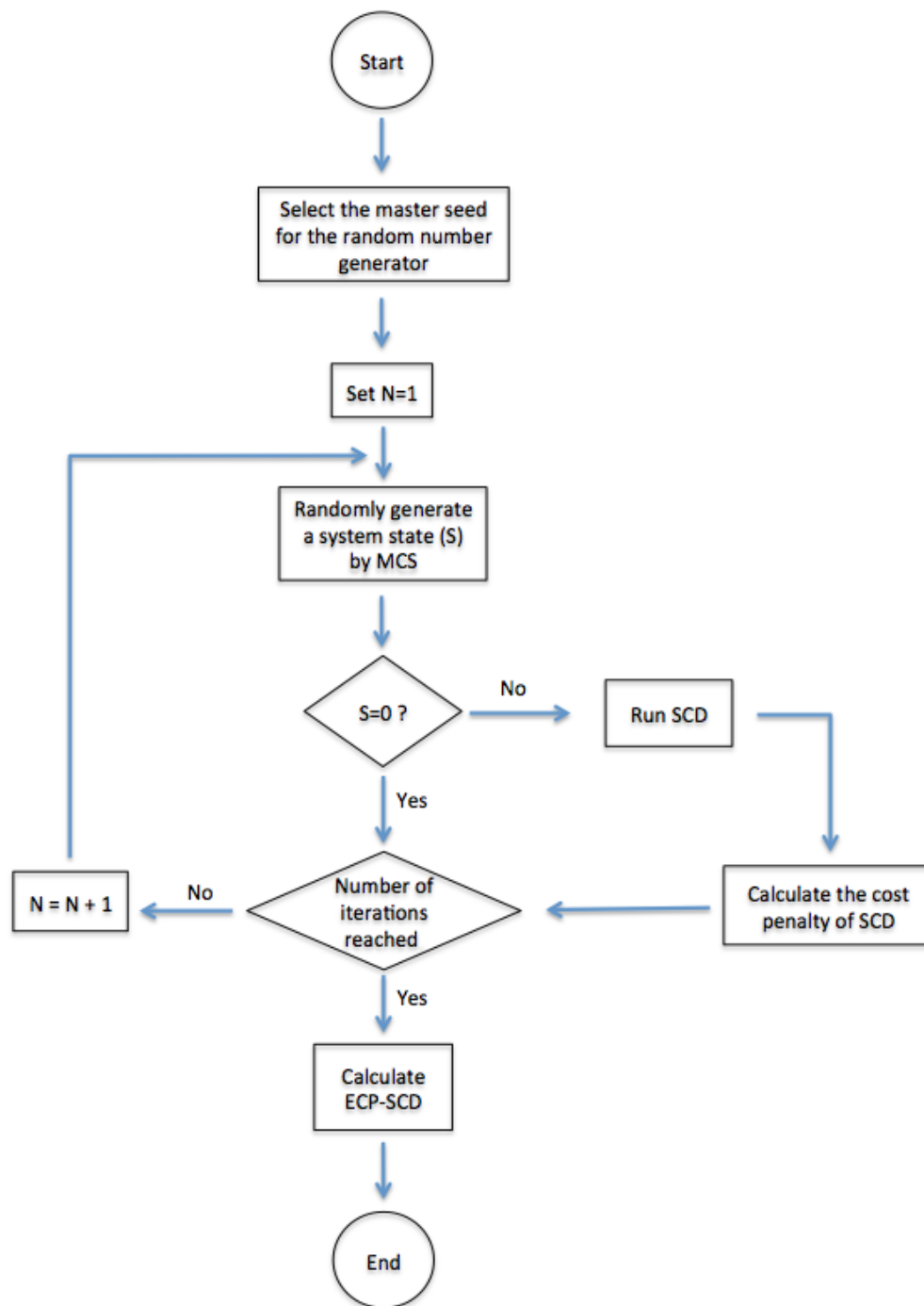


Figure 12: Overview of the Monte Carlo Simulation module for ECP_SCD

Chapter 3

Case Study & Results

Previous chapters have presented the algorithms developed for the index called Security Constrained Dispatch (SCD). The SCD model formulated in Chapter 2.5 was tested on the IEEE 30 bus test system using the DlgSILENT-PowerFactory software. In this chapter, case studies of applying above theories are presented for illustration purposes. This chapter is divided into 3 sections as follows: IEEE 30 bus test system data, SCD of the test system, and the contingency screening by SCD. Also, the result will be analyzed and the conclusion will be provided in the next chapter.

3.1 IEEE 30 Bus Test System

The IEEE 30 Bus Test Case represents a portion of the American Electric Power System (in the Midwestern US) as of December 1961. The data was kindly provided by Iraj Dabbagchi of AEP and entered in IEEE Common Data Format by Rich Christie at the University of Washington in August 1993.

The data, which used in this thesis, bases on the MATLAB M-files MatPower Example Cases [55]. This data is combined by two papers, O. Alsac & B. Stottand [2] and R.W. Ferrero et al [3]. V limits and line |S| limits taken from Alsac & Stott

Generator, Q limits were derived using their P_{\max} capacities. Also, the branch parameters was rounded up to nearest 0.01, shunt values divided by 100 and shunt on bus 10 moved to bus 5, load at bus 5 zeroed out. Generator locations, costs and limits and bus areas were taken from Ferrero.

IEEE 30 bus test system consists of six generators connected to bus 1, 2, 13, 22, 23 and 27; two switch shunts at bus 5 and bus 24, seven transformers and 34 transmission lines. The system has 20 load points totaling 189.2 MW and 107.2 Mvar. The one line diagram of the IEEE-30 bus system in DigSilent-PowerFactory software is shown in Figure 12. Bus, generator, transmission line and transformer data are given in Appendix A2.

3.2 ECP_SCD of the Test System

In this section, the result of ECP_SCD, variance, and standard deviation of the SCD are calculated and discussed. The procedure to obtain the results for each part using Digsilent-PowerFactor is described briefly.

3.2.1 Procedure and results of ECP SCD calculation

Step 1: Drawing one-line diagram of the IEEE 30 bus test system on DigSILENT-PowerFactory simulation software and put all the parameter data to all the components, which providing in Appendix A2. Then, run the power flow analysis to check the result and comparing with the result from MatPower simulation. Two results from both simulations should be the same.

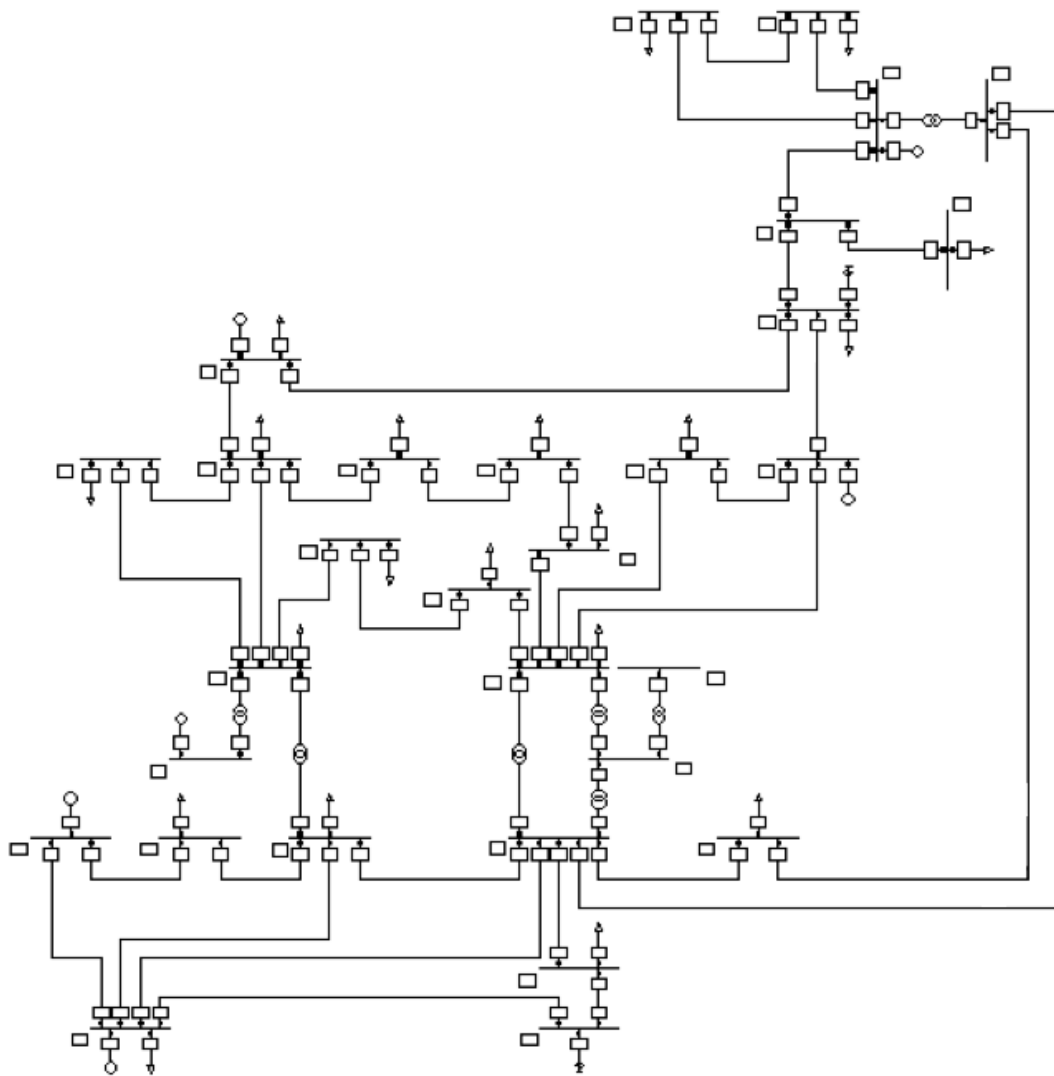


Figure 13: One-line diagram of the IEEE-30 bus system in DigSILENT-PowerFactory

Step2: Since the load shedding cost penalty doesn't contain in the MatPower IEEE 30 bus test system data, using the same amount of penalty load shedding cost and increasing each load point by 50% one at a time, we can see the effect of each load point by SCD. The SCD result for each load points in this case is shown in Figure 13.

As discussed in Chapter 2.2, the load point with the highest value of ECP_SCD supposed to have the highest cost penalty of load shedding. Figure 13 shows that the load point at bus 08 has the highest ECP_SCD cost, therefore, the load shedding cost penalty for load point at bus 08 is set at 10,000 \$/h, which is also the highest one. The rest of the load shedding cost penalty are separated in 7 groups, as shown in different colors in Figure 13, by the value of ECP_SCD. The new load shedding cost penalty for each load point is also shown in Table 2.

Step 3: After reset the load shedding penalty cost for all the load points, calculating the ECP_SCD cost for each contingency events. Since calculating ECP_SCD for all the contingency events will become very time-consuming and the probability of more than two components out of service at the same time is very low, we are considering only single and double contingency events in this thesis. The procedure to calculate ECP_SCD is in Chapter 2.6, and the flow chart is shown in Figure 10. The DPL code for calculating ECP_SCD value is shown in Appendix A3.

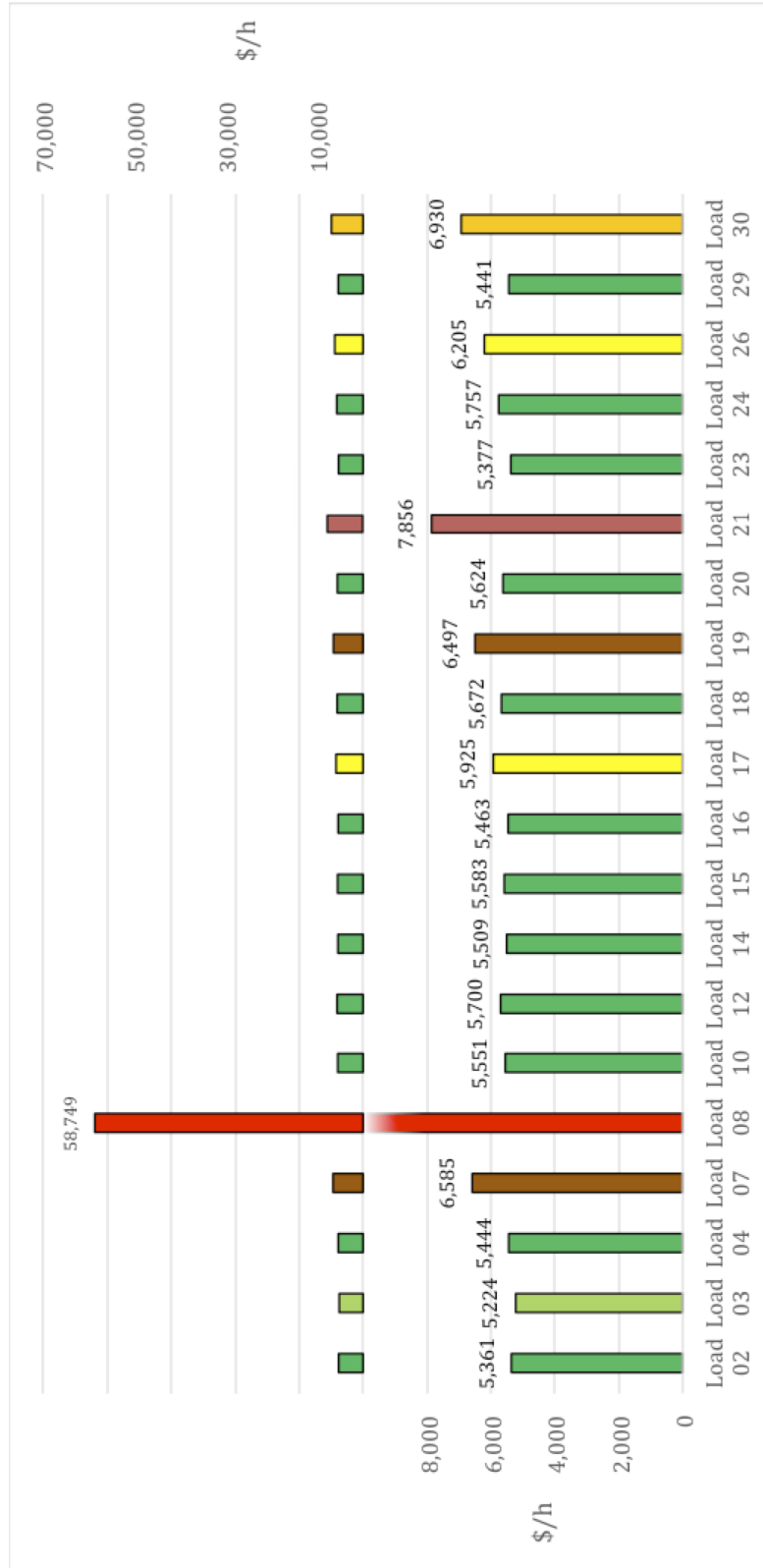






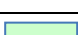


Figure 14: The ECP_SC D result with the same load shedding cost penalty for all the load points

Table 3: Cost penalty of load shedding for each load point.

Load shedding cost penalty (\$/h)	Load point at bus #	Color
10,000	08	
8,000	30	
7,000	21	
6,500	07,09	
6,000	17, 26	
5,500	02, 04, 10, 12, 14, 15, 16, 18, 20, 23, 24, 29	
5,000	03	

Step 4: Finally, the ECP_SCD, variance and standard deviation of ECP_SCD are calculated. The equations for these three numerical values are presented in chapter 2.5. To get a big picture of examining the system reliability by ECP_SCD, the system total load are corresponded by the daily load demand. The IEEE 30-bus test system daily load curve is taken from [5], and is shown in Figure 14. The total load from IEEE 30 bus test system data is set at 1, then increases and decreases by 5% from 0.9 to 1.55 scales according to the daily load curve. The results are also put in Table 3 ordering from load scaling factor 0.9 to 1.55. The red number in Table 3 is the result when LSF is 1, which is the normal load value from the data. Figure 15 is the result of ECP_SCD and daily load curve in the same graph. Figures 16, 17 and 18 show the bar chart of the ECP_SCD, variance and standard deviation of CP_SCD respectively.

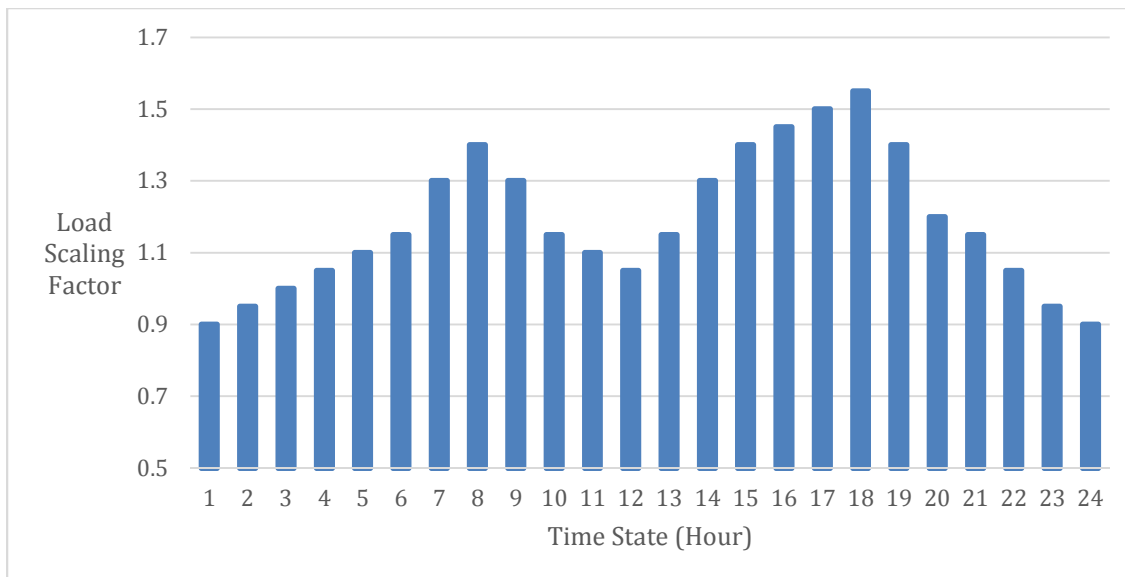


Figure 15: Daily load curve of IEEE 30 bus test system

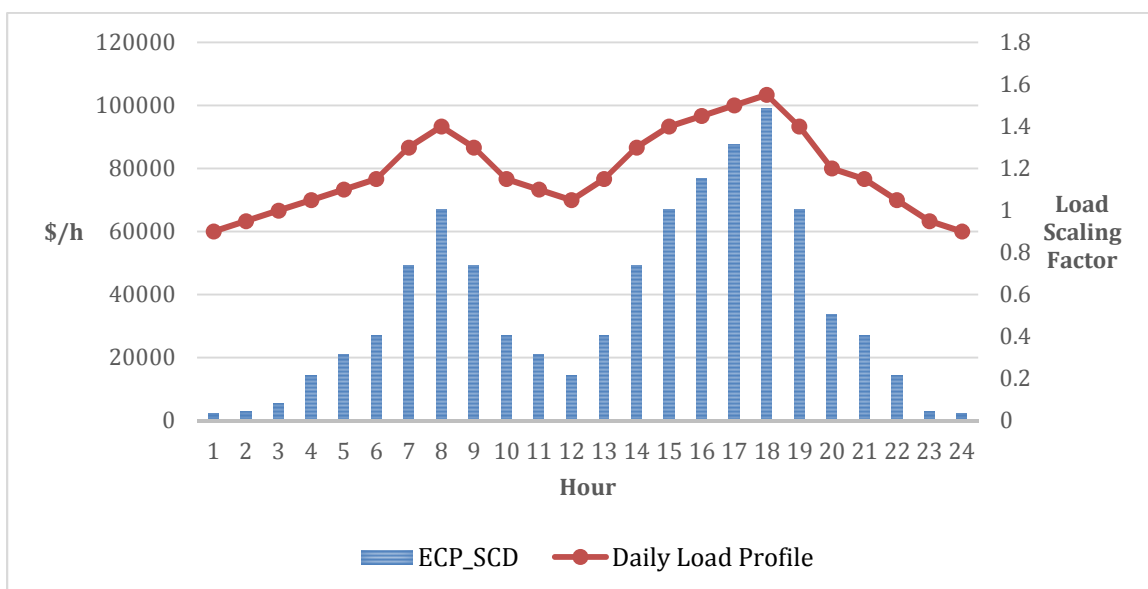


Figure 16: ECP_SCD result with the daily load curve

Table 4: Result of ECP_SCD

LSF	Active Power (MW)	Reactive Power (Mvar)	ECP_SCD	Variance	Standard Deviation	C.V.
0.9	170.28	96.48	2,232.18	127,086,156.00	11,273.25	19.80
0.95	179.74	101.84	3,017.44	211,979,755.00	14,559.52	20.72
1	189.2	107.2	5,564.56	359,564,112.00	18,962.18	29.35
1.05	198.66	112.56	14,438.22	586,362,174.00	24,214.92	59.63
1.1	208.12	117.92	20,994.91	916,960,534.00	30,281.36	69.33
1.15	217.58	123.28	27,175.36	1,390,096,935.00	37,284.00	72.89
1.2	227.04	128.64	33,847.43	2,039,374,684.00	45,159.44	74.95
1.25	236.5	134	41,297.48	2,887,368,156.00	53,734.24	76.86
1.3	245.96	139.36	49,269.87	4,044,592,403.00	63,597.11	77.47
1.35	255.42	144.72	57,856.87	5,533,060,094.00	74,384.54	77.78
1.4	264.88	150.08	66,950.20	7,389,306,460.00	85,961.08	77.88
1.45	274.34	155.44	76,795.43	9,688,323,137.00	98,429.28	78.02
1.5	283.8	160.8	87,485.56	12,489,920,836.00	111,758.31	78.28
1.55	293.26	166.16	99,091.70	15,855,893,461.00	125,920.19	78.69

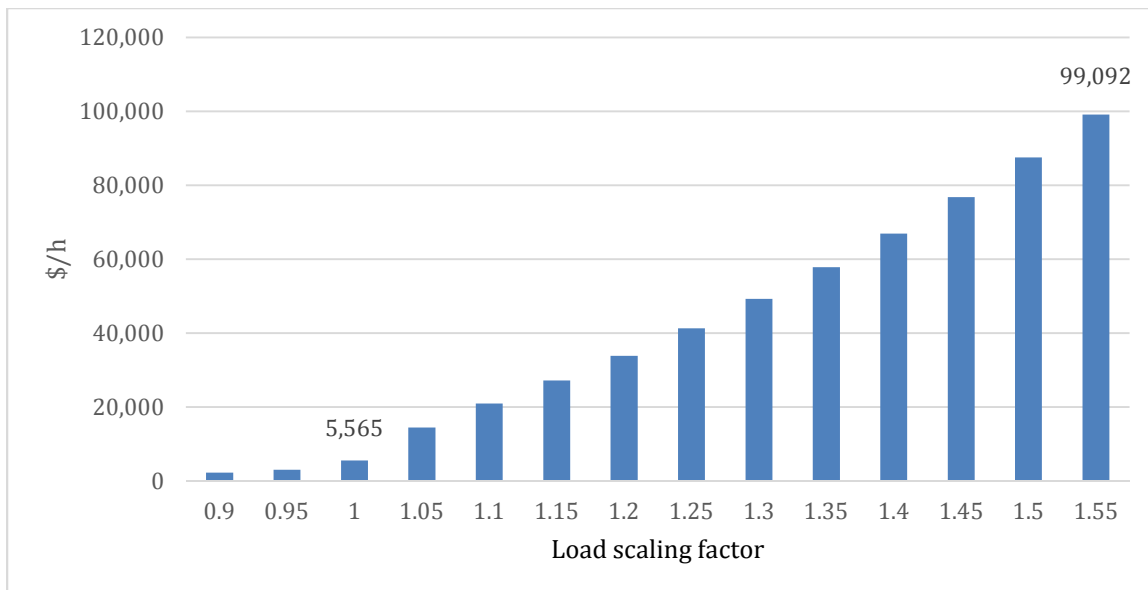


Figure 17: Result of ECP_SCD

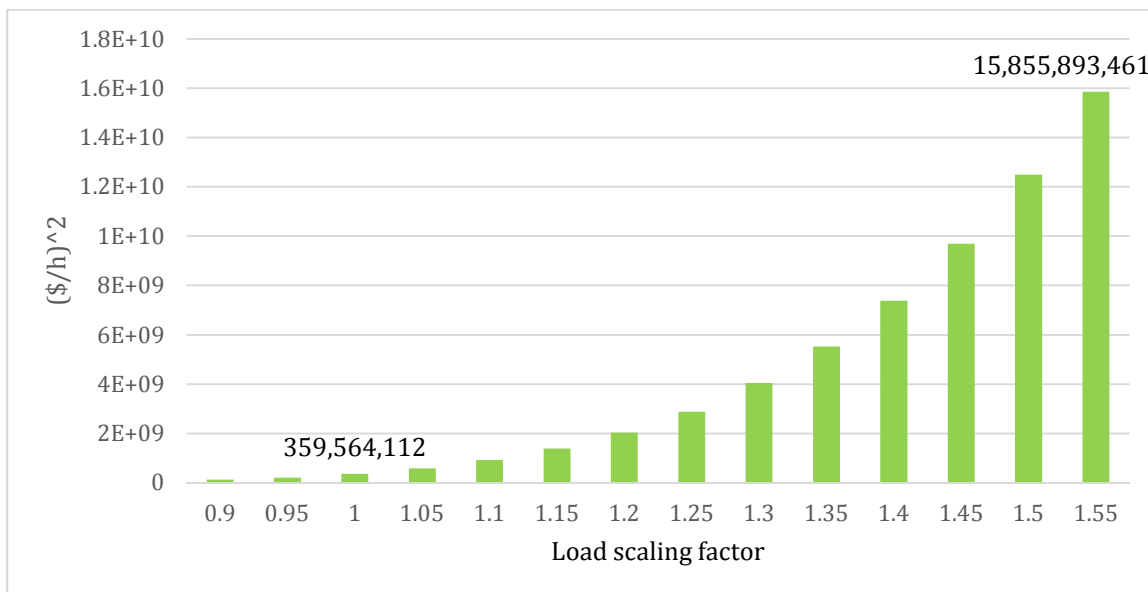


Figure 18: Variance of CP_SCD

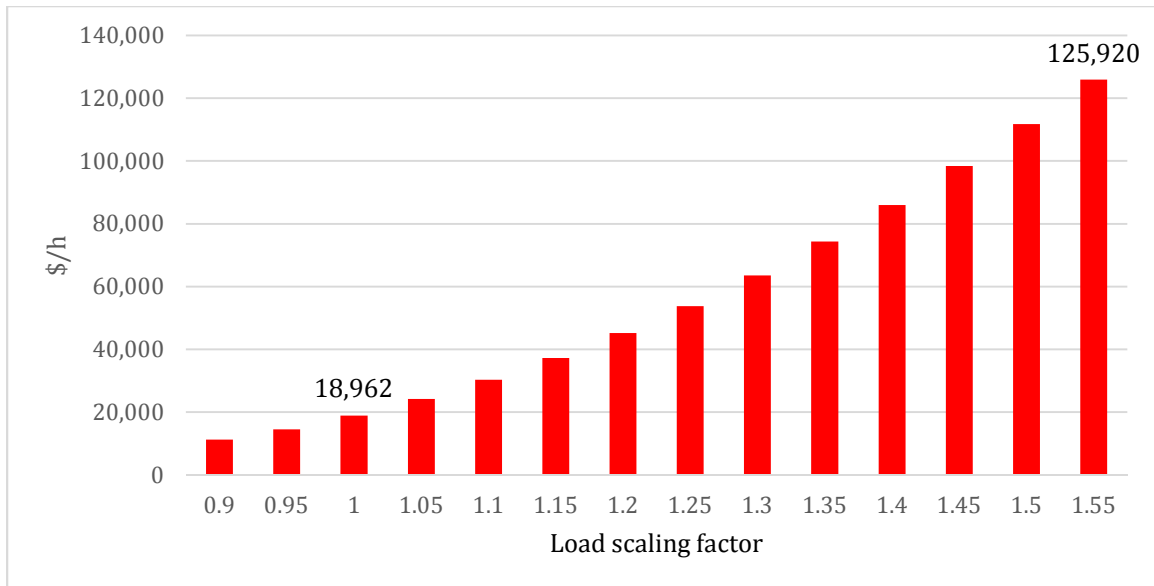


Figure 19: Standard deviation of CP_SCD

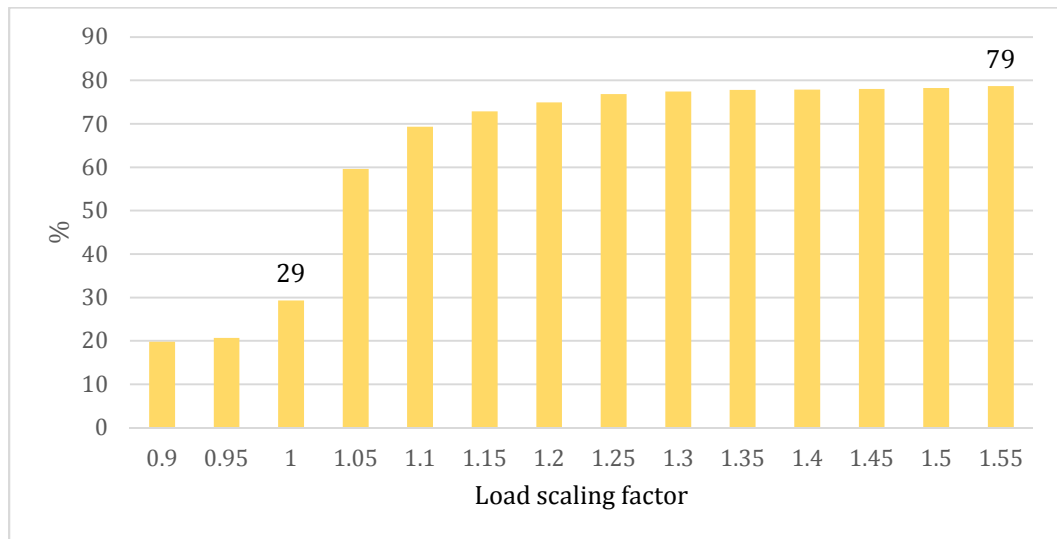


Figure 20: C.V. of CP_SCD

As discussion from previous chapter, ECP_SCD value shows the average cost penalty of the system in dollars per hour when the contingencies events occur at the particularly load amount, and can be the index that tells how good of the system can handle when contingency events occur. Also, the variance and standard deviation value shows how the cost penalty can vary in that moment. When the load scaling factor is more than one, most of the contingency events have to do the load shedding to get the system back to its steady-state. From Figure 17 and 18, the cost penalty of SCD will be closer to its average when the total load amount is smaller and increase a lot due to the load shedding involved for security correction. C.V. of CP_SCD is around 25% when the scale factor is one and increases a lot to 60% when the LSF change to 1.05. C.V. from Figure 20, C.V. increases when the total load increase, and after amount of the total load increase, the C.V. doesn't change that much in value. All three numerical values are non-linear curves due to the ECP_SCD computed by the non-linear calculation, which has many parameters (10 controls and 125 constraints parameters). As expected, the total load and ECP_SCD are related in the same way when considering the system reliability. When the total load is high, for example during peak load hour, the ECP_SCD also has a high value, which means the system has poor reliability. This consequence occurs due to the fact that more load shedding situations take place. On the other hand, low ECP_SCD indicates that the system has a great reliability, and can consist of the most contingencies event.

3.2.2 ECP_SCD by Monte Carlo Simulation

In this section, the Monte Carlo simulation will be used for calculating the ECP_SCD. In order to calculate this index, transmission line and generator unit states are chosen based on the probability of failure for the individual components. The availability of each component in a single state is determined by generating a random number in the range of zero to one. If the random number is greater than the probability of failure, the component is considered operational and available. Otherwise the component is considered failed. Then, the expected cost penalty is the average of the cost penalties for each state evaluated. Note that the same state can be evaluated more than once, and some states may never be evaluated due to the random sampling. Thus states that are more likely to occur have the greatest effect on the result.

DIGSILENT-PowerFactory, software has their own programming language called DPL, which similar to the C programming language and MATLAB. By means of a simple programming language, the Monte Carlo analysis can define an automation commands (scripts) to perform iterative calculations on the test case and post process the results. The script of Monte Carlo Simulation on DIGSILENT-PowerFactory is in Appendix A3.

The random seed number will be selected at 1 to initializes the random number generator. In this thesis, the random sampling states are simulated from 10,000 to 100,000 samplings. The result of ECP_SCD by Monte Carlo simulation shows in Figure 19, and the ECP_SCD results for each selected amount of sampling

state are really close to each other. From 10,000 to 100,000 sampling states the results only differ by 4%. Figure 19 indicates that around 75,000 to 100,000 sample states provide similarly as the results from normal statistic average value (5,564.56 \$/h). Also, Figure 20 shows the frequency of ECP_SCD by range of the penalty cost with 100,000 sampling state. Since this test system consist of 47 transmission lines which have a probability of failure set at 0.007 and 6 generators with 0.02 failure rate, the probability that all the components are in service is 0.6642, which is close to the result of Monte Carlo Simulation. The range between 0 to 50,000 \$/h is the most significant in this study because most of the penalty cost will fall in this group due to the higher probability of component outage of single contingency events.

The results of ECP_SCD from both Statistic Numerical Analysis and Monte Carlo Simulation are similar and really close in value. They also have the same disadvantage in that both techniques are time consuming. Monte Carlo Simulation seem a little bit faster due to the fact that some of contingency event aren't considered in calculation. Most of the random sampling states fall into the none contingency event which give the zero cost penalty, and sometime the random sampling events happen to be the same, which is only calculated once.

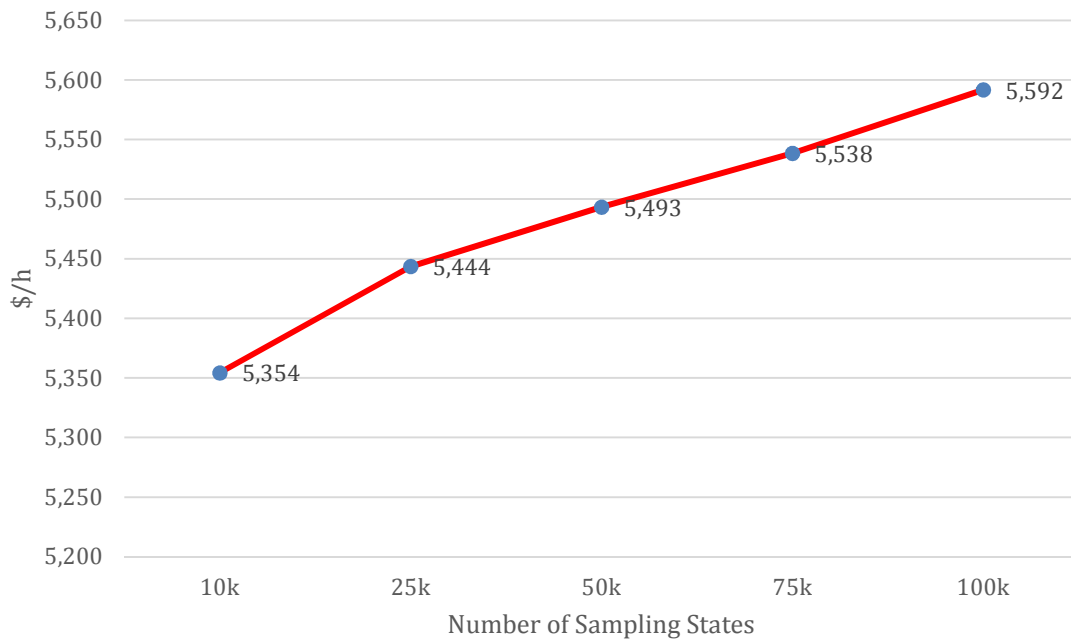


Figure 21: ECP_SCD by Monte Carlo Simulation

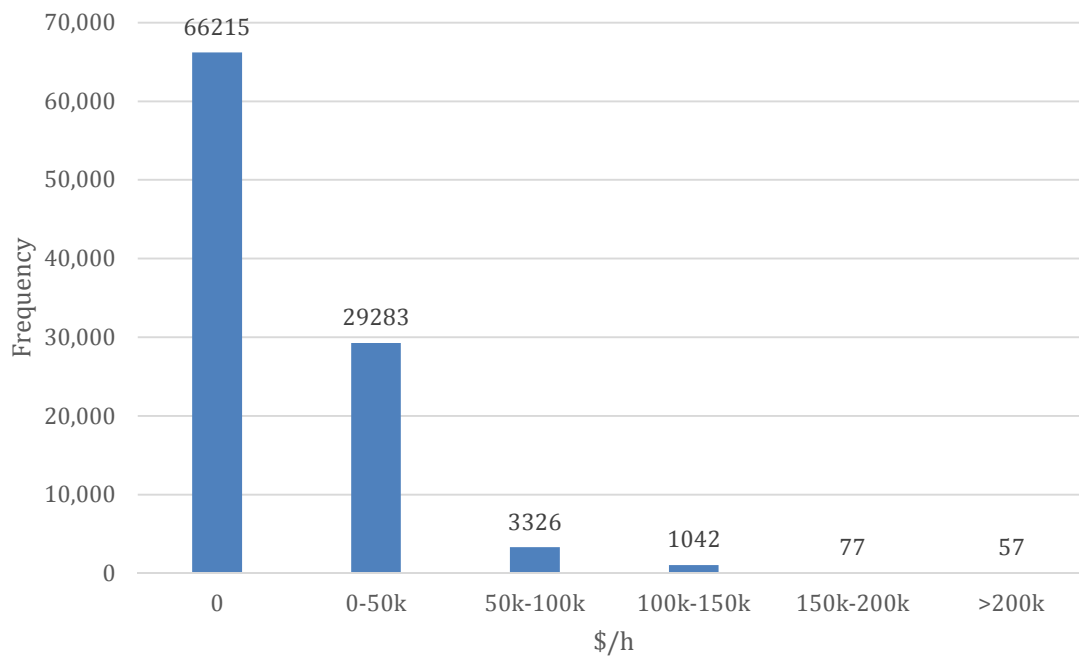


Figure 22: Frequency of ECP_SCD by Monte Carlo Simulation

However, to improve the system reliability, the ECP_SCD needs to be reduced. To prove this assumption, the results of ECP_SCD with varying failure rate of all the components and the ECP_SCD when increasing the transmission line limit are calculated.

3.2.3 ECP_SCD with decreasing the probability outage rate

In this section, the probability of elements outage will be decreased to see the change of the result of ECP_SCD. In this study, the base case has probability of transmission line outage 0.007 and the generator 0.02. The probability outage of all components will decrease 5% at the time from 100% to 80% as shown in Table 4. The results of ECP_SCD, variance, and standard deviation of ECP_SCD are shown in Figures 5, 6, and 7 respectively.

Table 5: Probability outage data

5% reduction in probability of failure	Transmission line	Generator
100%	0.007	0.02
95%	0.00665	0.019
90%	0.0063	0.018
85%	0.00595	0.017
80%	0.0056	0.016

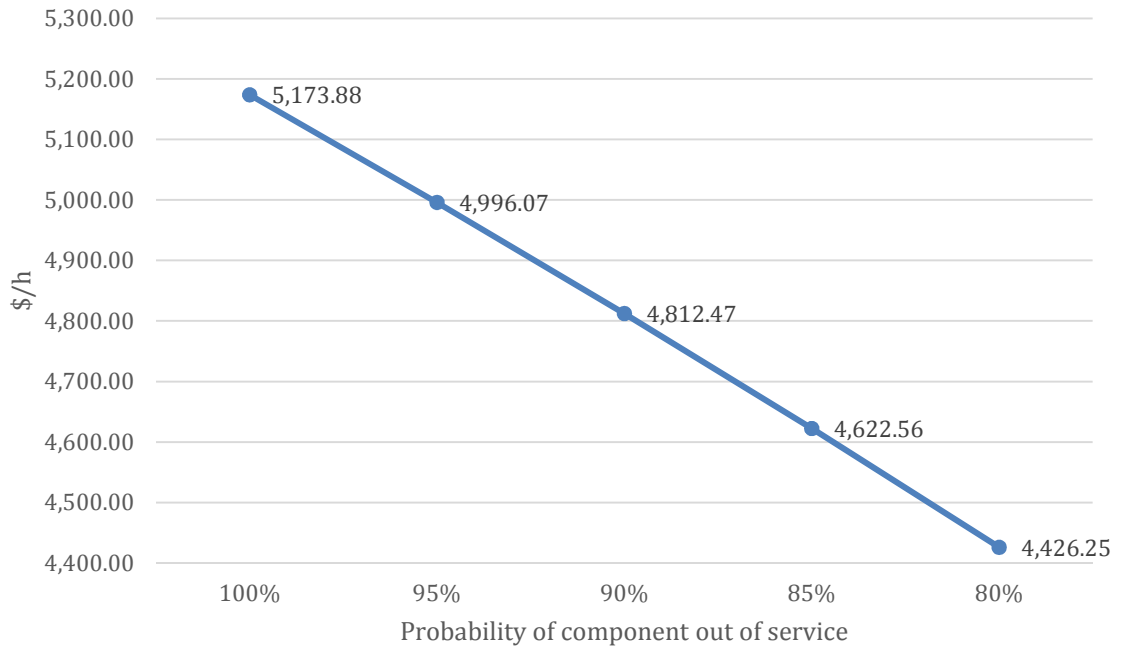


Figure 23: ECP_SCP when decreasing the probability outage rate

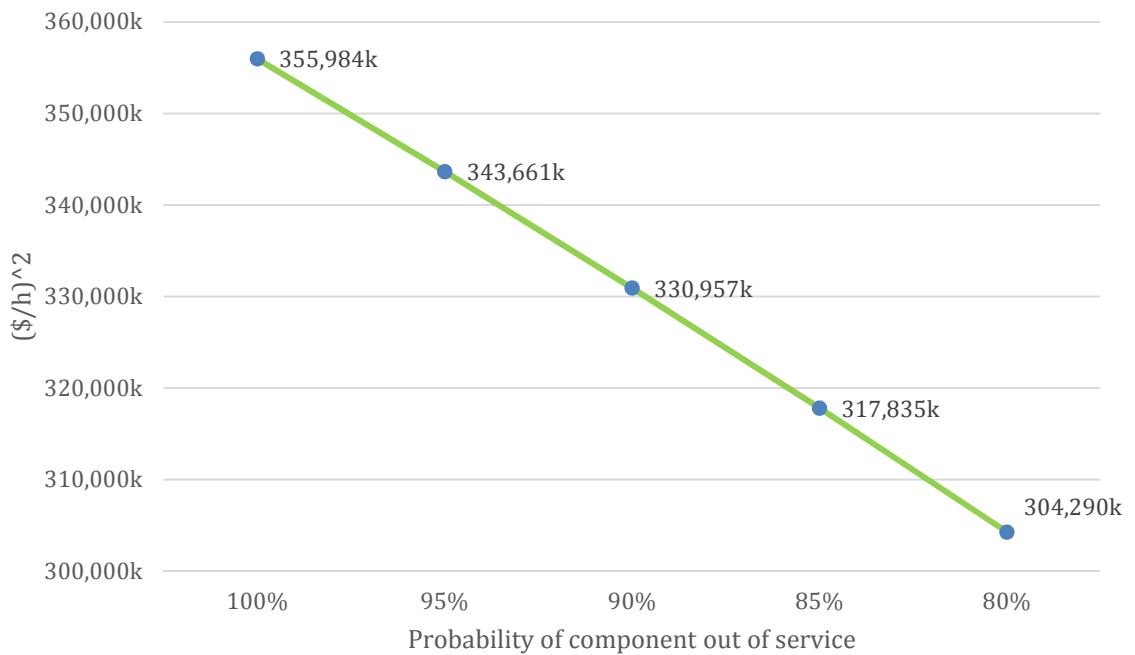


Figure 24: Variance of ECP_SCP when decreasing the probability outage rate

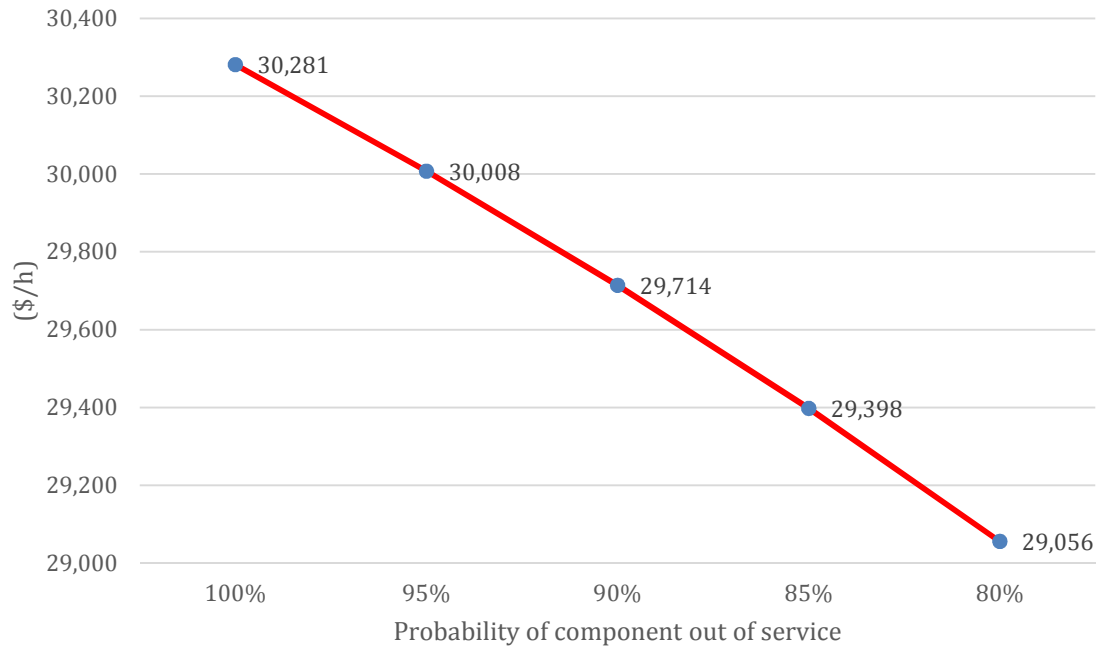


Figure 25: SD of ECP_SCP when decreasing the probability outage rate

As expected, the result of three numerical values decreases when the probability of component outage is decrease. When decreasing the probability of component outage by 5%, the ECP_SCD will slightly decrease around 3.5%. Therefore, the overall system reliability increases when the probability of component outage is decreased.

3.2.4 ECP_SCD when increasing the line limit

In this section, the transmission line limit will be increased by 50% one at a time to see the change of the ECP_SCD result. In this study, four transmission lines were chosen from the four highest lines loading percentage from OPF simulation.

These four transmission lines are line 06-08, line 15-23, line 21-22, and line 25-27 as shown in Figure 24 and line loading percentage represent in Table 5. In DigSILENT-PowerFactory, the line loading result after OPF simulation will represent in three different colors. The transmission line that has loading less than 80% is represented in black color, 80%-90% represented in orange color, and higher than 90% will be represented in red color. The result of OPF simulation is shown in Figure 24.

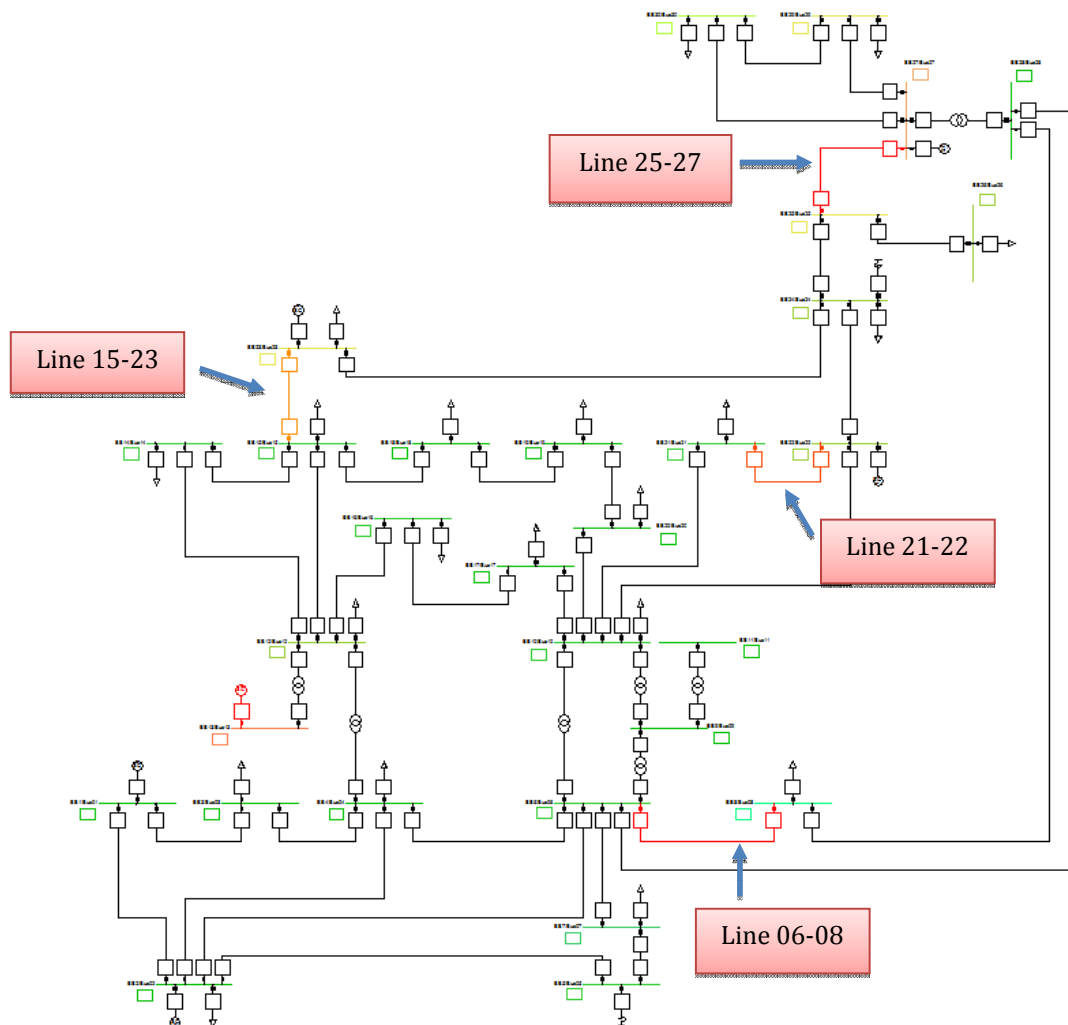


Figure 26: Result of OPF simulation

Table 6: Line loading result

Transmission line #	Line loading in %
Line 06-08	99.643
Line 25-27	96.801
Line 21-22	94.167
Line 15-23	83.012

The result of ECP_SCD when increasing the line-loading limit is shown in Figure 25. The pink area is the decreasing value of ECP_SCD when increasing that transmission line-loading limit and the blue area is the result of ECP_SCD. The result shows that increasing the transmission line-loading limit will decrease the ECP_SCD cost. Also, line-loading percentage seem to be related to the result of ECP_SCD. Increasing the line-loading limit of the transmission line that has a higher line loading percentage will decrease more value of ECP_SCD compare to the transmission line that has lower line loading percentage. In this case, Line 06-08 has a highest line loading percentage of the whole system, which is 99.643%. Increasing the line loading limit by 50% will decrease the result of ECP_SCD from 5,564.56 to 1418.65 \$/h, which is about 75% decreasing. For Line 15-23, which is the fourth highest rank of line loading percentage (83.012%), the ECP_SCD result decrease from 5,564.56 to 4885.92 \$/h, which is 12% decreasing.

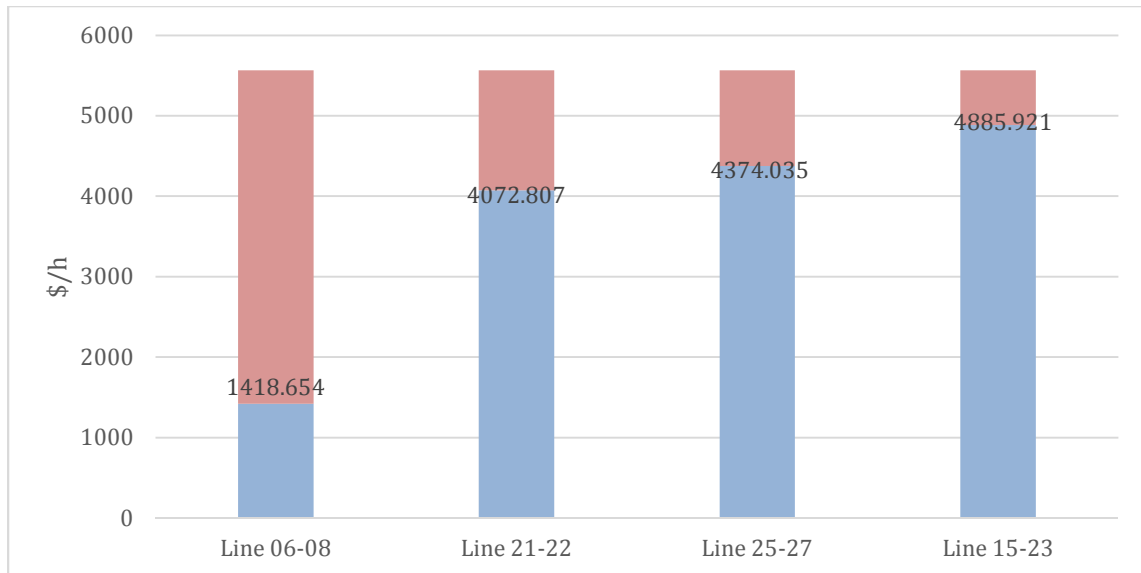


Figure 27: ECP_SCD when increasing the line-loading limit

3.3 Contingency Screening by SCD

Beside the result of ECP_SCD, Contingency Screening using the SCD is compared with the screening by the performance index. Contingency screening concept and equation are already described in Chapter 2.3. Parameter n and m in Performance Index' equation will be set at 5 to make equally considering between line loading and voltage violation. DlgSILENT-PowerFactory software has a Contingency Analysis function that can automatically generate contingency cases based on selected components. Also, this software has a set of predefined report formats called Report Contingency Analysis Results, which is useful for calculate the Performance Index,

To calculate the Performance Index, Loadings Violation and Maximum

Voltage Violations have been chosen as a report type. Loading Violations' report will show all overloaded components (according to the specified loading limit) for each contingency. Maximum Voltage Violations will report all voltage violations of a terminal (greater than or equal to the specified upper voltage limit) considering all contingencies. In this study, the loading limit will be set at 80% for all components. Figure 26 shows the result of power flow analysis on one line diagram of the test system when transmission line 06-08 is out of service. The red color transmission lines represent the overloading limit and the dark blue color on busbar means it is overvoltage limit. Contingency Analysis results that taken from DIgSILENT-PowerFactory and Performance Index calculation results for top 10 contingency events are listed in Table 6.

In this thesis, SCD will also be used for Contingency Screening. The top 10 contingency events that have a highest value of SCD are ranked in Table 7. In addition, Table 8 provides result comparison between Contingency Screening by Performance index and SCD. Although, the top three contingency events are the same for both techniques, all rankings after the third are slightly different. Additional, seven out of ten contingency events will rank in the top ten; one is really close to top ten, other two-outage events ranking is out of range.

Table. 10 shows the results of contingency screening by SCD with different load scaling factor. Although the total load is increased by 55% at LSF 1.55, result of the top 10 contingency events similar to the result of normal load value. Therefore, this study shows that the SCD index can be used for contingency screening, and will

give the similarly results compare with the screening performance index. Since the result of SCD is the optimal operating cost using the real system data that simulate and test throughout this thesis, contingency screening analysis by SCD index can be used in real life for system planning and study contingency events.

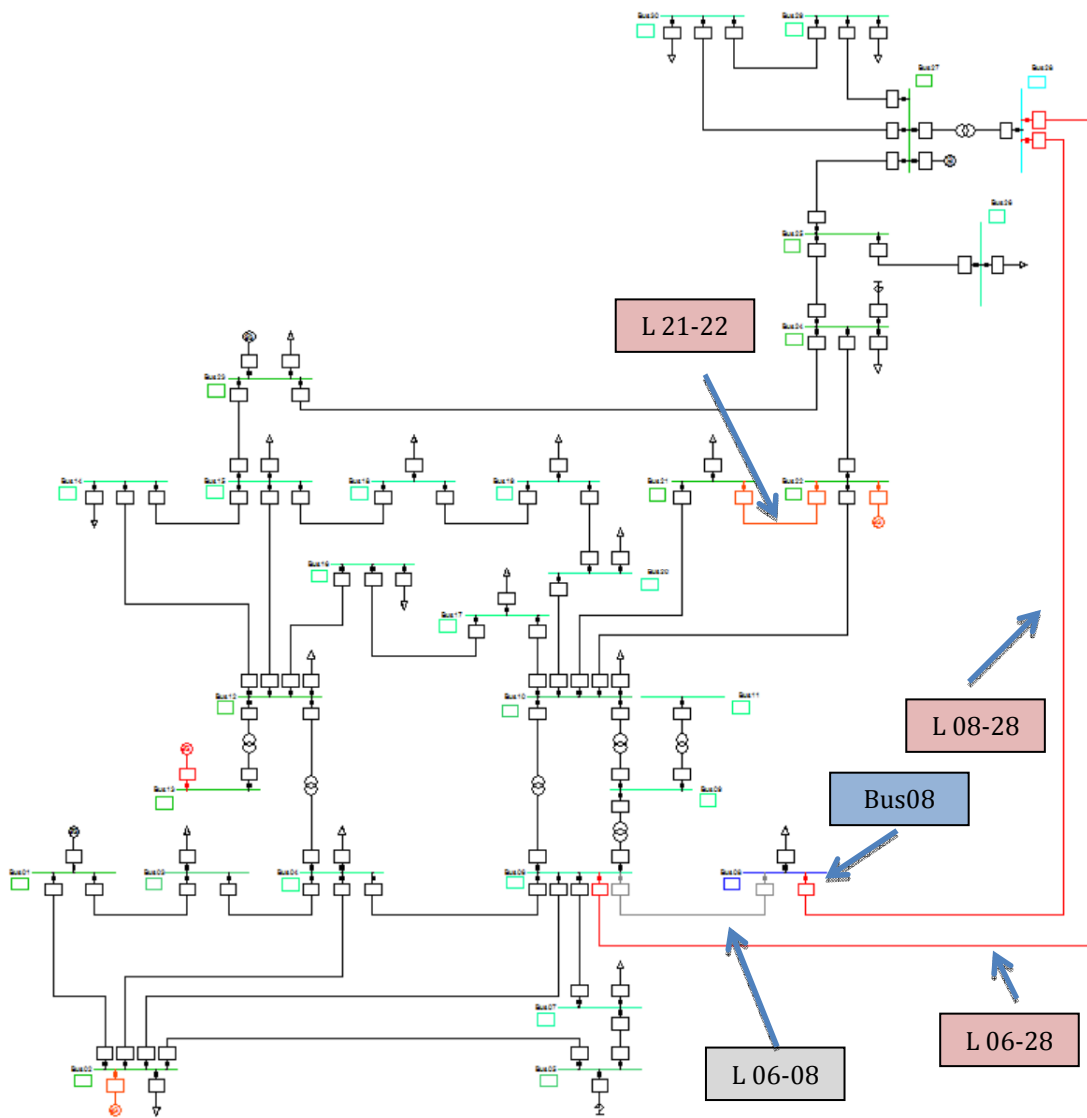


Figure 28: Load flow analysis when transmission line 06-08 out of service

Table 7: Contingency Screening by Performance Index

Component Outage	Overloading Limit	PIP/PIV	PI
L 06-08	08-28	8.502839	11.6079
	21-22	0.777361	
	06-28	1.494184	
	Bus08	0.8335155	
L 08-28	06-08	5.129512	5.955893
	21-22	0.826382	
Gen27	06-08	3.074208	4.795711
	21-22	0.756465	
	Bus26	0.006581253	
	Bus27	0.03641983	
	Bus29	0.041047152	
	Bus30	0.043884741	
Gen22	06-08	1.939096	4.785149
	15-23	0.408659	
	23-24	0.730588	
	23-24	1.706806	
	Bus08	4.57336E-05	
	Bus09	0.00536142	
	Bus10	0.021098933	
	Bus11	0.00536142	
	Bus17	0.010619923	
	Bus18	0.000685933	
	Bus19	0.002816788	
	Bus20	0.005078505	
	Bus21	0.084192952	
	Bus22	0.116494876	

Component Outage	Overloading Limit	PIP/PIV	PI
L 15-23	06-08	1.68218	4.678432
	21-22	1.226992	
	22-24	0.658215	
	23-24	1.111044	
L 10-20	06-08	1.751616	4.453683
	21-22	0.515801	
	15-18	1.301429	
	15-23	0.461496	
	18-19	0.403963	
	Bus18	0.001172524	
	Bus19	0.006196145	
	Bus20	0.012009206	
Gen01	06-08	1.240445	4.10284
	21-22	0.991028	
	22-24	0.40402	
	24-25	0.433455	
	25-27	1.033893	
T6 12-13/ Gen13	06-08	1.873517	4.012778
	15-23	1.144107	
	21-22	0.995154	
T7 28-27	06-08	2.285516	3.844458
	21-22	1.084996	
	25-27	0.473946	
L 10-22	06-08	1.750898	3.709325
	21-22	1.958427	

Table 8: Contingency Screening by SCD

Component outage	SCD (\$/h)
06-08	120877.30
08-28	98261.29
Gen27	74681.44
T7 28-27	60147.23
T6 12-13/ Gen13	36468.88
Gen22	31205.27
25-26	21567.22
Gen02	653.79
Gen01	625.40
06-07	602.37

Table 9: Comparing results of Contingency Screening by PI vs. SCD

Component outage	Ranking by SCD	Ranking by PI
06-08	1	1
08-28	2	2
Gen27	3	3
T7 28-27	4	9
T6 12-13/ Gen13	5	8
Gen22	6	4
25-26	7	40
Gen02	8	15
Gen01	9	7
06-07	10	37

Table 10:
Contingency
screening by SCD
with different load
scaling factor

Ranking	Load Scaling factor											
	0.9	0.95	1	1.05	1.1	1.15	1.2	1.25	1.4	1.45	1.5	1.55
1	06-08	06-08	06-08	06-08	06-08	06-08	06-08	06-08	en 13	Gen 13	Gen 13	Gen 13
2	08-28	08-28	08-28	08-28	08-28	08-28	Gen27	Gen27	en27	Gen02	Gen02	Gen02
3	Gen27	Gen27	Gen27	Gen27	Gen27	Gen27	08-28	08-28	Gen02	Gen27	Gen27	Gen27
4	T7 28-27	T7 28-27	T7 28-27	T7 28-27	25-26	25-26	Gen 13	08-28	06-08	06-08	Gen01	Gen01
5	25-26	25-26	25-26	T7 28-27	T7 28-27	25-26	25-26	Gen02	Gen01	Gen01	06-08	06-08
6	Gen02	Gen02	Gen22	Gen 13	Gen 13	Gen 13	T7 28-27	Gen02	Gen22	Gen22	Gen22	Gen22
7	Gen01	Gen01	25-26	Gen22	Gen22	Gen22	06-07	T7 28-27	08-28	06-07	06-07	06-07
8	Gen22	Gen22	Gen02	Gen01	06-07	06-07	Gen22	06-07	06-07	08-28	Gen23	Gen23
9	Gen 13	Gen 13	Gen01	Gen23	Gen01	Gen23	10-20	Gen22	25-26	25-26	08-28	15-18
10	Gen 23	01-03	06-07	06-07	Gen23	10-20	Gen23	10-20	10-20	Gen23	15-18	12-16

Chapter 4

Conclusion

This thesis introduces an index called Expected Cost Penalty due to Deviation from Security Constrained Dispatch (ECP_SCD), which is an optimal operating cost of the system following contingency and security corrections event. The power system operator can use this index to represent how good of the system can handle when contingency events occur by the average of the penalty costs of all contingency events. As expected, when the total load is high, for example during peak load hour, the ECP_SCD also has a high value, which means that, most of the time when contingency events occur, the system operator has to pay a lot of money to keep the remaining system operate in steady state. This consequence occurs due to the fact that more load shedding situations take place. On the other hand, low ECP_SCD indicates that the system has a great ability to handle the required loads without exceeding their limits, and can consist most of the contingencies event.

When decrease the probability of component outage by 5%, the ECP_SCD will slightly decrease around 3.5%. Therefore, the overall system reliability increases when the probability of component outage is decreased. Increasing the transmission line-loading limit will also decrease the ECP_SCD cost. Line-loading percentage seem

to be related to the result of ECP_SCD. Increasing the line-loading limit of the transmission line that has a higher line loading percentage from the normal OPF situation will decrease more value of ECP_SCD compare to the transmission line that has lower line loading percentage.

The results of ECP_SCD from both Statistic Numerical Analysis and Monte Carlo Simulation are similar and fairly close in value. Both techniques contain the same disadvantage in that both are time consuming. Monte Carlo Simulation seem a little bit faster due to some of contingency event doesn't consider in calculation. Most of the random sampling states fall into the none contingency event which give the zero cost penalty, and sometime the random sampling events happen to be the same, which are only calculated once.

Finally, SCD index can be used for contingency screening, and will give the similar results compared with the screening performance index. Since the result of SCD is the optimal operating cost using the real system data that simulate and test throughout this thesis, contingency screening analysis by SCD index can be used in real life for system planning and study contingency events.

References

- [1] M. B. Cain, R. P. O'Neill and A. Castillo, "History of Optimal Power Flow and Formulations," Federal Energy Regulatory Commission, Dec. 2012. Available: <http://www.ferc.gov/industries/electric/indus-act/market-planning/opf-papers/acopf-1-history-formulation-testing.pdf>
- [2] A. J. Wood and B. F. Wallenberg, "Power Generation, Operation and Control," 2nd ed., New York: John Wiley & Sons, 1996.
- [3] J. Carpentier, "Contribution to the economic dispatch problem," Bulletin de la Societe Francoise des Electriciens, vol. 3, no. 8, pp. 431–447, 1962, in French.
- [4] J. A. Momoh, M. E. El-Harwary and Ramababu Adapa, "A review of selected optimal power flow literature to 1993, part I and II," IEEE Transactions on Power System, vol. 14, no. 1, pp. 96-111, Feb. 1999.
- [5] K. S. Pandya and S. K. Joshi, "A survey of optimal power flow methods," Journal of Theoretical and Applied Information Technology, vol. 4, no. 5, pp. 450–458, 2008.
- [6] S. Frank, I. Steponavice, and S. Rebennack, "Optimal power flow: A bibliographic survey I—Formulations and deterministic methods," Energy Systems, vol. 3, no. 3, pp. 221–258, 2012. Available: <http://dx.doi.org/10.1007/s12667-012-0056-y>.
- [7] S. Frank, I. Steponavice, and S. Rebennack, "Optimal power flow: A bibliographic survey II—Non-deterministic and hybrid methods," Energy Systems, vol. 3, no. 3, pp. 259–289, 2012. Available: <http://dx.doi.org/10.1007/s12667-012-0057-x>.
- [8] D. B. Das and C. Patvardhan, "Useful multi-objective hybrid evolutionary approach to optimal power flow," Generation, IEE Proceedings-Transmission and Distribution, vol. 150, no. 3, pp. 275-282, 13 May 2003.
- [9] J.G. Vlachogiannis and K.Y. Lee, "Reactive Power Control Based on Particle Swarm Multi-Objective Optimization", Proceedings of 13th International Conference on Intelligent Systems Application to Power Systems, Arlington, VA, Nov. 6-10 2005.
- [10] M. Tripathy and S. Mishra, "Bacteria Foraging-Based Solution to Optimize Both Real Power Loss and Voltage Stability Limit," IEEE Transactions on Power Systems, vol. 22, no. 1, pp. 240-248, Feb 2007.

- [11] Z. L. Gaing and X. H. Liu, "New Constriction Particle Swarm Optimization for Security-Constrained Optimal Power Flow Solution," International Conference on Intelligent Systems Applications to Power Systems, pp.1-6, Nov. 5-8 2007.
- [12] N. Aminudin, T. K. A. Rahman, and I. Musirin, "Optimal Power Flow for Load Margin Improvement using Evolutionary Programming," The 5th Student Conference on Research and Development, pp.1-6, 12-11 Dec. 2007.
- [13] M. A. Abido, "Multiobjective Particle Swarm Optimization for Optimal Power Flow Problem," The 12th International Middle-East Power System Conference, pp. 392-396, Mar. 12-15 2008.
- [14] M. Varadarajan and K. S. Swarup, "Solving Multi-Objective Optimal Power Flow using Differential Evolution," IET Generation Transmission & Distribution, vol. 2, no. 5, pp. 720-730, Sep. 2008.
- [15] K. Zehar and S. Sayah, "Optimal Power Flow with Environmental Constraint using a Fast Successive Linear Programming Algorithm: Application to the Algerian Power System." Energy Conversion and Management, vol. 49, no. 11, pp. 3362–3366, Nov. 2008.
- [16] B. Gasbaoui and B. Allaoua, "Ant Colony Optimization Applied on Combinatorial Problem for Optimal Power Flow Solution," Leonardo Journal of Sciences, vol. 14, pp. 1–17, 2009.
- [17] M. S. Kumari and S. Maheswarapu, "Enhanced Genetic Algorithm based computation technique for multi-objective Optimal Power Flow solution," International Journal of Electrical Power & Energy Systems, vol. 32 no. 6, pp. 736–742, Jul. 2010.
- [18] J. Aghaei, A. L. Ara, and M. Shabani, "Fuzzy Multi-Objective Optimal Power Flow Considering UPFC," International Journal of Innovative Computing, Information and Control, vol. 8, no. 2, pp. 1155–1166, Feb. 2012.
- [19] J. A. Momoh, J. Z. Zhu, G. D. Boswell, and S. Hoffman, "Power System Security Enhancement by OPF with Phase Shifter," IEEE Transactions on Power Systems, vol.16, no. 2, pp. 287-293, May 2001.
- [20] S. Gope and T. Malakar, "Contingency Constraint Corrective Rescheduling with the Presence of Wind Farm," International Conference on Sustainable Energy and Intelligent Systems, pp. 137-142, Jul. 20-22 2011.

- [21] R. N. Banu and D. Devaraj, "Optimal Power Flow for Steady State Security Enhancement using Genetic Algorithm with FACTS Devices," IEEE Region 10 and the Third International Conference on Industrial and Information Systems, pp.1-6, Dec. 8-10 2008.
- [22] C. Nnonyelu and T. Madueme, "Power System Contingency Analysis: A Study of Nigeria's 330KV Transmission Grid," In proceeding of: Energy Source for Power Generation, At Electrical Engineering, University of Nigeri, Nsukka, vol. 4, Jul. 2013
- [23] Z. Hussain, Z. Chen, and P. Thogersen, "Fast and Precise Method of Contingency Ranking in Modern Power System," IEEE Jordan Conference on Applied Electrical Engineering and Computing Technologies, pp. 1-7, Dec. 6-8 2011.
- [24] S. Pajic, "Power System State Estimation and Contingency Constrained Optimal Power Flow - A Numerically Robust Implementation," Ph.D.'s Thesis, Worcester Polytechnic Institute, Apr. 2007.
- [25] S. R. Dahman, "N-1-1 Contingency Analysis using PowerWorld Simulator," PowerWorld Corporation, March 2010. Available: <http://www.powerworld.com/Document/20Library/SimulatorN-1-1.pdf>.
- [26] F. Milano, C. A. Canizares, and A. J. Conejo, "Sensitivity-Based Security-Constrained OPF Market Clearing Model," IEEE Transactions on Power Systems, vol. 20, no. 4, pp. 2051-2060, Nov. 2005.
- [27] P. E. O. Yumbala, J. M. Ramirez, and C. A. Coello, "Optimal Power Flow Subject to Security Constraints Solved with a Particle Swarm Optimizer," IEEE Transactions on Power Systems, Vol. 23, No. 1, pp. 33-40, Feb. 2008.
- [28] Z. L. Gaing and C. H. Lin, "Contingency-Constrained Optimal Power Flow Using Simplex-Based Chaotic-PSO Algorithm," Applied Computational Intelligence and Soft Computing, 2011.
- [29] V. C. Ramesh and X. Li, "A Fuzzy Multi-Objective Approach to Contingency Constrained OPF", IEEE Transactions on Power Systems, vol. 12, no. 3, pp. 1348-1354, Aug. 1997.
- [30] N. Fan, R. Chen, and J. Watson, "N-1-1 Contingency-Constrained Optimal Power Flow by Interdiction Methods," IEEE Power and Energy Society General Meeting, pp. 1-6, 22-26 Jul. 2012

- [31] F. Zaoui and S. Fliscounakis, "A Direct Approach for the Security Constrained," IEEE PES Power Systems Conference and Exposition, pp. 1562-1569, Oct. 29-Nov. 1 2006.
- [32] L. A. Finley, T. R. Standish, and R. C. Phillips, "Optimizing System Performance Through Dynamic Load Shed Scheduling," IEEE Transactions on Power Apparatus and Systems, vol. PAS-104, no. 6, pp. 1286-1289, Jun. 1985.
- [33] G. B. Shrestha and K. C. Lee, "Load Shedding Schedules Considering Probabilistic Outages," The 7th International Power Engineering Conference, vol. 2, pp. 950-955, Nov. 29-Dec. 2 2005.
- [34] B. F. Rad and M. Abedi, "An Optimal Load-Shedding Scheme During Contingency Situations using Meta-Heuristics Algorithms with Application of AHP Method," The 11th International Conference on Optimization of Electrical and Electronic Equipment, pp. 167-173, May 22-24 2008.
- [35] M. T. Hagh and S. Galvani, "A Multi Objective Genetic Algorithm for Weighted Load Shedding," The 18th Iranian Conference on Electrical Engineering, pp. 867-873, May 11-13 2010.
- [36] B. Charoenphan and K. Audomvongseree, "Optimal Load Shedding Scheme under Contingency Condition Considering Voltage Stability Problem," International Conference on Electrical Engineering/Electronics Computer Telecommunications and Information Technology, pp. 1006-1010, May 19-21 2010.
- [37] S. Su and K. Tanaka, "An Efficient Voltage Stability Ranking using Load Shedding for Stabilizing Unstable Contingencies," Proceedings of the 44th International Universities Power Engineering Conference, pp. 1-5, Sept. 1-4 2009.
- [38] C. M. Grinstead and J. L. Snell. "Introduction to Probability." The CHANCE Project, Jul. 2006. Available:
http://www.dartmouth.edu/~chance/teaching_aids/books_articles/probability_book/amsbook.mac.pdf
- [39] J. Condren, T.W. Gedra, and P. Damrongkulkamjorn, "Optimal power flow with expected security costs," IEEE Transactions on Power Systems, vol. 21, no. 2, pp. 541-547, May 2006
- [40] J. Condren and T.W. Gedra, "Expected-Security-Cost Optimal Power Flow with Small-Signal Stability Constraints," IEEE Transactions on Power Systems, vol. 21, no. 4, pp. 1736-1743, Nov. 2006

- [41] L. Yang, J. Jian, and T. Li, "Parallel Interior-Point Algorithm Based on MCWC for ESC-OPF," International Conference on Information Technology and Computer Science, vol. 2, pp. 267-270, Jul. 25-26 2009.
- [42] R. S. Wibowo, N. Yorino, Y. Zoka, Y. Sasaki, and M. Eghbal, "FACTS Allocation Based on Expected Security Cost by Means of Hybrid PSO," Asia-Pacific Power and Energy Engineering Conference, pp.1-4, Mar. 28-31 2010.
- [43] J. He, L. Cheng, D. S. Kirschen, and Y. Sun, "Optimising the Balance between Security and Economy on a Probabilistic Basis," IET Generation, Transmission & Distribution, vol. 4, no. 12, pp. 1275-1287, Dec. 2010
- [44] M. E. El-Hawary, and G. A. N. Mbamalu, "A Comparison of Probabilistic Perturbation and Deterministic Based Optimal Power Flow Dolutions," IEEE Transactions on Power Systems, vol. 6, no. 3, pp. 1099-1105, Aug. 1991.
- [45] A.Schellenberg, W. Rosehart, and J. Aguado, "Cumulant Based Stochastic Optimal Power Flow (S-OPF) for Variance Optimization," IEEE Power Engineering Society General Meeting, vol. 1, pp. 473-478, Jun. 12-16 2005.
- [46] M. Dadkhah and B. Venkatesh, "Probabilistic - Optimal Power Flow for Radial Distribution Systems with Wind Generators," Proceedings of the World Congress on Engineering, vol. 2, Jul. 3-5 2013.
- [47] A. Papoulis and S. Pillai, "Probability, Random Variables, and Stochastic Processes," 4th ed., McGraw Hill, 2002.
- [48] M. Davari, F. Toorani, H.Nafisi, M. Abedi, and G. B. Gharehpetian, "Determination of Mean and Variance of LMP using Probabilistic DCOPF and T-PEM," IEEE 2nd International Power and Energy Conference, pp. 1280-1283, Dec. 1-3 2008.
- [49] I. Erlich, G. K. Venayagamoorthy, and N. Worawat, "A Mean-Variance Optimization algorithm," IEEE Congress on Evolutionary Computation, pp. 1-6, Jul. 18-23 2010.
- [50] I. Erlich, W. Nakawiro, and M. Martinez, "Optimal Dispatch of Reactive Sources in Wind Farms," IEEE Power and Energy Society General Meeting, pp.1-7, Jul. 24-29 2011.
- [51] W. Nakawiro, I. Erlich, and J. L. Rueda, "A Novel Optimization Algorithm for Optimal Reactive Power Dispatch: A Comparative Study," The 4th International Conference on Electric Utility Deregulation and Restructuring and Power Technologies, pp.1555-1561, July 6-9 2011.

[52] J. D. Glover, M.S. Sarma, and T.J. Overbye, "Power System Analysis and Design," Fifth Edition, Cengage Learning, 2010.

[53] A. Ghosh, "Power Flow Analysis," E-Learning Courses from the IITs & IISc, Available: http://nptel.ac.in/courses/Webcourse-contents/IIT-KANPUR/power-system/ui/Course_home-4.htm

[54] DIgSILENT, "Power Factory 15 User Manual," DIgSILENT GmbH, Gomaringen, Germany, Dec. 2013. Available: www.digsilent.de

[55] R. D. Zimmerman and C. E. Murillo-Sánchez, "Matpower 4.1 User's Manual," Power Systems Engineering Research Center (Pserc), Dec. 2011, Available: <http://www.pserc.cornell.edu/matpower>

[56] R. Billinton and W. Li, "Reliability Assessment of Electric Power Systems Using Monte Carlo Methods," Plenum Press, 1994.

[57] F. X. B. Llavall, "reliability worth assessment of radial system with Distribution Generation," Illinois Institute of Technology, Chicago, Jul 2011.

[58] R. Billinton and L. Wenyuan, "Consideration of multi-state generating unit models in composite system adequacy assessment using Monte Carlo simulation," Canadian Journal of Electrical and Computer Engineering, vol.17, no.1, pp. 24-28, Jan. 1992.

[59] Y. Gao, M. Zhou, G. Li, Y. Huang, L. Xiao and R. Li, "Monte Carlo Simulation Based Available Transmission Capability Calculation," 2005 IEEE/PES Transmission and Distribution Conference and Exhibition: Asia and Pacific, pp.1-6, 2005.

[60] S. J. Kamat and W. E. Franzmeier, "Determination of reliability using event-based Monte Carlo simulation, Part2," IEEE Trans. Reliability, vol. R-25, no. 3, pp. 254-255, 1976.

[61] Z. Liming, C. Guoqiang, Y. Jianwei and J. Limin, "Monte-Carlo simulation based on FTA in reliability analysis of door system," 2010 The 2nd International Conference on Computer and Automation Engineering (ICCAE), vol.5, pp.713-717, 26-28 Feb. 2010.

[62] S. J. Kamat and M. W. Riley, "Determination of reliability using event-based Monte Carlo simulation," IEEE Trans. Reliability, vol. R-24, no. 1, pp. 73-75, 1975.

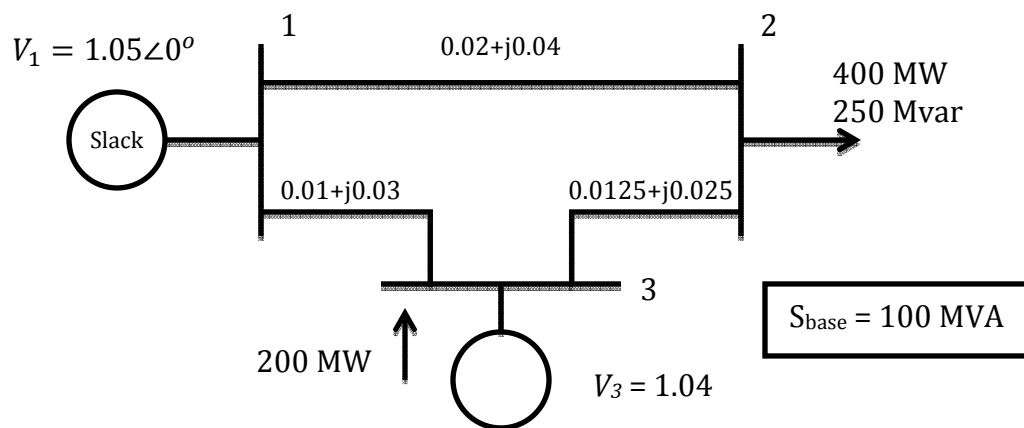
[63] A. M. Reind and M. T. Schilling, "Reliability Assessment of the Brazilian Power System Using Enumeration and Monte Carlo," IEEE Transactions on Power Systems, vol.23, no.3, pp.1480-1487, Aug. 2008.

- [64] L. Goel, "A Framework to Implement Supply and Demand Side Contingency Management in Reliability Assessment of Restructured Power Systems," 2007. IEEE Power Engineering Society General Meeting, pp.1, 24-28 June 2007.
- [65] S. Asgarpour and S. K. Panarelli, "Expected Cost Penalty due to Deviation from Economic Dispatch for interconnected power systems," IEEE Transactions on Power Systems, vol.10, no.1, pp.441-447, Feb 1995.
- [66] D. Y. Wang, Y. T. Ami and E. Chebli, "Evaluation of Low-Voltage Network Systems Reliability Using Probabilistic Methods," Proceedings of the 10th International Conference on Probabilistic Methods Applied to Power Systems, PMAPS '08, pp. 1-6, 25-29 May 2008.
- [67] F. Capitanescu, M. Glavic and L. Wehenke, "An interior-point method based optimal power flow," University of Liège, Montefiore Institute, 4000 Liège, Belgium, Jun. 2005.

Appendix

A1 Example of Power Flow Analysis on 3 Bus System

Step 1: Represent the system by its one line diagram.



Step 2: Convert all quantities to Per Unit. In this case, V_1 , V_3 and all the impedances are already in per unit values

Since $S_{base} = 100$ MVA

$$\text{In Bus 2: } P_2 = -(400)/100 = -4 \text{ p.u.}$$

$$Q_2 = -(250)/100 = -2.5 \text{ p.u.}$$

$$\text{In Bus 3: } P_3 = 200/100 = 2 \text{ p.u.}$$

Step 3: Obtain the Y_{bus} matrix.

$$Y_{11} = [Y_{12} + Y_{13}] = (0.02 + j0.04)^{-1} + (0.01 + j0.03)^{-1} = 20 - j50$$

$$Y_{12} = Y_{21} = -(0.02 + j0.04)^{-1} = -10 + j20$$

$$Y_{13} = Y_{31} = -(0.01 + j0.03)^{-1} = -10 + j30$$

$$Y_{22} = [Y_{12} + Y_{13}] = (0.02 + j0.04)^{-1} + (0.0125 + j0.025)^{-1} = 26 - j52$$

$$Y_{23} = Y_{32} = -(0.0125 + j0.025)^{-1} = -16 + j32$$

$$Y_{33} = [Y_{23} + Y_{13}] = (0.01 + j0.03)^{-1} + (0.0125 + j0.025)^{-1} = 26 - j62$$

When putting this all together, the Y_{bus} matrix will be:

$$Y_{bus} = \begin{bmatrix} 20 - j50 & -10 + j20 & -10 + j30 \\ -10 + j20 & 26 - j52 & -16 + j32 \\ -10 + j30 & -16 + j32 & 26 - j62 \end{bmatrix}$$

Then convert Y_{bus} matrix to be the polar form

$$Y_{bus} = \begin{bmatrix} 53.85165 \angle -1.1903 & 22.36068 \angle 2.0344 & 31.62278 \angle 1.8925 \\ 22.36068 \angle 2.0344 & 58.13777 \angle -1.1071 & 35.77709 \angle 2.0344 \\ 31.62278 \angle 1.8925 & 35.77709 \angle 2.0344 & 67.23095 \angle -1.1737 \end{bmatrix}$$

Note: the angles are in radians for this example.

Step 4: Classify all the buses.

Table A1: Buses classify result

Bus number	Bus type	Given parameters	Unknown parameters
1	Slack Bus	V, δ	P, Q
2	Generator Bus	$P, V $	Q, δ
3	Load Bus	P, Q	$ V , \delta$

Step 5: Choose the initial values of the voltage magnitudes $|V|^{(0)}$ of all load buses and angles $\delta^{(0)}$ of the voltages of all the buses (unless it is specified) except the slack bus (usually 1 and 0 respectively).

Assume: $|V_2| = 1$

$$\delta_2 = 0$$

$$\delta_3 = 0$$

Step 6: Use the estimated values from step 6 to calculate approximation for the real and reactive power, and the difference with the value that was actually given.

From:

$$P_2 = |Y_{21}||V_2||V_1| \cos(\theta_{21} + \delta_1 - \delta_2) + |Y_{22}||V_2|^2 \cos(\theta_{22} + \delta_2 - \delta_2) \\ + |Y_{23}||V_2||V_3| \cos(\theta_{23} + \delta_3 - \delta_2)$$

$$P_2 = (22.36068)(1)(1.05) \cos(2.0344 + 0 - 0) \\ + (58.13777)(1)(1) \cos(-1.1071 + 0 - 0) \\ + (35.77709)(1)(1.04) \cos(2.0344 + 0 - 0)$$

$$\therefore P_2 = -1.136$$

$$P_3 = |Y_{31}||V_3||V_1| \cos(\theta_{31} + \delta_1 - \delta_3) + |Y_{32}||V_3||V_2| \cos(\theta_{32} + \delta_2 - \delta_3) \\ + |Y_{33}||V_3|^2 \cos \theta_{33}$$

$$P_3 = (31.62278)(1.04)(1.05) \cos(1.8925) + (35.77709)(1.04) \cos(2.0344) \\ + 67.23095(1.04^2) \cos(-1.1737)$$

$$\therefore P_3 = 0.566$$

$$Q_2 = -|Y_{21}||V_2||V_1| \sin(\theta_{21} + \delta_1 - \delta_2) + |Y_{22}||V_2|^2 \sin\theta_{22} \\ - |Y_{23}||V_2||V_3| \sin(\theta_{23} + \delta_3 - \delta_2)$$

$$Q_2 = -(22.36068)(1.05) \sin(2.0344) + (58.13777) \sin(-1.1071) \\ - (35.77709)(1.04) \sin(2.0344)$$

$$\therefore Q_2 = -2.282$$

Calculate real and reactive power mismatch

$$\Delta P_2^{(0)} = P_2 - P_2^{(0)} = -4.0 - (-1.136) = -2.864$$

$$\Delta P_3^{(0)} = P_3 - P_3^{(0)} = 2.0 - (0.566) = 1.434$$

$$\Delta Q_2^{(0)} = Q_2 - Q_2^{(0)} = -2.5 - (-2.282) = -0.218$$

Step 7: Use the estimated values from step 6 to form the Jacobian Matrix. In

this example, the Jacobian matrix is a 3x3 matrix.

$$J = \begin{bmatrix} \frac{\partial P_2}{\partial \delta_2} & \frac{\partial P_2}{\partial \delta_3} & \frac{\partial P_2}{\partial |V_2|} \\ \frac{\partial P_3}{\partial \delta_2} & \frac{\partial P_3}{\partial \delta_3} & \frac{\partial P_3}{\partial |V_2|} \\ \frac{\partial Q_2}{\partial \delta_2} & \frac{\partial Q_2}{\partial \delta_3} & \frac{\partial Q_2}{\partial |V_2|} \end{bmatrix}$$

$$\frac{\partial P_2}{\partial \delta_2} = -|V_2||Y_{21}||V_1| \sin(\delta_2 - \delta_1 - \theta_{21}) - |V_2||Y_{23}||V_3| \sin(\delta_2 - \delta_3 - \theta_{23})$$

$$\frac{\partial P_2}{\partial \delta_3} = |V_2||Y_{23}||V_3|\sin(\delta_2 - \delta_3 - \theta_{23})$$

$$\begin{aligned} \frac{\partial P_2}{\partial |V_2|} &= |V_2||Y_{22}|\cos\theta_{22} + |Y_{21}||V_1|\cos(\delta_2 - \delta_1 - \theta_{21}) + |Y_{22}||V_2|\cos(-\theta_{22}) \\ &\quad + |Y_{23}||V_3|\cos(\delta_2 - \delta_3 - \theta_{23}) \end{aligned}$$

$$\frac{\partial P_3}{\partial \delta_2} = |V_3||Y_{32}||V_2|\sin(\delta_3 - \delta_2 - \theta_{32})$$

$$\frac{\partial P_3}{\partial \delta_3} = -|V_3||Y_{31}||V_1|\sin(\delta_3 - \delta_1 - \theta_{31}) - |V_3||Y_{32}||V_2|\sin(\delta_3 - \delta_2 - \theta_{32})$$

$$\frac{\partial P_3}{\partial |V_2|} = |V_3||Y_{32}|\cos(\delta_3 - \delta_2 - \theta_{32})$$

$$\frac{\partial Q_2}{\partial \delta_2} = |V_2||Y_{21}||V_1|\cos(\delta_2 - \delta_1 - \theta_{21}) + |V_2||Y_{23}||V_3|\cos(\delta_2 - \delta_3 - \theta_{23})$$

$$\frac{\partial Q_2}{\partial \delta_3} = -|V_2||Y_{23}||V_3|\cos(\delta_2 - \delta_3 - \theta_{23})$$

$$\begin{aligned} \frac{\partial Q_2}{\partial |V_2|} &= -|V_2||Y_{22}|\sin\theta_{22} + |Y_{21}||V_1|\sin(\delta_2 - \delta_1 - \theta_{21}) + |Y_{22}||V_2|\sin(-\theta_{22}) \\ &\quad + |Y_{23}||V_3|\sin(\delta_2 - \delta_3 - \theta_{23}) \end{aligned}$$

The Jacobien Matrix is as follow:

$$\begin{bmatrix} 54.28 & -33.28 & 24.86 \\ -33.28 & 66.04 & -16.64 \\ -27.14 & 16.64 & 49.72 \end{bmatrix}$$

Step 8: Solve the unknown's mismatch.

$$\begin{bmatrix} -2.864 \\ 1.434 \\ -0.218 \end{bmatrix} = \begin{bmatrix} 54.28 & -33.28 & 24.86 \\ -33.28 & 66.04 & -16.64 \\ -27.14 & 16.64 & 49.72 \end{bmatrix} \begin{bmatrix} \Delta\delta_2^{(0)} \\ \Delta\delta_3^{(0)} \\ \Delta|V_2^{(0)}| \end{bmatrix}$$

$$\Delta\delta_2^{(0)} = -0.04528$$

$$\Delta\delta_3^{(0)} = -0.00787$$

$$\Delta|V_2^{(0)}| = -0.02655$$

Step 9: Obtain the updates values.

$$\delta_2^{(1)} = 0 + (-0.04528) = -0.04528$$

$$\delta_3^{(1)} = 0 + (-0.00787) = -0.00787$$

$$|V_2^{(1)}| = 1 + (-0.02655) = 0.97345$$

Step 10: Check if all the mismatches are below a small number. Otherwise repeat step 7-9 until obtaining an accurate value

$$\begin{aligned} \delta_2^{(3)} &= -0.047058 + (-0.0000038) = -0.04706 \text{ radian} \\ &= -2.6963 \text{ degree} \end{aligned}$$

$$\begin{aligned} \delta_3^{(3)} &= -0.008703 + (-0.0000024) = -0.008705 \text{ radian} \\ &= -0.4987 \text{ degree} \end{aligned}$$

$$|V_2^{(3)}| = 0.971684 + (-0.0000044) = 0.97168 \text{ p.u.}$$

Step 11: Calculate all the rest parameter:

$$P_1 = |Y_{11}||V_1^2|\cos\theta_{11} + |Y_{12}||V_1||V_2|\cos(\theta_{12} + \delta_3 - \delta_1) \\ + |Y_{13}||V_1||V_3|\cos(\theta_{13} + \delta_3 - \delta_1)$$

$$Q_1 = -|Y_{11}||V_1^2|\sin\theta_{11} - |Y_{12}||V_1||V_2|\sin(\theta_{12} + \delta_2 - \delta_1) \\ - |Y_{13}||V_1||V_3|\sin(\theta_{13} + \delta_3 - \delta_1)$$

$$Q_3 = -|Y_{31}||V_3||V_1|\sin(\theta_{31} + \delta_1 - \delta_3) - |Y_{32}||V_3||V_2|\sin(\theta_{32} + \delta_2 - \delta_3) \\ - |Y_{33}||V_3^2|\sin\theta_{33}$$

$$\therefore P_1 = 2.1842 \text{ p.u.} \rightarrow = 218.42 \text{ MW}$$

$$Q_1 = 1.4085 \text{ p.u.} \rightarrow = 140.85 \text{ Mvar}$$

$$Q_3 = 1.4618 \text{ p.u.} \rightarrow = 146.18 \text{ MW}$$

A2 IEEE 30 Bus Test System Data

Table A2: Bus Data Format

Bus number	Type	Pg	Qg	Bs	Vmax	Vmin
01	3	0	0	0	1.05	0.95
02	2	21.7	12.7	0	1.1	0.95
03	1	2.4	1.2	0	1.05	0.95
04	1	7.6	1.6	0	1.05	0.95
05	1	0	0	0.19	1.05	0.95
06	1	0	0	0	1.05	0.95
07	1	22.8	10.9	0	1.05	0.95
08	1	30	30	0	1.05	0.95

Bus number	Type	Pg	Qg	Bs	Vmax	Vmin
09	1	0	0	0	1.05	0.95
10	1	5.8	2	0	1.05	0.95
11	1	0	0	0	1.05	0.95
12	1	11.2	7.5	0	1.05	0.95
13	2	0	0	0	1.1	0.95
14	1	6.2	1.6	0	1.05	0.95
15	1	8.2	2.5	0	1.05	0.95
16	1	3.5	1.8	0	1.05	0.95
17	1	9	5.8	0	1.05	0.95
18	1	3.2	0.9	0	1.05	0.95
19	1	9.5	3.4	0	1.05	0.95
20	1	2.2	0.7	0	1.05	0.95
21	1	17.5	11.2	0	1.05	0.95
22	2	0	0	0	1.1	0.95
23	2	3.2	1.6	0	1.1	0.95
24	1	8.7	6.7	0.04	1.05	0.95
25	1	0	0	0	1.05	0.95
26	1	3.5	2.3	0	1.05	0.95
27	2	0	0	0	1.1	0.95
28	1	0	0	0	1.05	0.95
29	1	2.4	0.9	0	1.05	0.95
30	1	10.6	1.9	0	1.05	0.95

Bus type:

PQ bus = 1

PV bus =2

Reference bus =3

Pg: real power demand in MW

Qg: reactive power demand in MVar

Bs: shunt susceptance in MVar (injected at V = 1.0 p.u.)

Vmax/ Vmin: maximum/minimum voltage magnitude in p.u.

Table A3: Generator Data Format

Bus #	Pg	Qg	Pmax	Pmin	Qmax	Qmin	Vg	a	b	c
1	23.54	0	80	0	150	-20	1	0.02	2	0
2	60.97	0	80	0	60	-20	1	0.0175	1.75	0
13	37	0	40	0	44.7	-15	1	0.025	3	0
22	21.59	0	50	0	62.5	-15	1	0.0625	1	0
23	19.2	0	30	0	40	-10	1	0.025	3	0
27	26.91	0	55	0	48.7	-15	1	0.00834	3.25	0

Bus #: Generator at bus number #

Pg: real Power output in MW

Qg: reactive power output in MVAR

Pmax/ Pmin: maximum/minimum real power output in MW

Qmax/ Qmin: maximum/minimum reactive power output in MVAR

Vg: voltage magnitude setpoint in p.u.

a,b,and c, parameters defining total polynomial cost function (highest order coefficients first)

In this data, the cost function is a second-degree polynomial equation since the greatest power is two (N-1). Therefore, the equation of generator cost is:

$$\text{generator cost} = ax^2 + bx + c$$

Table A4: Transmission Line Data Format

From bus # to bus #	R	X	B	R'	X'	B'	MVA rate	Irated
01-02	0.02	0.06	0.03	3.645	10.935	164.609	130	0.556
01-03	0.05	0.19	0.02	9.1125	34.628	109.739	130	0.556
02-04	0.06	0.17	0.02	10.935	30.983	109.739	65	0.278
02-05	0.05	0.2	0.02	9.1125	36.45	109.739	130	0.556
02-06	0.06	0.18	0.02	10.935	32.805	109.739	65	0.278
03-04	0.01	0.04	0	1.8225	7.29	0	130	0.556
04-06	0.01	0.04	0	1.8225	7.29	0	90	0.385
05-07	0.05	0.12	0.01	9.1125	21.87	54.8697	70	0.299
06-07	0.03	0.08	0.01	5.4675	14.58	54.8697	130	0.556
06-08	0.01	0.04	0	1.8225	7.29	0	32	0.137
06-28	0.02	0.06	0.01	3.645	10.935	54.8697	32	0.137
08-28	0.06	0.2	0.02	10.935	36.45	109.739	32	0.137
10-17	0.03	0.08	0	5.4675	14.58	0.	32	0.137
10-20	0.09	0.21	0	16.403	38.273	0.	32	0.137
10-21	0.03	0.07	0	5.468	12.758	0.	32	0.137
10-22	0.07	0.15	0	21.87	47.385	0.	32	0.137
12-14	0.12	0.26	0	12.758	23.693	0.	32	0.137
12-15	0.07	0.13	0	16.403	36.45	0.	32	0.137
12-16	0.09	0.2	0	40.095	36.45	0.	32	0.137
14-15	0.22	0.2	0	20.048	40.095	0.	16	0.068
15-18	0.11	0.22	0	18.225	36.45	0.	16	0.068

From bus # to bus #	R	X	B	R'	X'	B'	MVA rate	Irated
15-23	0.1	0.2	0	14.58	34.628	0.	16	0.068
16-17	0.08	0.19	0	10.935	23.693	0.	16	0.068
18-19	0.06	0.13	0	5.4675	12.758	0.	16	0.068
19-20	0.03	0.07	0	1.8225	3.645	0.	32	0.137
21-22	0.01	0.02	0	21.87	32.805	0.	32	0.137
22-24	0.12	0.18	0	23.693	49.208	0.	16	0.068
23-24	0.13	0.27	0	34.628	60.143	0.	16	0.068
24-25	0.19	0.33	0	45.563	69.255	0.	16	0.068
25-26	0.25	0.38	0	20.048	38.273	0.	16	0.068
25-27	0.11	0.21	0	40.095	76.545	0.	16	0.068
27-29	0.22	0.42	0	58.32	109.35	0.	16	0.068
27-30	0.32	0.6	0	43.74	82.013	0.	16	0.068
29-30	0.24	0.45	0	3.645	10.935	0.	16	0.068

From bus # to bus #: transmission line from bus number # to bus number #

R: resistance in p.u.

X: reactance in p.u.

B: total line susceptance in p.u.

R: resistance in real unit in MW/km

X: reactance in real unit in MVAR/km

B: susceptance in real unit in uS/km

MVA rate: long term rating in MVA

Irated: current rating in kA

Table A5: Transformer Data Format

From bus # to bus #	R	X	R1	X1	MVA rate
T1 04-12	0	0.26	0	0.169	65
T2 06-09	0	0.21	0	0.1365	65
T3 06-10	0	0.56	0	0.1792	32
T4 09-10	0	0.11	0	0.0715	65
T5 09-11	0	0.21	0	0.1365	65
T6 12-13	0	0.14	0	0.091	65
T7 28-27	0	0.4	0	0.26	65

From bus # to bus #: transmission line from bus number # to bus number #

R: resistance in p.u.

X: reactance in p.u.

R1: positive sequence resistance in p.u.

X1: positive sequence reactance in p.u.

MVA rate: long term rating in MVA

Table A6: Generator Cost Data in Piecewise Linear Format

Gen 1		Gen 2		Gen 13	
Power (MW)	Cost (\$/h)	Power (MW)	Cost (\$/h)	Power (MW)	Cost (\$/h)
0	0	0	0	0	0
4	8.32	4	7.28	2	6.1
8	17.28	8	15.12	4	12.4
12	26.88	12	23.52	6	18.9
16	37.12	16	32.48	8	25.6
20	48	20	42	10	32.5
24	59.52	24	52.08	12	39.6
28	71.68	28	62.72	14	46.9
32	84.48	32	73.92	16	54.4
36	97.92	36	85.68	18	62.1
40	112	40	98	20	70
44	126.72	44	110.88	22	78.1
48	142.08	48	124.32	24	86.4
52	158.08	52	138.32	26	94.9
56	174.72	56	152.88	28	103.6
60	192	60	168	30	112.5
64	209.92	64	183.68	32	121.6
68	228.48	68	199.92	34	130.9
72	247.68	72	216.72	36	140.4
76	267.52	76	234.08	38	150.1
80	288	80	252	40	160

Gen 22		Gen 23		Gen 27	
Power (MW)	Cost (\$/h)	Power (MW)	Cost (\$/h)	Power (MW)	Cost (\$/h)
0	0	0	0	0	0
2.5	2.8906	1.5	4.5563	2.75	9.0006
5	6.5625	3	9.225	5.5	18.127
7.5	11.016	4.5	14.006	8.25	27.380
10	16.25	6	18.9	11	36.759
12.5	22.266	7.5	23.906	13.75	46.264
15	29.063	9	29.025	16.5	55.896
17.5	36.641	10.5	34.256	19.25	65.653
20	45.	12	39.6	22	75.537
22.5	54.141	13.5	45.056	24.75	85.546
25	64.063	15	50.625	27.5	95.682
27.5	74.766	16.5	56.306	30.25	105.94
30	86.25	18	62.1	33	116.33
32.5	98.516	19.5	68.006	35.75	126.85
35	111.56	21	74.025	38.5	137.49
37.5	125.39	22.5	80.156	41.25	148.25
40	140.	24	86.4	44	159.15
42.5	155.39	25.5	92.756	46.75	170.17
45	171.56	27	99.225	49.5	181.31
47.5	188.52	28.5	105.81	52.25	192.58
50.	206.25	30.	112.5	55.	203.98

Power: real power in MW

Cost: cost in \$/h

A3 DPL Code

SCD for Single Contingency

```

string str,s1,s2,s3,p1;
int error, error2,a,b;
double cost, max,SumCostLS,CostLS,c,i;
object F, C, Omax, SumGrid,Q;
set S,T,V;
ClearOutput();

Cost.Resize(0,0);
LS.Resize(0,0);
T.Clear();
S = SEL.AllLines();           ! get all components
T.Add(S);
S = SEL.GetAll('ElmTr2');
T.Add(S);
S = SEL.AllSym();
T.Add(S);
S = SEL.AllLoads();
V.Add(S);

!Show total cost with all lines on service
SumGrid = SummaryGrid();

F=T.First();
while(F)
{
F.ShowFullName();
F=T.Next();
}

a=1;
b=1;

F =T.First();

while(F)
{
F:outserv=1;
printf('When %o is out of service',F);

i=1;

```

```

while(i<=10)
{
  Opf:kpenalty_min=i;
  printf('i = %f',i);
  error = Opf.Execute();
  if (error)
  {
    i+=0.1;
  }
  else
  {
    s1 = SumGrid.lnr('c:cst_disp');
    s2 = SumGrid.unr('c:cst_disp');
    printf('%s = %5.3f [%s] for PF\n',s1, SumGrid:c:cst_disp, s2);
    LS.Set(b,a,0);
    Cost.Set(b,a,SumGrid:c:cst_disp);
    F:outserv=0;

    break;
  }
  Cost.Set(b,a,0);
}
c=Cost.Get(b,a);
printf('c = %5.3f \n', c);
if (c=0)
{

error2=OpfLS.Execute();
if (error2)
{
  Cost.Set(b,a,999);
  F:outserv=0;
}
else

{
  SumCostLS=SumGrid:c:cst_disp;
  Q=V.First(); !load 2
  CostLS=Q:c:Pmism*5500*-1;
  SumCostLS+=CostLS;

  Q=V.Next(); ! load 3
  CostLS=Q:c:Pmism*5000*-1;
  SumCostLS+=CostLS;

  Q=V.Next(); ! load 4
  CostLS=Q:c:Pmism*5500*-1;
  SumCostLS+=CostLS;
}
}

```

```
Q=V.Next(); !load 7
CostLS=Q:c:Pmism*6500*-1;
SumCostLS+=CostLS;

Q=V.Next(); !load 8
CostLS=Q:c:Pmism*10000*-1;
SumCostLS+=CostLS;

Q=V.Next(); !load 10
CostLS=Q:c:Pmism*5500*-1;
SumCostLS+=CostLS;

Q=V.Next(); !load 12
CostLS=Q:c:Pmism*5500*-1;
SumCostLS+=CostLS;

Q=V.Next(); !load 14
CostLS=Q:c:Pmism*5500*-1;
SumCostLS+=CostLS;

Q=V.Next(); !load 15
CostLS=Q:c:Pmism*5500*-1;
SumCostLS+=CostLS;

Q=V.Next(); !load 16
CostLS=Q:c:Pmism*5500*-1;
SumCostLS+=CostLS;

Q=V.Next(); !load 17
CostLS=Q:c:Pmism*6000*-1;
SumCostLS+=CostLS;

Q=V.Next(); !load 18
CostLS=Q:c:Pmism*5500*-1;
SumCostLS+=CostLS;

Q=V.Next(); !load 19
CostLS=Q:c:Pmism*6500*-1;
SumCostLS+=CostLS;

Q=V.Next(); !load 20
CostLS=Q:c:Pmism*5500*-1;
SumCostLS+=CostLS;

Q=V.Next(); !load 21
CostLS=Q:c:Pmism*8000*-1;
SumCostLS+=CostLS;
```

```

Q=V.Next ();      !load 23
CostLS=Q:c:Pmism*5500*-1;
SumCostLS+=CostLS;

Q=V.Next ();      !load24
CostLS=Q:c:Pmism*5500*-1;
SumCostLS+=CostLS;

Q=V.Next ();      !load 26
CostLS=Q:c:Pmism*6000*-1;
SumCostLS+=CostLS;

Q=V.Next ();      !load 29
CostLS=Q:c:Pmism*5500*-1;
SumCostLS+=CostLS;

Q=V.Next ();      !load 30
CostLS=Q:c:Pmism*7000*-1;
SumCostLS+=CostLS;

Cost.Set (b, a, SumCostLS);
LS.Set (b, a, 1);
printf( 'load shedding cost = %5.3f \n', SumCostLS);
P:outserv=0;

}

}
b+=1;
P:outserv=0;
P=T.Next ();
}

```

SCD for Double Contingencies

```

string str,s1,s2,s3,p1;
int err, error2, a, b,z,i,j;
double cost, max,c,SumCostLS,CostLS;
object P, O, Omax, SumGrid,X,Q;
set S,T,U,V;

ClearOutput();

SumGrid = SummaryGrid();
Cost.Resize(0,0);
Iteration.Resize(0,0);
UnSupplied.Resize(0,0);

T.Clear();
U.Clear();
S = SEL.AllLines();
T.Add(S);
U.Add(S);
S = SEL.GetAll('ElmTr2');
T.Add(S);
U.Add(S);
S = SEL.AllSym();
T.Add(S);
U.Add(S);
S = SEL.AllLoads();
V.Add(S);

O = T.First();

a=1;
z=1;
while(O)
!for(j=1;j<2;j=j+1)
{
X = U.First();
b=1;
while (X)
{
if (a>=b)
{
Cost.Set(b,a,0);
UnSupplied.Set(b,a,8888);
X.ShowFullName();
X = U.Next();
}
}
}

```

```

printf('aaaa %f',b);
b+=1;
}
else
{
  C:outserv=1;
  X:outserv=1;
  printf('aaaa %f',b);
  printf('When %o and %o are out of service',C,X);

  i=1;
  Opf:kpenalty_min=1;
  while(i<=10)
  { printf('%f',i);
    err = Opf.Execute();
    if (err)
    {
      i+=0.1;
      Opf:kpenalty_min=i;

      c=Cost.Set(b,a,0);
    }
    else
    {
      s1 = SumGrid.lnr('c:cst_disp');
      s2 = SumGrid.unr('c:cst_disp');
      printf('%s = %5.3f [%s] for OPF\n',s1, SumGrid:c:cst_disp, s2);
      Cost.Set(b,a,SumGrid:c:cst_disp);
      UnSupplied.Set(b,a,SumGrid:c:n_unsup);
      Iteration.Set(b,a,i);
      Opf:kpenalty_min=1;
      C:outserv=0;
      X:outserv=0;

      break;
    }
  }
  printf('bbbb %f',b);
  c=Cost.Get(b,a);
  if(c>0)
  {

    Opf:kpenalty_min=1;
    C:outserv=0;
    X:outserv=0;
  }
  else
  {

err = OpfLS.Execute();

if (err)
  { OpfLS:iInit=1;
    err=OpfLS.Execute();

```

```

        if(err)
        { Cost.Set(b,a,123456);
          OpfLS:iInit=0;
          Opf:kpenalty_min=1;
          C:outserv=0;
          X:outserv=0;
        }
        else
        {
          SumCostLS=SumGrid:c:cst_disp;
Q=V.First(); !load 2
CostLS=Q:c:Pmism*5500*-1;
SumCostLS+=CostLS;

Q=V.Next(); ! load 3
CostLS=Q:c:Pmism*5000*-1;
SumCostLS+=CostLS;

Q=V.Next(); ! load 4
CostLS=Q:c:Pmism*5500*-1;
SumCostLS+=CostLS;

Q=V.Next(); ! load 7
CostLS=Q:c:Pmism*6500*-1;
SumCostLS+=CostLS;

Q=V.Next(); !load 8
CostLS=Q:c:Pmism*10000*-1;
SumCostLS+=CostLS;

Q=V.Next(); !load 10
CostLS=Q:c:Pmism*5500*-1;
SumCostLS+=CostLS;

Q=V.Next(); !load 12
CostLS=Q:c:Pmism*5500*-1;
SumCostLS+=CostLS;

Q=V.Next(); !load 14
CostLS=Q:c:Pmism*5500*-1;
SumCostLS+=CostLS;

Q=V.Next(); !load 15
CostLS=Q:c:Pmism*5500*-1;
SumCostLS+=CostLS;

Q=V.Next(); !load 16
CostLS=Q:c:Pmism*5500*-1;
SumCostLS+=CostLS;

Q=V.Next(); !load 17
CostLS=Q:c:Pmism*6000*-1;
SumCostLS+=CostLS;

```

```

Q=V.Next();    !load 18
CostLS=Q:c:Pmism*5500*-1;
SumCostLS+=CostLS;

Q=V.Next();    !load 19
CostLS=Q:c:Pmism*6500*-1;
SumCostLS+=CostLS;

Q=V.Next();    !load 20
CostLS=Q:c:Pmism*5500*-1;
SumCostLS+=CostLS;

Q=V.Next();    !load 21
CostLS=Q:c:Pmism*8000*-1;
SumCostLS+=CostLS;

Q=V.Next();    !load 23
CostLS=Q:c:Pmism*5500*-1;
SumCostLS+=CostLS;

Q=V.Next();    !load24
CostLS=Q:c:Pmism*5500*-1;
SumCostLS+=CostLS;

Q=V.Next();    !load 26
CostLS=Q:c:Pmism*6000*-1;
SumCostLS+=CostLS;

Q=V.Next();    !load 29
CostLS=Q:c:Pmism*5500*-1;
SumCostLS+=CostLS;

Q=V.Next();    !load 30
CostLS=Q:c:Pmism*7000*-1;
SumCostLS+=CostLS;

        Cost.Set(b,a,SumCostLS);
        UnSupplied.Set(b,a,SumGrid:c:n_unsup);
        Iteration.Set(b,a,99);
        printf( 'load shedding cost = %5.3f \n', SumCostLS);
        Opf:kpenalty_min=1;
        C:outserv=0;
        X:outserv=0;
        OpfLS:iInit=0;
    }
}
else
{
    SumCostLS=SumGrid:c:cst_disp;

```



```
Q=V.First(); !load 2
CostLS=Q:c:Pmism*5500*-1;
SumCostLS+=CostLS;

Q=V.Next(); !load 3
CostLS=Q:c:Pmism*5000*-1;
SumCostLS+=CostLS;

Q=V.Next(); !load 4
CostLS=Q:c:Pmism*5500*-1;
SumCostLS+=CostLS;

Q=V.Next(); !load 7
CostLS=Q:c:Pmism*6500*-1;
SumCostLS+=CostLS;

Q=V.Next(); !load 8
CostLS=Q:c:Pmism*10000*-1;
SumCostLS+=CostLS;

Q=V.Next(); !load 10
CostLS=Q:c:Pmism*5500*-1;
SumCostLS+=CostLS;

Q=V.Next(); !load 12
CostLS=Q:c:Pmism*5500*-1;
SumCostLS+=CostLS;

Q=V.Next(); !load 14
CostLS=Q:c:Pmism*5500*-1;
SumCostLS+=CostLS;

Q=V.Next(); !load 15
CostLS=Q:c:Pmism*5500*-1;
SumCostLS+=CostLS;

Q=V.Next(); !load 16
CostLS=Q:c:Pmism*5500*-1;
SumCostLS+=CostLS;

Q=V.Next(); !load 17
CostLS=Q:c:Pmism*6000*-1;
SumCostLS+=CostLS;

Q=V.Next(); !load 18
CostLS=Q:c:Pmism*5500*-1;
SumCostLS+=CostLS;

Q=V.Next(); !load 19
CostLS=Q:c:Pmism*6500*-1;
SumCostLS+=CostLS;

Q=V.Next(); !load 20
CostLS=Q:c:Pmism*5500*-1;
SumCostLS+=CostLS;
```

```

Q=V.Next();           !load 21
CostLS=Q:c:Pmism*8000*-1;
SumCostLS+=CostLS;

Q=V.Next();           !load 23
CostLS=Q:c:Pmism*5500*-1;
SumCostLS+=CostLS;

Q=V.Next();           !load24
CostLS=Q:c:Pmism*5500*-1;
SumCostLS+=CostLS;

Q=V.Next();           !load 26
CostLS=Q:c:Pmism*6000*-1;
SumCostLS+=CostLS;

Q=V.Next();           !load 29
CostLS=Q:c:Pmism*5500*-1;
SumCostLS+=CostLS;

Q=V.Next();           !load 30
CostLS=Q:c:Pmism*7000*-1;
SumCostLS+=CostLS;

        Cost.Set(b,a,SumCostLS);
        UnSupplied.Set(b,a,SumGrid:c:n_unsup);
        Iteration.Set(b,a,99);
        printf( 'load shedding cost = %5.3f \n', SumCostLS);
        Opf:kpenalty_min=1;
        C:outserv=0;
        X:outserv=0;
    }

    }
    b+=1;
    X.ShowFullName();
X = U.Next();
}
z+=1;

}
a+=1;
C = T.Next();
}

```

ECP_SCD

```

double a,b,c,d,e,f,g,h,m,x,y,z;
int i,j,k,l;
ClearOutput();

m=AIS.Get(1,1); !prob of all components in service
!ECP-SCD 100
a=OPF.Get(1,1); ! opf of (n-0)
for(i=1;i<48;i=i+1)
{ b=One_Out.Get(i,1);
  c=Prob_One_Out.Get(i,1);
  d=(b-a)*c;
  g=h+c; !sum up the prob
  h=g;
  e=f+d; ! sum up the result
  f=e;
}
l=2;
for(j=1;j<48;j=j+1)
{ for(k=1;k<48;k=k+1)
  { b=Two_Out_100.Get(k,j);
    c=Prob_Two_Out.Get(k,j);
    d=(b-a)*c;
    g=h+c; !sum up the prob
    h=g;
    e=f+d; ! sum up the result
    f=e;
  }
  l+=1;
}
printf('%f',h+m);
f=f/(h+m);
Result.Set(1,1,f);
x=f;

!Variance 100
for(i=1;i<48;i=i+1)
{ b=One_Out.Get(i,1);
  c=Prob_One_Out.Get(i,1);
  d=(pow(b-a-x,2))*c;
  y=z+d;
  z=y;
}
l=2;
for(j=1;j<48;j=j+1)
{ for(k=1;k<48;k=k+1)
  { b=Two_Out_100.Get(k,j);
    c=Prob_Two_Out.Get(k,j);
    d=(pow(b-a-x,2))*c;
    y=z+d;
    z=y;
  }
  l+=1;
}
z=z/(h+m);
Result.Set(1,2,z);

```

Monte Carlo Simulation

```

double d,st,t,a,b,c,i,j,k,l,x,y,z,e,f,g,h,m,n,o,p,q; !
ClearOutput();
Result.Resize(0,0);      !clear all result from previous simulation
Result2.Resize(0,0);
Result3.Resize(0,0);
Result4.Resize(0,0);
CompOut3.Resize(0,0);
CompOut4.Resize(0,0);
CompOut5.Resize(0,0);
CompOut6.Resize(0,0);

!InOut
for (j=1;j<=100000;j=j+1)
{
for (i=1;i<=41;i=i+1)
{
c=Random(0,1);
if (c<0.993)
{d=0;
Result.Set(j,i,d);
}
else
{d=1;
Result.Set(j,i,d);
}
}
}

for (i=42;i<=47;i=i+1)
{
c=Random(0,1);
if (c<0.98)
{d=0;
Result.Set(j,i,d);
}
else
{d=1;
Result.Set(j,i,d);
}
}
}

!Count Unit Out
for (j=1;j<=100000;j=j+1)
{
b=0;
for (i=1;i<=47;i=i+1)
{
c=Result.Get(j,i);
a=b+c;
b=a;
}
}

```

```

    Result2.Set(j,1,b);
}

!Count Unit Out by number
l=1;
for(j=0;j<=47;j=j+1)
{
    b=0;
    for(i=1;i<=100000;i=i+1)
    { k=Result2.Get(i,1);
      if (k=j)
      { a=b+1;
        b=a;
      }
      Result3.Set(l,1,b);
    }
    l=l+1;
}

!Get Result
h=1;
m=1;
n=1;
p=1;
for(j=1;j<=100000;j=j+1)
{
    a=Result2.Get(j,1);
    !printf('j=%f a= %f',j,a);
    if (a=0)
    {
        Result4.Set(j,1,0);
        !printf('ha ha ha');
    }
    else if (a=1)
    {
        for(i=1;i<=47;i=i+1)
        {
            b=Result.Get(j,i);
            !printf('%f %f', j,i);
            if(b=1)
            {
                x=OneOut.Get(i,1);
                Result4.Set(j,1,x);
            }
        }
    }
    else if (a=2)
    { g=0;

```

```

for(i=1;i<=47;i=i+1)
{
!printf('for=%f ',i);
b=Result.Get(j,i);
if(b=1)
{ !printf('i=%f ',i);
e=i;
!printf('e=%f ',e);

! g=g+1;
! break;
for(i=e+1;i<=47;i=i+1)
{
b=Result.Get(j,i);
if (b=1)
{
f=i;
!printf('f= %f',f);
x=TwoOut.Get(f,e);
Result4.Set(j,1,x);
}
}
}
!break;
}
}

else if (a=3)
{
for(i=1;i<=47;i=i+1)
{ e=i;
b=Result.Get(j,i);
if(b=1)
{
CompOut3.Set(h,1,i); !CompOut3#1
for(i=e+1;i<=47;i=i+1)
{
b=Result.Get(j,i);
if (b=1)
{ f=i;
CompOut3.Set(h,2,i); !CompOut3#1
for(i=f+1;i<=47;i=i+1)
{
b=Result.Get(j,i);
if (b=1)
{
CompOut3.Set(h,3,i); !CompOut3#1
}
}
}
}
}
}
}
}

```



```
!!!!

else if (a>=7)
{
    Result4.Set(j,1,0);
    !z=z+1;
}
!printf('Interation=%f ',j);
}

for(j=1;j<=100000;j=j+1)
{
    a=Result4.Get(j,1);
    b=c+a;
    c=b;
}

!c=c/10000;
printf('Avg Cost Penalty=%f ',c);
```